THE UNIVERSITY OF MICHIGAN

COLLEGE OF ENGINEERING

High Altitude Engineering Laboratory

Departments of

Aerospace Engineering

Atmospheric and Oceanic Science

Final Report

SATELLITE MEASUREMENT OF STRATOSPHERIC POLLUTANTS AND MINOR CONSTITUENTS BY SOLAR OCCULTATION: A PRELIMINARY REPORT

by

S. R. Drayson
F. L. Bartman
W. R. Kuhn
R. Tallamraju

ORA Project 011023

under contract with:

NATIONAL OCEANIC AND ATMOSPHERIC ADMINISTRATION

GRANT NG-10-72

administered through

OFFICE OF RESEARCH ADMINISTRATION ANN ARBOR

November 1972

ens

UMR 7752

Abstract

The feasibility of determining concentrations of pollutants and minor constituents from satellite measurement of solar occultation absorption in the infrared is examined. The molecules considered include water vapor, O_3, OH, CO_2, CO, CH_4, N_2O, NO, NO_2, N_2O_5, HNO_3, and also aerosols. A survey of experimentally and theoretically determined concentrations and of infrared spectral properties is made for each constituents. Atmospheric applications and estimates of stratospheric absorption are included.

TABLE OF CONTENTS

TABLE OF CONTENTS (cont.)

TABLE OF CONTENTS (cont.)

TABLE OF CONTENTS (cont.)

Chapter 1. Introduction

The atmosphere of the earth is a complex medium in which many physical and chemical processes are continually modifying its composition, dynamics, temperature etc. Most of this occurs naturally in the atmosphere but man's activities are also causing change both on a local and a global scale. While there is still a tendency to study the different phenomena on an individual basis, it is apparent that a true picture of the atmosphere can evolve only by considering the interaction of all of the individual components.

The minor atmospheric constituents are of great importance. For instance, ozone in the stratosphere prevents lethal solar radiation from reaching the surface. Most of these minor constituents are involved in chemical and photochemical reactions which ultimately effect the distribution of all of them, but are also modified by atmospheric transport phenomena, horizontal and vertical, large scale and eddies of all scales.

In the troposphere mixing is good and measurements are comparitively easy to make. In the stratosphere the atmosphere is much more stable so that eddy mixing processes are much less efficient. Much more dissociating radiation can reach these levels so that the chemical processes are different from those in the troposphere. Many of them are not completely understood and measurements of their concentrations are poor or completely missing.

Man is modifying his natural environment by polluting it with gasses, dust and aerosols. Many do not reach stratospheric levels, but some do diffuse upwards and others are deposited in the stratosphere by aircraft. The fate of these pollutants is a matter of speculation and concern, particularly as it may modify the climate of the earth.

Thus there is a need for the global measurements of the distribution of minor constituents in the stratosphere as an aid to understanding the natural processes in the atmosphere, gauging the possible effect of pollutants and the actual monitoring of pollutants. A satellite would provide an ideal platform provided a suitable experiment could be devised. The purpose of this study is to investigate the feasibility of one method, solar occultation.

This report contains the results of the first six months of an investigation into the feasibility of determining concentrations of minor constituents in the stratosphere by satellite measurement of the attenuation of solar radiation along a tangent path through the atmosphere. The aim of the study is to answer such questions as:

What constituents may be measured by this technique?

How accurately can the concentrations be measured?

What is the altitude range?

What vertical resolution can be attained?

How does the method compare with other techniques, particularly satellite methods?

What inversion techniques can be employed?

Before these questions can be adequately answered we must know what range of concentrations we can reasonably expect in the stratosphere. A literature search of measurements and theoretical calculations of stratospheric distributions was made for many of the minor constituents. In addition, for each of them a critical evaluation was made of our knowledge of the spectral properties of each molecule. This study was confined to the infrared region of the spectrum as oxygen and ozone may be expected to absorb most of the radiation in the ultraviolet region. Finally, the findings on the distributions

and spectral properties have been combined to calculate the approximate absorption at various tangent heights, using a procedure described in the Appendix. Dust and aerosols are considered in a separate chapter.

It should be stressed that this document is not a final report on a completed investigation. It represents an interim summary of progress. It was prepared in the fall of 1972 so that any references that appeared or became available to the authors later than September 1972 are not included.

Chapter 2. Molecules Containing Hydrogen and Oxygen (O_3, H_2O, OH)

2.1 Ozone

2.1.1 Distribution

Ozone, although a minor constituent, plays a significant role in the meteorological processes of the earth's atmosphere as well as preventing solar ultra violet radiation from reaching the earth's surface and terminating biological processes. Were it not for the small amount of ozone in the stratosphere, there would be no temperature inversion near 10 km elevation and one can imagine that circulation systems, cloud coverage etc. would be much different from what we find today. Thus it is important to monitor atmospheric ozone in order to detect any changes - man induced or otherwise - in its amount and distribution.

The primary reactions leading to the formation and destruction of ozone in the stratosphere have been known for many years (see, e.g. Craig, (1965)). Ozone is produced in a three body collision including atomic and molecular oxygen, and is primarily destroyed by photo dissociation. These processes produce a maximum ozone concentration at a height of about 25 km ($5 \times 10^{12}/cm^3$). At 50 km the concentration has decreased to approximately $5 \times 10^{10}/cm^3$. Recently, other constituents have been found to influence atmospheric ozone, such as water vapor (Hunt, 1966) and nitrogen oxides (Johnston, 1971) and while inclusion of these molecules may alter significantly the total ozone amount, the general profile is essentially the same, i.e., a lower stratospheric maximum, with much smaller amounts in both the troposphere and mesosphere. In this section we briefly review the observations of atmospheric ozone, with particular emphasis in the height range of approximately 10 to 50 km.

Total atmospheric ozone as a function of season is shown in Fig.2. 1. 1 and is taken from Dopplick (1970). This distribution was compiled from monthly mean Umkehr measurements (Ozone Data for the World [Meteorological Service of Canada 1960-1968]) and represents 2-9 year averages for longitudes of approximately 75W. Total ozone amount is a maximum at high latitudes in late winter and early spring, reaching values of about 0. 45 and 0. 35 atm cm in the northern and southern hemispheres respectively. These maxima are produced primarily by an increase in ozone in the low stratosphere (Dutsch, 1970). The poleward ozone gradient is still present in the summertime, but not so much so as in the winter. The lesser amounts in tropical regions (0. 25-0. 28 atm cm) are due to the "thicker" equatorial troposphere and associated circulation system. Note that there is more ozone in the high latitudes of the northern hemisphere than in the southern hemisphere. The maximum is also reached somewhat later in the southern hemisphere with the high values extending longer into summer (see e. g. Willett, 1968).

Significant longitudinal variations in total ozone have also been detected from remote soundings of Nimbus 3 data (Prabhakara, Salmonson, Conrath, Steranda, and Allison, 1971). During June and July of 1969, ozone minima were detected over northeast India (0. 25 atm cm) and North Africa (0. 27 atm cm) and are thought to be associated with upper air high pressure systems causing a net divergence of ozone from the outward flow. Regions of high ozone amount ($\sim$ 0. 3 atm cm) are located over Southeast Asia and Africa and are thought to be associated with the easterly jet stream.

In addition to the large seasonal variation in total ozone, harmonic analysis of mean monthly ozone data (Shah, 1967) revealed a 26 month quasi-biennial oscillation. This oscillation has been confirmed for both the Northern

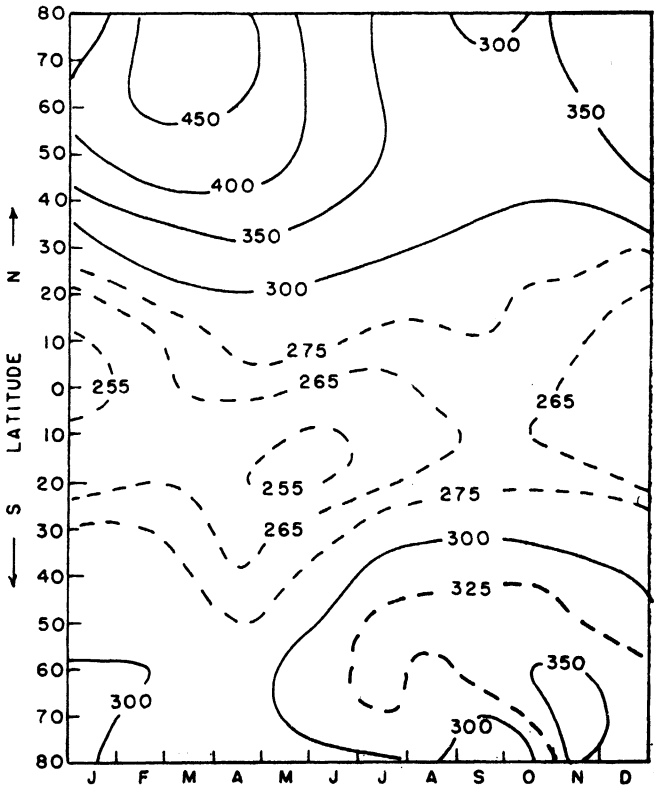

Fig. 2.1.1 Total atmospheric ozone (x10^3 atm-cm) as a function of latitude and season. From Dopplick (1972).

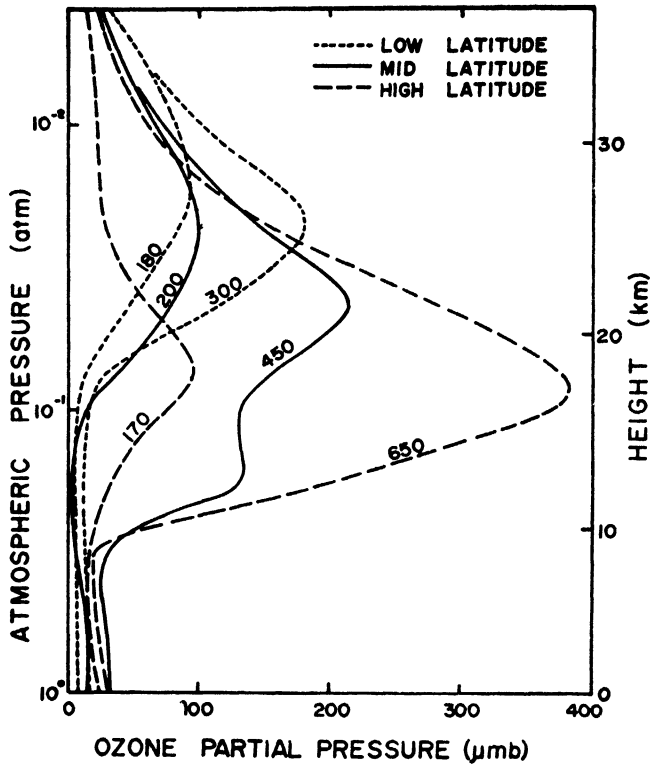

Fig. 2.I. 2 Standard ozone profiles for lowest and highest total ozone (atm-cm) for low-, mid-, and high latitude series. From Mateer, Heath, and Krueger(1971).

and Southern hemispheres, with Northern hemisphere data showing the oscillation extending from equatorial to polar latitudes. The oscillation follows a meridional wave pattern with a maximum at the equator and a wavelength of about 30 degrees latitude. There is no systematic progression in phase with latitude, there being a simultaneous occurrence of wave crests at temperate and polar latitudes. There have been observed no significant longitudinal variations in amplitude, although there are differences in phase.

Typical vertical profiles of atmospheric ozone are shown in Fig. 2.1.2 and are taken from the work of Mateer, Heath, and Krueger (1971). These ozone profiles were developed from data from direct soundings at the Canal Zone (Hering and Borden, 1965), Boulder, Colorado (Dutsch, 1966), and Resolute, Canada (advance of publication). Large variations in ozone amount are possible; at high latitudes values may reach 0.650 atm cm while smaller amounts are found in the lower latitudes with lowest values reaching 0.180 atm cm. Note also that the peak in the distribution increases in elevation with decreasing latitude. The double maximum in the mid latitude profile with maximum ozone is probably due to an intrusion of ozone rich polar air into the mid latitude troposphere (see following discussion).

A number of latitudinal vertical ozone distributions have been constructed (Ramanathan and Kulkarni, 1960; Dopplick, 1970; Dutsch, 1970) and Figs. 2.1.3 and 2.1.4 show the results of Dopplick and Dutsch respectively. Note that their results (Fig. 2.1.3 a, c and 2.1.4) are qualitatively quite similar. Dopplick's global seasonal northern hemisphere results were from data as described earlier. Southern hemisphere profiles are reflected from corresponding Northern hemisphere latitudes and adjusted to the correct Southern hemisphere total ozone amounts. Dutsch implies his profiles are constructed from both the Umkehr method and direct soundings, and are for the Northern hemisphere only.

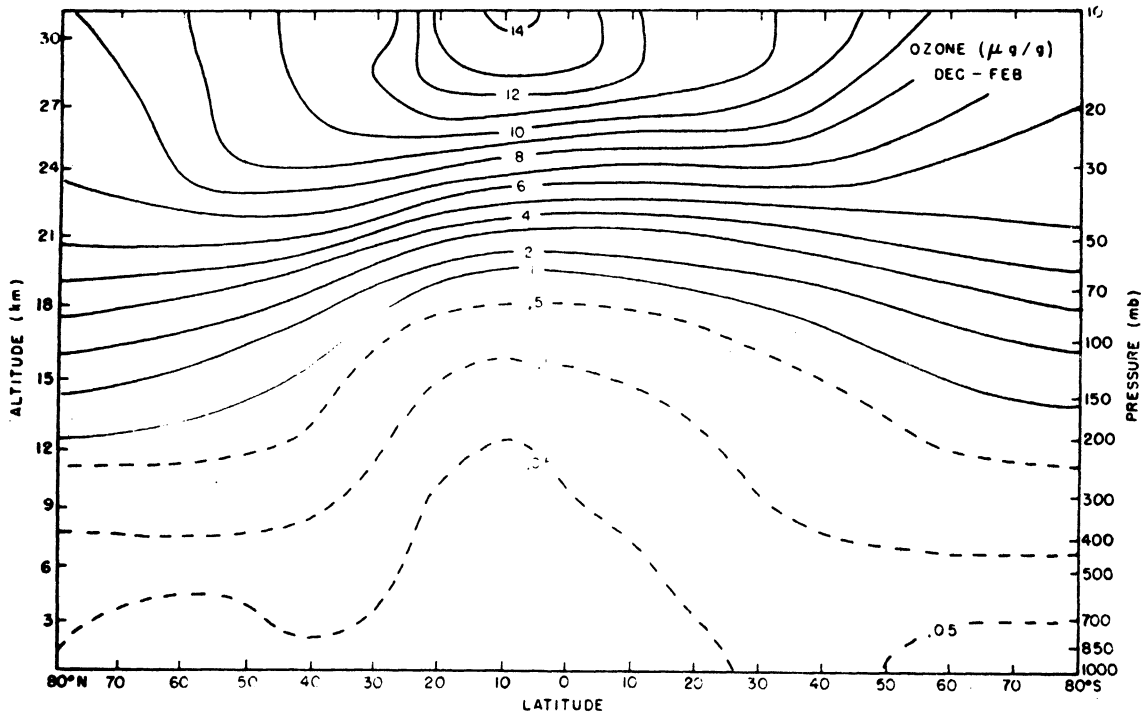

Fig. 2.1.3a Mean ozone (μg/gm for December-February. From Dopplick (1972).

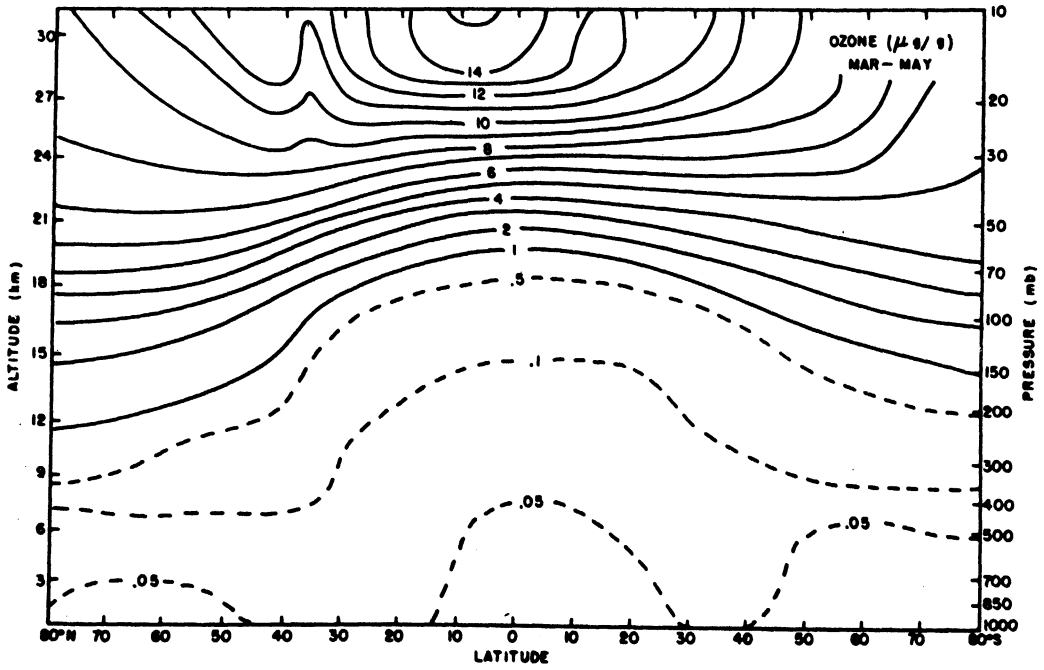

Fig. 2.1.3b Mean ozone (μm/gm) for March-May. From Dopplick (1970).

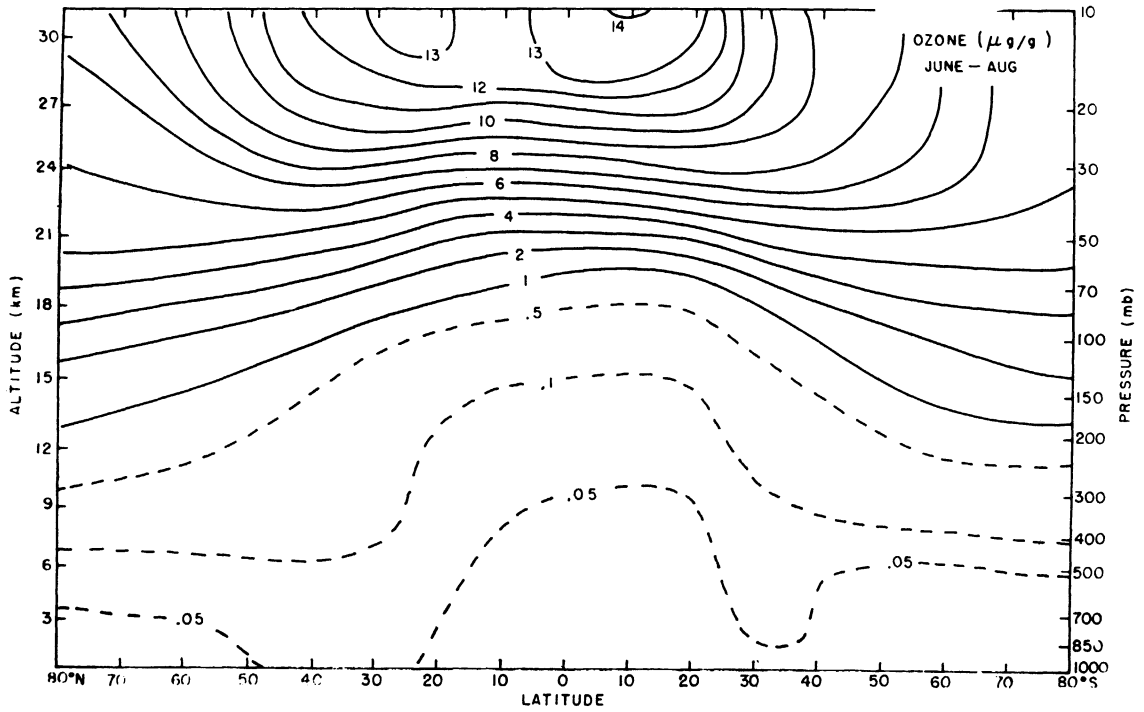

Fig. 2.1.3c Mean ozone (μg/gm) for June-August. From Dopplick (1972).

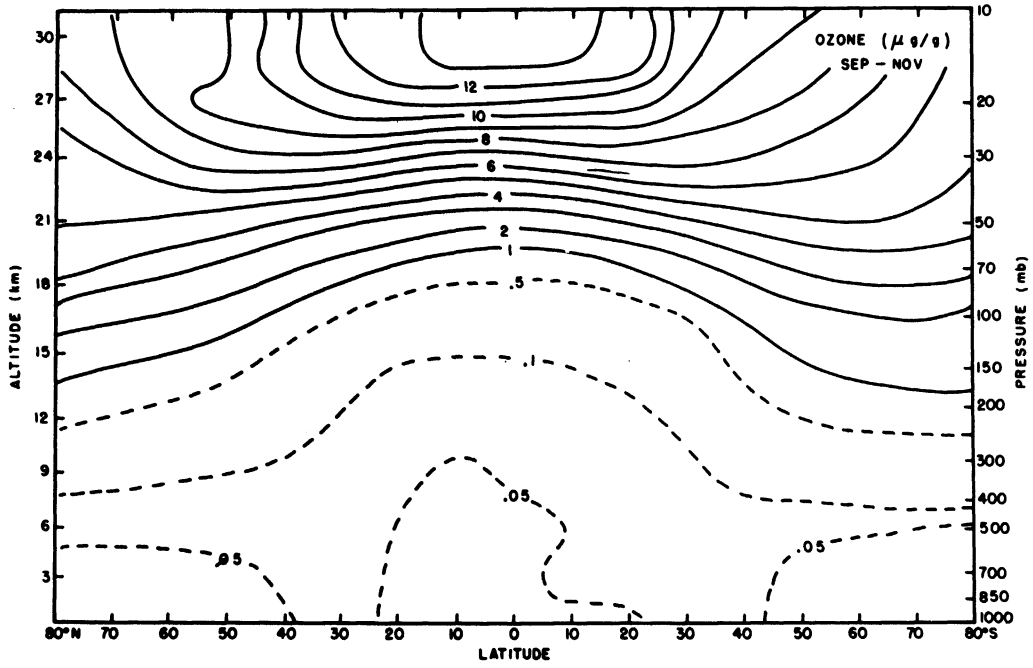

Fig. 2.1.3d Mean ozone (μg/gm) for September-November. From Dopplick (1970).

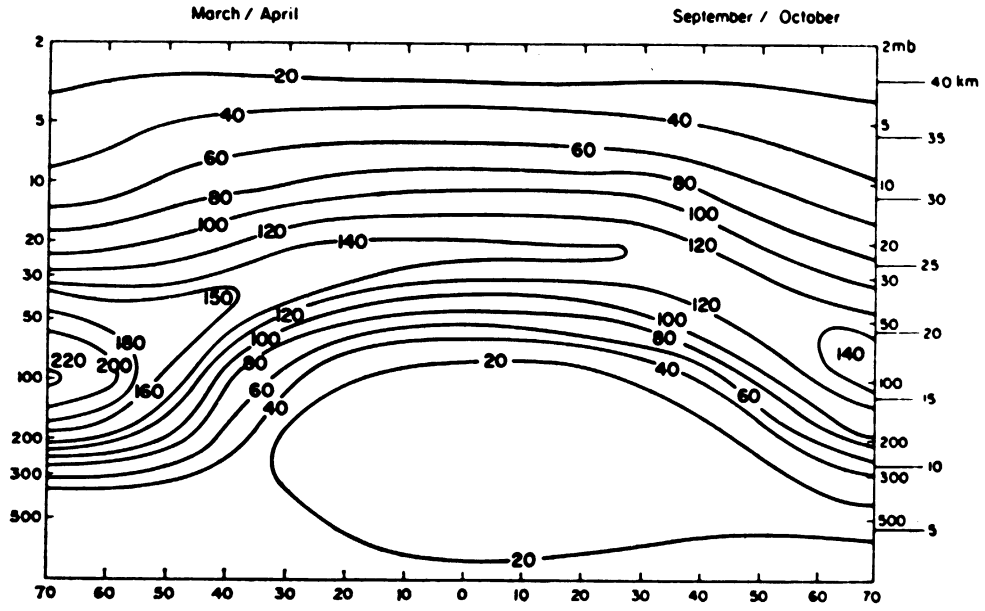

Fig. 2.1.4a Latitudinal cross section of vertical ozone distribution; early spring compared with early fall, northern hemisphere data. From Dutsch (1970).

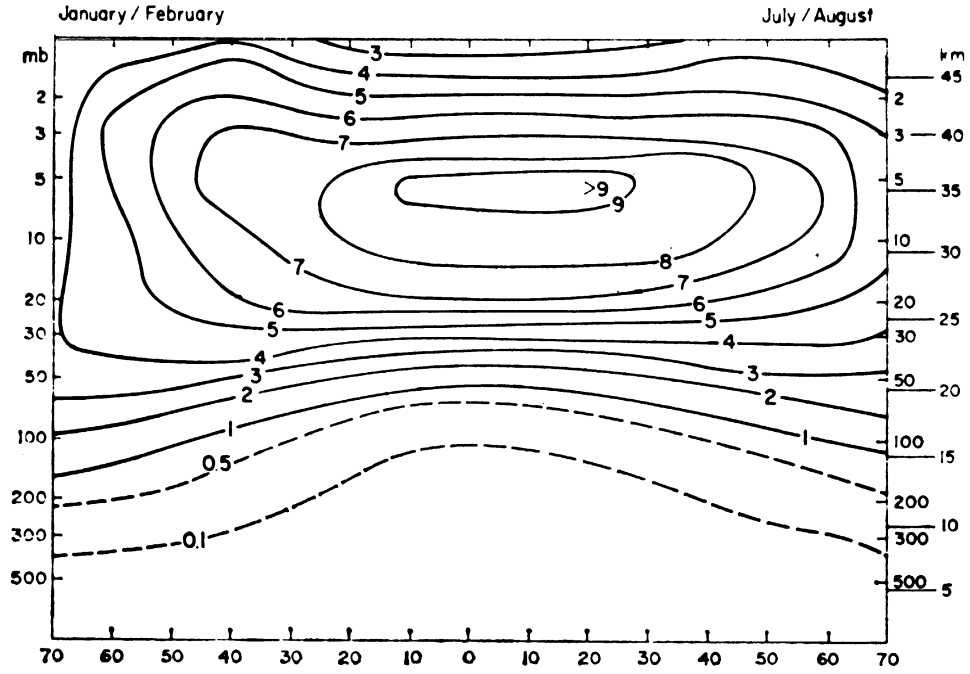

Fig. 2.1.4b Latitudinal cross section of the vertical distribution of ozone to air (number) mixing ratio; late winter compared with late summer, northern hemisphere data. From Dutsch (1970).

In the very low stratosphere, (see Fig. 2.1.4a), concentrations near the equator are less than near the poles, while in the mid stratosphere the equatorial regions have the larger concentrations of ozone, (e.g., Randhawa, 1971 has found an order of magnitude more ozone in the upper stratosphere near the equator than at the poles) with the maximum gradient occurring in the fall. In mid latitudes, the most rapid increase in concentration occurs near the ozone maximum, and is most prominent in February. The maximum increase in the low stratosphere occurs 1 to 2 months later, while the tropospheric maximum is not reached until summer (Dutsch, 1970).

The diurnal variation of ozone appears to be significant only in the mid and upper mesosphere. Hilsenrath (1971) has measured ozone by a chemiluminescent self pumping parachute sonde released from a rocket over Wallops Island in March, and he finds above 60 km the predawn ozone concentration is twice as large as is measured after sunrise. Similarly, Randhawa (1971) employed a rocket-borne ozonesonde and found a diurnal variation at 50 km of nearly a factor of 3 at the Panama Canal Zone (9^{o} 20'N) in November.

It is well known that at times the ozone profile is highly structured (see, e.g., Breiland 1967; Danielson, 1968), and a well developed secondary ozone maximum appears (see Fig. 2.1.5). This structure is thought to occur when high latitude stratospheric air is transported southward and into the low latitude troposphere. This ozone rich stratospheric air produces a lower elevation secondary ozone maximum; one also finds as would be expected, a secondary tropopause produced by the intrusion of the high latitude polar air. The smaller scale structure can be explained in a similar manner. Indeed Breiland has demonstrated that the gradient of ozone partial pressure is related to the vertical gradient of potential temperature, i.e., an increase in thermal stability leads to an increase in the vertical gradient of the partial pressure of ozone.

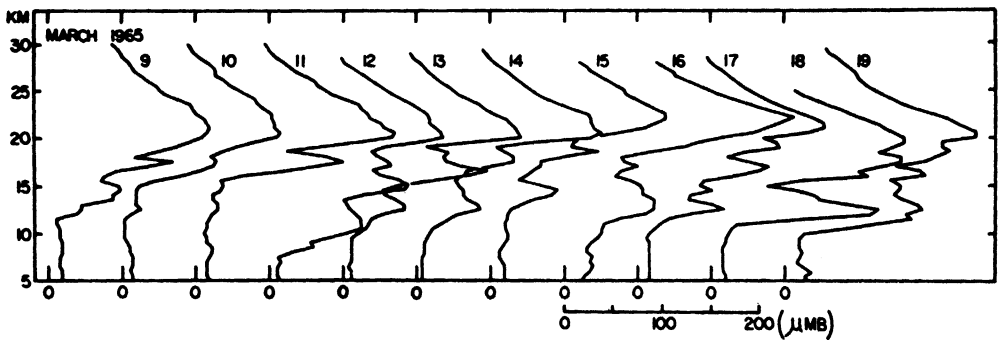

Fig. 2.1.5 Vertical distribution of atmospheric ozone (μmb) showing development of secondary maxima. From Breiland (1967).

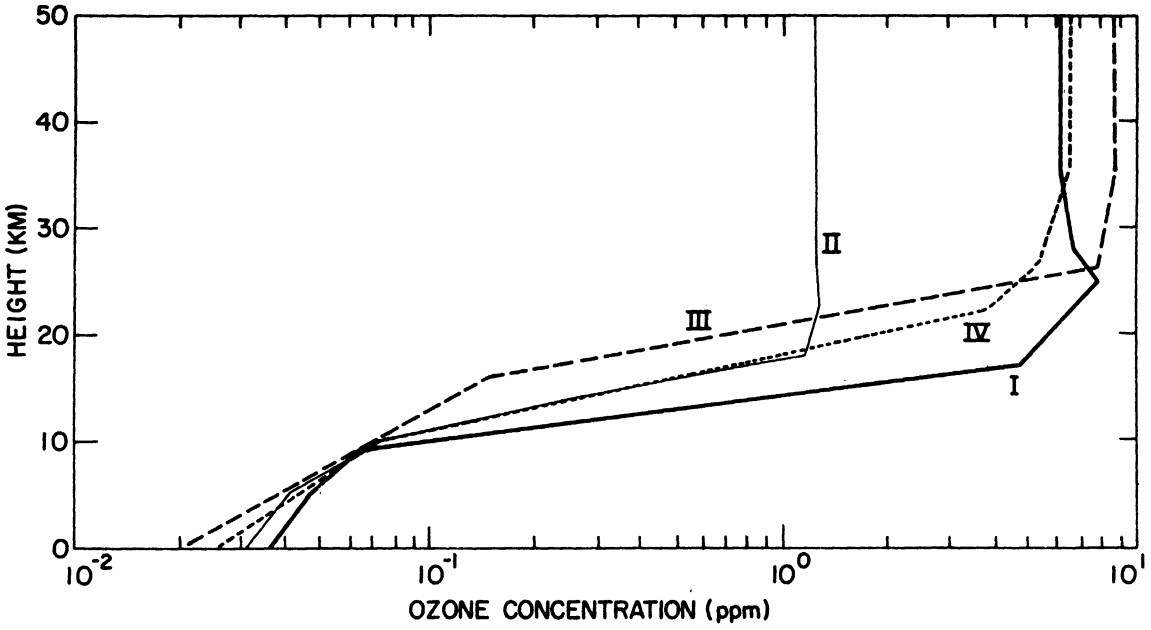

Fig. 2.1.6 Model ozone profiles used in estimates of stratospheric tangent mass paths.

Strong seasonal transitions in wind and temperature in the upper atmosphere do not seem to influence very much ozone concentration up to 50 km. Hilsenrath (1971) measured ozone mixing ratios at Pt. Barrow, Alaska during a winter to summer transition on January 30th and January 11th in 1969 for which the temperature on the 30th at 60 km was 50^{o}K lower than on the 11th, while the opposite was true at 40 km. The mixing ratios were essentially the same on both days between 30 and 50 km. Above 50 km, the ozone concentration increased by almost a factor of four.

The four representative ozone profiles to be used in this study are shown in Fig. 2.1.6. Profile I corresponds to a total ozone amount of 0.650 atm cm, and is representative of the maximum ozone amount one might find at high latitudes (from Mateer et. at., 1971). Profile II is from the same authors, and represents a high latitude minimum (0.170 atm cm), while Profile III illustrates large ozone concentrations above the ozone maximum (.300 atm cm). Profile IV corresponds to a typical mid-latitude distribution. Note that for any height, the extreme variations in the volumetric mixing ratios are about an order of magnitude.

2.1.2 Spectral properties of the ozone molecule (ir region)

Ozone is a triatomic molecule belonging to the symmetry group C_{2v}. The apex angle is $116^{o}45'$, and the bond lengths are approximately 1.26A in the ground state. The dipole moment has been determined from an analysis of the microwave spectrum, and is 0.150 debye. The fundamental vibrational modes have been identified, and occur at 1103 cm^{-1} (ν_1), 701 cm^{-1} (ν_2), and 1042 cm^{-1} (ν_3). Band strengths of the fundamentals as well as some of the overtone and combination bands have been measured by McCaa and Shaw (1967), and their results are reproduced in Table 2.1.1

Band (cm^{-1})	Strength (cm^{-2} atm^{-1})
1042(ν_3)	350.
1103(ν_1)	10.4
2110	32.
701(ν_2)	18.
1728	1.35
1792	.54
2779	.66
3042	3.0
3181	.33

Table 2.1.1: Band strengths for selected infrared bands of the ozone molecule. From McCaa and Shaw (1967)

Note that the ν_3 band is at least an order of magnitude stronger than the other bands which have been measured. The ν_3 band strength as determined by McCaa and Shaw is in reasonably good agreement with the earlier measurements of Walshaw (1954, 1957) whose data, if extrapolated to zero mass path, yield a value of 360 atm^{-1} cm^{-2}, while his empirical formula gives 376 atm^{-1} cm^{-2} To the authors' knowledge, there are no other measurements for the weaker bands which can be compared with those from McCaa and Shaw. Measurements are made difficult because of the highly reactive nature of ozone, and because large paths are required due to the small band strengths.

Theoretical studies of line strengths and positions of the infrared bands of ozone have dealt almost solely with the 9 micron region, primarily because of the importance of the ν_3 band to atmospheric radiation calculations. Early theoretical studies included those of Kaplan, Migeotte, and Neven (1956), who evaluated line strengths and positions for the spectral interval from 1052.66 to 1057.67 cm^{-1}, and compared their results with high resolution measurements

of the solar spectrum; good agreement was found up to rotational level seventeen. The more recent evaluation of Clough and Kneizys (1965) extended over the spectral region from 995 to 1070 cm^{-1}, and included the Coriolis effect as well as a second order distortion term. They indicate that their theoretical absorption contours are in satisfactory agreement with experimental absorption spectra taken over the interval from 1000 to 1150 cm^{-1}; the spectral resolution was 0.08 and 0.06 cm^{-1} for the ν_3 and ν_1 bands respectively. While these studies may be all right for energy budget calculations, it is doubtful if they are adequate for such applications as remote sensing. Indeed, Drayson and Young (1967) and Goldman et. al. (1970) have found large discrepancies between absorption contours calculated from theoretical parameters and observational results. Also, there has been little study of the half-width variation within the band; estimates for the mean half-width have been made by Kaplan (1959) and Walshaw (1955), who give values of 0.089 and 0.076 cm^{-1} (STP) respectively.

Recently, Aida (1971) presented a paper at the Symposium on Radiation held in Sendai, Japan, in which he calculated band parameters for the 9 micron region and found good agreement with experimental results. Much of the improvement which he found was apparently due to his inclusion of some of the weaker bands in this region. Any final conclusion concerning his results should await publication.

2.1.3 Results

The tangent path ozone amounts (atm cm) for profiles I through IV (see Fig. 2.1.6) are shown in Fig. 2.1.7. The method for computing these profiles is given in Appendix A. Profile III representing the maximum ozone

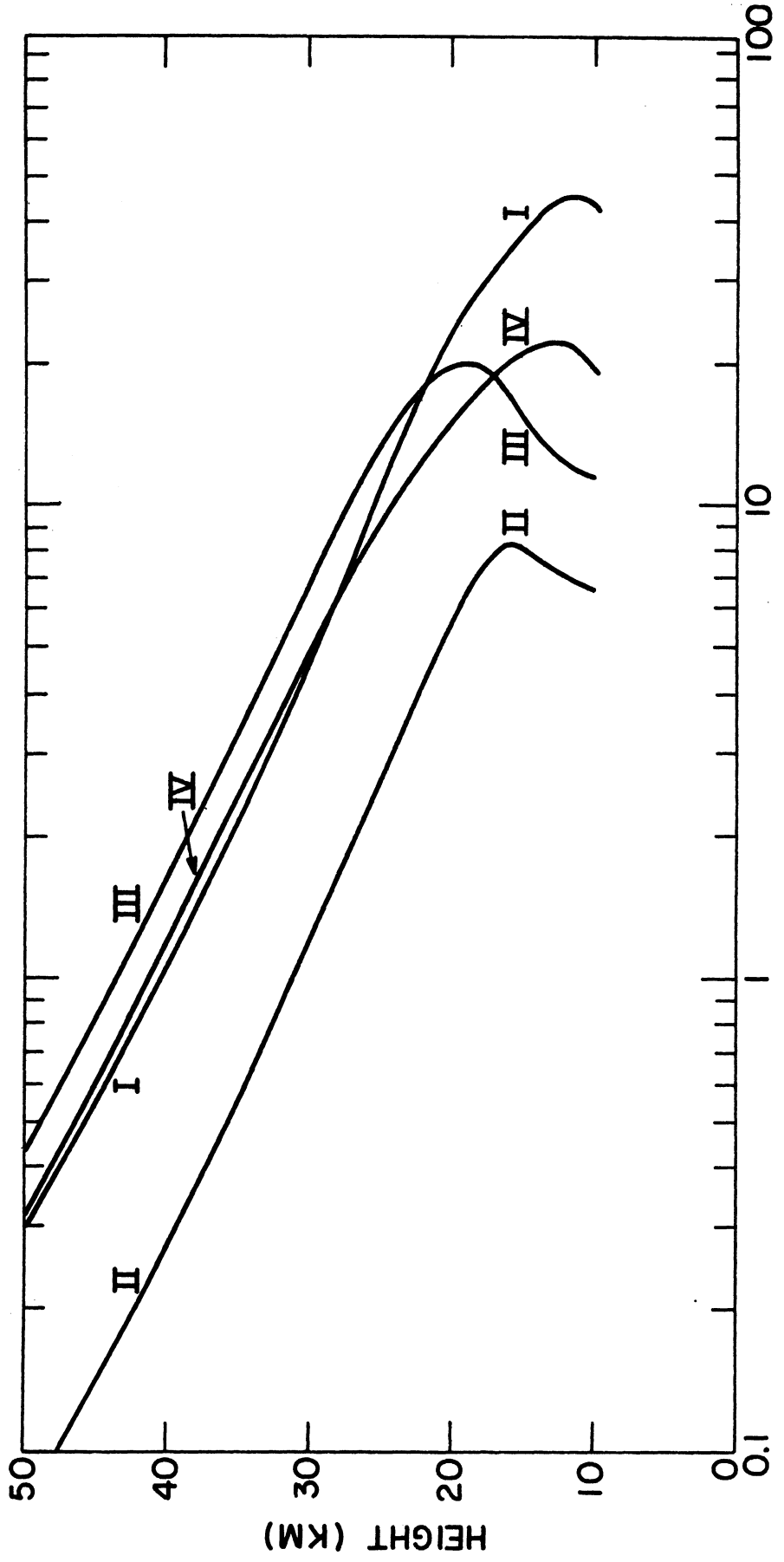

Fig. 2.1.7 Ozone tangent mass paths (atm-cm) based on model ozone profiles from Fig. 2.1.6.

amounts found in the mid and upper stratosphere and profile II for the high latitude minimum differ by approximately a factor of six for any given height; these two profiles are used in the following discussion.

The absorption contours given by McCaa and Shaw (1967) for the nine bands 701, 1042, 1103, 1728, 1792, 2110, 2779, 3042, and 3181 cm^{-1} have been used to estimate the absorption for profiles II and III in Fig. 2.1.7 and are summarized in Table 2.1.2. For each case, the maximum percent absorption shown on the contour has been used. One should bear in mind that these contours correspond to room temperature which differs significantly from the tangent path temperature. This varies from about 220 K near the tropopause to about 270 K at the stratopause. The temperature effect on the absorption becomes quite significant especially for transitions which do not involve the ground state. In addition, most of the stratospheric pressures and mass paths do not correspond to pressures and mass paths used by McCaa and Shaw; thus only a limited number of comparisons are possible. It is hoped that in future work we shall be able to carry out line by line calculations and produce high resolution absorption profiles which correspond to stratospheric pressures and mass paths as well as temperatures.

The ν_1 and ν_2 bands show similar absorptions as one might expect because of their similar strengths (see Table 2.1.1). At 16 km, e.g., both give a maximum absorption greater than 30-35% for Profile II. For Profile III, the maximum absorption has not fallen to the above value until a height of 24 km is reached. At this elevation, Profile II gives an absorption of 15% for the ν_1 band and somewhat larger for the ν_2 band.

Only for Profile III does one get significant absorption from the 1728 and 1792 cm^{-1} bands in the lower stratosphere. Profile II yields absorp-

tions of only 10 and 5% respectively for a height of 24 km. Also, even for the largest tangent paths represented by Profile III, maximum absorption from the 2779 and 3181 cm^{-1} bands is only 4 and 9% respectively at the 24 km height. Maximum absorption for the 3042 cm^{-1} band is somewhat larger, being 18% at 16 km and 10% at 24 km for Profile II; Profile III yields an absorption of 25% at 24 km.

Significant absorption is found for the 2110 cm^{-1} band well above the 24 km height, where the maximum absorption is 40 and 75% for Profiles II and III respectively; at 16 km, the absorption from II has increased to about 70%.

As one would expect, the greatest absorption is from the strong ν_3 band. The band center is effectively saturated at heights of 24 and 16 km for Profiles III and II respectively. Thus this band would produce measurable absorption well into the mid-stratosphere. Even for Profile II, the absorption is still 88% at the 24 km level.

Band (cm^{-1}) Height (km)	1042(ν_3)	1103(ν_1)	2110	701(ν_2)	1728	1792	2779	3042	3181
16 II	100	>30-35	70	>30-35				18	
24II	88	15	40	>15	10	5		10	
24III	100	30-35	75	30-35			4	25	9

Table 2.1.2: Maximum absorption (%) for Profiles II and III for selected ozone bands.

2.2 Water Vapor

2.2.1 Distribution

The significance of atmospheric water vapor to biological and atmospheric processes is well known. Water vapor is as important in sustaining biological activity as is oxygen. In addition water vapor is the most significant gas in maintaining the tropospheric temperature structure, not only through its gaseous absorption and emission properties of planetary and solar radiation but also in the liquid and solid state as clouds whereby much of the planetary radiation is prevented from escaping the earth, and also in shielding the earth from solar radiation. Water vapor is not as important in the stratosphere in maintaining the thermal structure although it has been determined that reactions of water vapor with ozone reduce the ozone concentration which, as indicated previously, shields the earth from harmful ultraviolet radiations. In addition, high flying aircraft may induce cloud formation which could alter the radiation balance of certain regions over the earth. Remote soundings of stratospheric water vapor would provide the continuous coverage necessary to monitor such possible effects.

Typically, water vapor concentrations are found to decrease exponentially in the troposphere. The source of most of this vapor is the oceans. The tropopause provides a barrier to vertical motions and most of the vapor is "trapped" in the troposphere, with stratospheric concentrations thought to be primarily controlled by the tropopause saturation vapor pressure. Total atmospheric water vapor averages about 2 precipitable cm with maxima (4 cm) and minima (<1 cm) over the equator and poles, respectively. Large longitudinal variations are also evident (Fig. 2.2.1) e.g., the yearly average water content over central South America is about three times larger than over

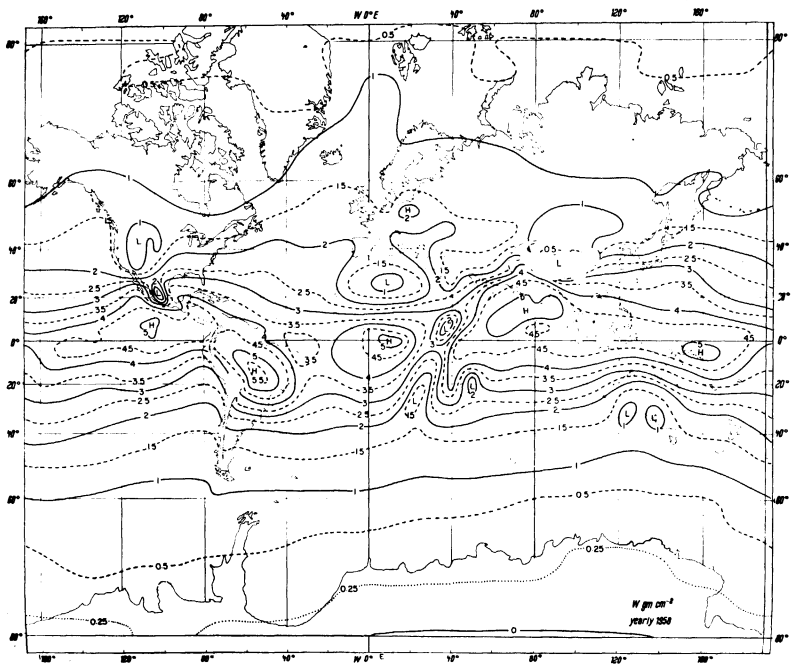

Fig. 2.2.1 Time average of the vertically integrated values of specific humidity (precipitable water) in units of gm/cm^2 for yearly data. Isoline spacing (full curves) 1 gm/cm^2. From Starr, Peixoto, and McKean, (1969).

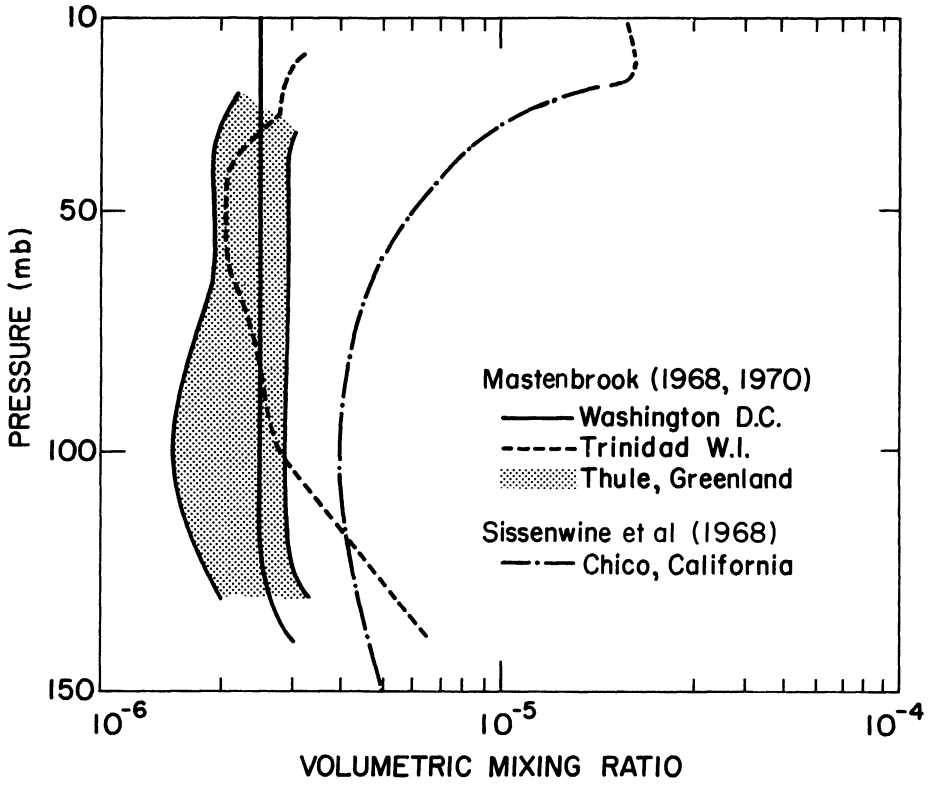

Fig. 2.2.2 Comparisons of lower stratospheric profiles for atmospheric water vapor.

south central Africa. The vertical distribution of water vapor and its variation with latitude, longitude, and season are now reasonably well known at least up to the mid troposphere (see, e. g., Taljaard, Van Loon, Crutcher and Jenne, 1969; and Crutcher and Van Loon, 1970) and we shall here only discuss those observations made in the stratosphere.

Early studies of stratospheric water vapor are somewhat suspect because of the high degree of instrumental sophistication required to measure such small amounts of water vapor. In addition, water vapor contamination from the instrument itself is a source of some uncertainty. Studies prior to 1961 have been carefully reviewed by Gutnick (1962)who called attention to "the widely divergent and apparently inexplicable stratospheric humidity data" e. g., the results of Japanese investigators indicated a much higher concentration (mixing ratio of 3×10^{-4} gm/gm) than those of the British group (4×10^{-5} gm/gm).

Gutnick (1962) also gives a mean annual vertical profile to 31 km, which as pointed out by Sissenwine, Grantham, and Salmala (1968) would give noctilucent clouds over most of the earth and water vapor partial pressures exceeding the total atmospheric pressure if his mean profile is extrapolated upward. More recent observations indicate smaller stratospheric concentrations; Houghton (1963) measured the absorption of solar radiation in the 6. 3μm region and found mixing ratios of 1.5×10^{-6} and 5×10^{-5} gm/gm in the low and mid stratosphere respectively. Williamson and Houghton (1965) measured the downward planetary radiation in the 6. 3μm band, and found a similar value for the lower stratosphere (3×10^{-6} gm/gm).

Recently there have been a number of studies of stratospheric water vapor over particular regions, the most extensive being that of Mastenbrook (1968, 1971) over Washington, D. C. during the 6 year period from 1964-1969. These measurements were made from descent balloon soundings with a frost point hygrometer. The median of Mastenbrook's values is plotted in Fig. 2. 2. 2.

The volumetric mixing ratio varies from 1 to 4 ppm between 40 and 80 mb, with a mode of 2.5 ppm. At higher and lower elevations the mode is also 2.5 but the distributions are skewed toward higher concentrations which is thought due to water vapor contamination from the instrument at the higher levels, and at lower levels the increase is probably due to the close proximity to the tropopause.

Three soundings were also made at Thule, Greenland (Mastenbrook, 1968) in July and August 1965 and stratospheric mixing ratios were not much different from those found in lower latitudes, being about 1.5 to 3.5 x 10^{-6} gm/gm (Fig. 2.2.2). Measurements at Trinidad during 1964-1965 also by Mastenbrook (1968) gave the same results as for Washington, D. C. for the 50-60 mb range but were larger at lower elevations than the Washington, D. C. results (Fig. 2.2.2).

Also plotted in Fig. 2.2.2 is a mid latitude yearly average humidity profile for Chico California (Sissenwine et. al. (1968)). This profile is the result of seventeen observations made from a balloon carrying an alpha radiation hygrometer. The dashed portion of the curve is the result of only one sounding. As in the case of Mastenbrook's profiles, the humidity reaches a minimum near the tropopause, but then shows a slight maximum near 25 mb with a gradual decrease upward. Thus in the vicinity of 25 mb, Sissenwine et. al.'s profile yields almost an order of magnitude more water vapor than does that of Mastenbrook. Sissenwine et. al. speculate that tropospheric water vapor may pass into the stratosphere in mid latitudes when multiple tropopauses are present, and also that ice crystals from convective clouds which penetrate the stratosphere over continental mid latitude regions in summer could vaporize

and produce a high water vapor content. It is however, interesting that Mastenbrook does not find such large stratospheric values over any of the three sites used for his measurements.

The only direct measurements of water vapor near the stratopause are those of Scholz, Ehhalt, Heidt, and Martell (1970) who used a hydrogen cooled cryocondenser carried on a rocket. Measurements were made at White Sands in September, 1968 in the height range of 44-62 km. The volumetric mixing ratio was found to be within the range of 3 to 10 ppm.

An annual cycle in stratospheric water vapor has been detected by Mastenbrook (1971)[1] as well as a linear increase over a 6 year period of about 1 ppm. It can be seen from Fig. 2.2.3. that the annual cycle is present at least to 100 mb with the amplitude being greatest (50 ppm) at the 300 mb level and decreasing with decreasing pressure. At the 100 mb level the amplitude is only about 0.5 ppm and less than 0.2 ppm above 80 mb. There is also some indication of a phase shift; in the upper troposphere, the maximum water vapor content occurs in summer, while at 80 mb the maximum is in winter.

The only latitudinal study of stratospheric water vapor is that of McKinnon and Morewood (1970) who measured solar absorption in the ν_1 and ν_3 bands (2.59μ). These spectra were obtained from jet aircraft from April 1967 through May 1968 over North and South America (70N to 40S) in the height range of 10.7 to 18.3 km. At all latitudes, concentrations of water vapor were found to reach a minimum about 2 km above the tropopause and then remain nearly constant to 18.3 km. A large seasonal variation was

---

[1]Sissenwine et. al. (1968) point out that their data appear to show an annual cycle but harmonic analysis did not show these cycles to be statistically significant.

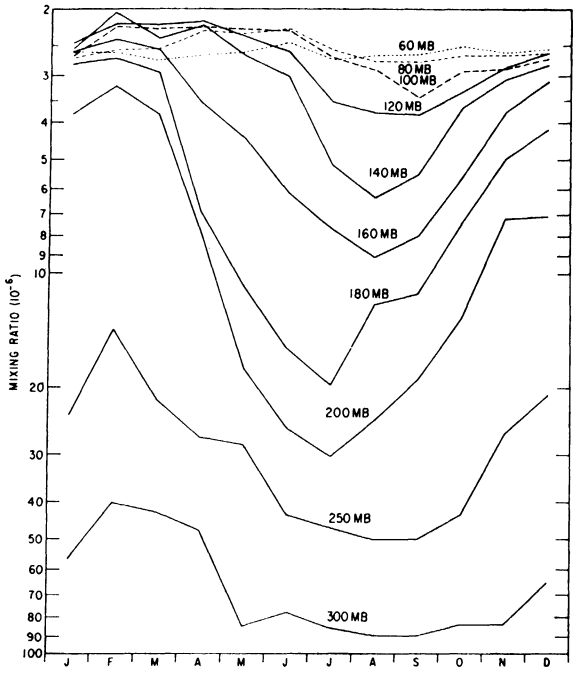

Fig. 2. 2. 3 Seasonal variability of mixing ratio for selected pressure levels as determined from three-month running medians. From Mastenbrook (1971).

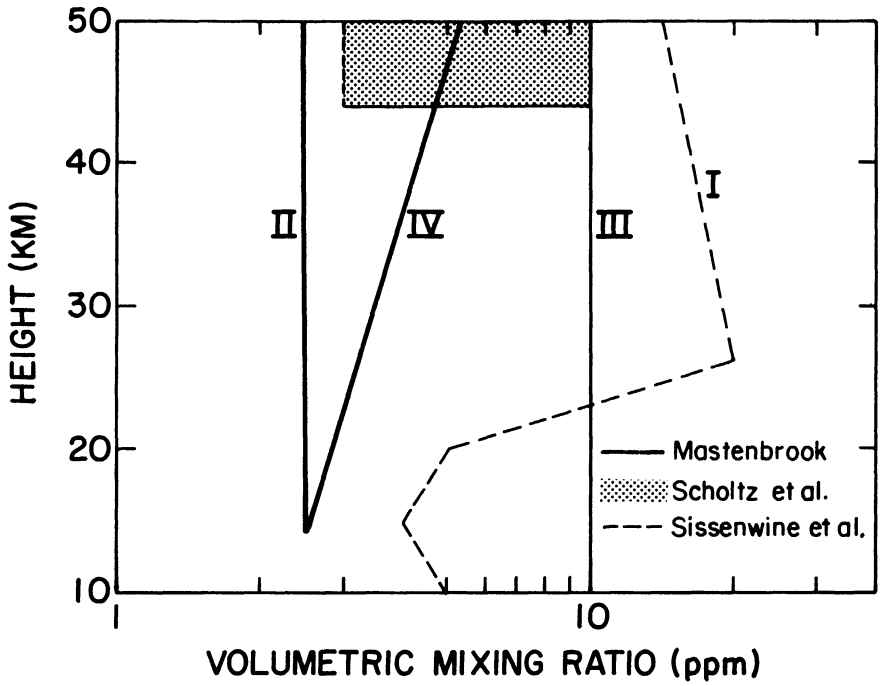

Fig. 2. 2. 4 Model water vapor profiles used in estimates of stratospheric tangent mass paths.

detected below the tropopause, the mixing ratios being four to eight times larger in summer than in winter; stratospheric variations were only a few percent. The latitudinal variation in mixing ratio above 17.7 km obtained during January-March is rather small, representative values being 1.75×10^{-6} gm/gm at 65N, 1.45×10^{-6} at 25N, 1.6×10^{-6} at 7N, and 1.25×10^{-6} at 30S. It is interesting to note that the minimum concentration does not occur over the equator, as one would expect if the equatorial tropopause were the only controlling region for stratospheric water vapor.

Water vapor profiles which were chosen for the tangent path calculations are shown in Fig. 2.2.4. The extreme distributions are represented by Sissenwine et. al.'s (1968) results and those of Mastenbrook (1971). Note that the variation is slightly less than an order of magnitude.

2.2.2 Infrared spectral properties

There have probably been more studies, both theoretical and experimental, devoted to the spectral characteristics of water vapor than any other nonlinear triatomic molecule. H_2O belongs to the point group C_{2v} and has three fundamental vibrational bands, ν_1 and ν_3, with band centers at 3657.05 and 3755.92 cm^{-1} respectively, and the strong bending mode ν_2, located at 1594.78 cm^{-1}. In addition, there is the strong pure rotational band centered about 125 cm^{-1} (band strength $\sim$ 1440 cm^{-2} atm^{-1}). The most abundant isotope (99.73%) is H_2O^{16}, which has a dipole moment of 1.87 debye.

In addition to the fundamentals, there are important water vapor bands throughout the visible and infrared spectrum, and because of the quite different moments of inertia, the rotational structure of these bands is very complex. The strengths of many of these bands are given in Table 2.2.1.

Transition	Band Center (cm^{-1})	Strength ($cm^{-2}atm^{-1}$)
000-100 (ν_1)	3757.05	11.2
000-010 (ν_2)	1594.78	223.
000-001 (ν_3)	3755.92	167.
000-411	18394	.0005
000-203	17495	.003
000-401	16899	.008
000-302	16898	.0008
000-321	16822	.005
000-113	15832	.0005
000-311	15348	.005
000-103	14319	.03
000-400	14221	.003
000-301	13831	.08
000-202	13828	< .0005
000-221	13653	.2
000-013	12565	.003
000-112	12408	.2
000-211	12151	.002
000-210	12140	.003
000-131	11813	.05
000-003	11032	.05
000-102	10869	.01
000-201	10613	.3
000-300	10600	.02
000-121	10329	.05
000-220	10284	.001
000-041	9834	.002
000-012	9000	.008
000-121	8807	.21
000-210	8762	.0003
000-130	8274	.0002
000-031	8374	.0008
000-002	7445	.03
000-101	7250	40.0
000-200	7201	.40
000-021	6871	.3
000-120	6775	.005
000-011	5331	5.9
000-110	5235	.2
000-030	4667	.008

Table 2.2.1: Band intensities for visible and infrared water vapor bands (from Goody, 1964; intensities given by Goody are in cm)

There is still much uncertainty regarding the strengths of many of these weaker bands; indeed, even for the strong ν_2 band, Penner (1959) gives a value some ten percent smaller than that reported by Goody. Note that the above listings all involve transitions with the ground state and will thus not be strongly temperature dependent. Upper state bands depend critically on temperature, and are not included in the above listing.

There have been numerous low and medium resolution measurements of water vapor, notable being those of Palmer (1960) for the rotational band, and Burch, Gryvnak, Singleton, France and Williams (1962) for the fundamentals as well as the Ω bands (000-011 and 000-110). Palmer examined the spectral region from 200 to 500 cm^{-1} and expressed the transmission as averages over 50 cm^{-1} intervals. Burch et. al. present graphs of total band absorptance vs. either mass path or pressure, as well as representative absorption curves. The more recent high resolution work includes that of Babrov (1967) and Fridovich and Kinard (1972) (for earlier work, see Goody, 1964). Babrov analyzed 12 lines in the ν_1 and 30 lines in the ν_3 band by a curve of growth method, while Fridovich and Kinard determined intensities of 7 lines in the ν_2 band, and compared their results with other investigators. They found, for example, the line strength at 1429.96 cm^{-1} to be 981 cm/gm, while Prinz (1968) gives 725, and Krakow and Healy (1969) give1116 cm/gm. These results indicate that while H_2O has been extensively investigated, there is still need for improvement in the band parameters; Goldman and Kyle (1968) reach the same conclusion from an investigation of the 2.7μm band for averages over intervals smaller than about 10 cm^{-1}.

The most detailed compilation of band parameters (line positions, strengths and half-widths) is that of Benedict (unpublished), Benedict and Calfee (1967) and Gates, Calfee, Hansen, and Benedict (1964). Calculations

for 6100 lines extend over the spectral range from 0.74 to 4444 cm^{-1}. The bands included are the fundamentals, $2\nu_2$, $3\nu_2$, $\nu_2\nu_3$, $\nu_1\nu_2$, as well as the hot bands 021-010, 100-010, 020-010, 001-010, 030-010, 011-010, and 110-010. The isotopes H_2O^{17} and H_2O^{18} are included along with HDO. Results are presented in a form such that strengths corresponding to different temperatures can be computed. Half-widths are based on the earlier results of Benedict and Kaplan (1964, 1959), who used Anderson's theory to calculate the widths of many pure rotational transitions for both self broadened H_2O, and H_2O broadened by nitrogen and oxygen. They found large variations from line to line in both absolute value as well as in the ratio of self to nitrogen broadening. Also there is a good correlation between nitrogen and oxygen broadening. An intensity weighted mean half width for oxygen broadening is 0.04155 (STP) and for nitrogen broadening 0.08767 cm^{-1}. To the author's knowledge, there are no comparable studies for the visible water vapor bands.

It should be obvious that we have not attempted to review all, or even most of those papers which have made significant contributions to the spectral properties of water vapor, but only those which relate directly to the present work.

2.2.3 Preliminary results for the infrared water vapor bands

Tangent path water vapor amounts for the profiles of Fig. 2.2.4 are given in Fig. 2.2.5. The profile of Sissenwine et. al. (1968) gives the largest tangent paths above the height of 20 km, being some 40 atm cm at 20 km and decreasing to 0.65 atm cm at the stratopause. The minimum distribution shown is that of Mastenbrook (1970), and is about a factor of six less than that of Sissenwine et. al. These two profiles, I and II, will be used in the following analysis.

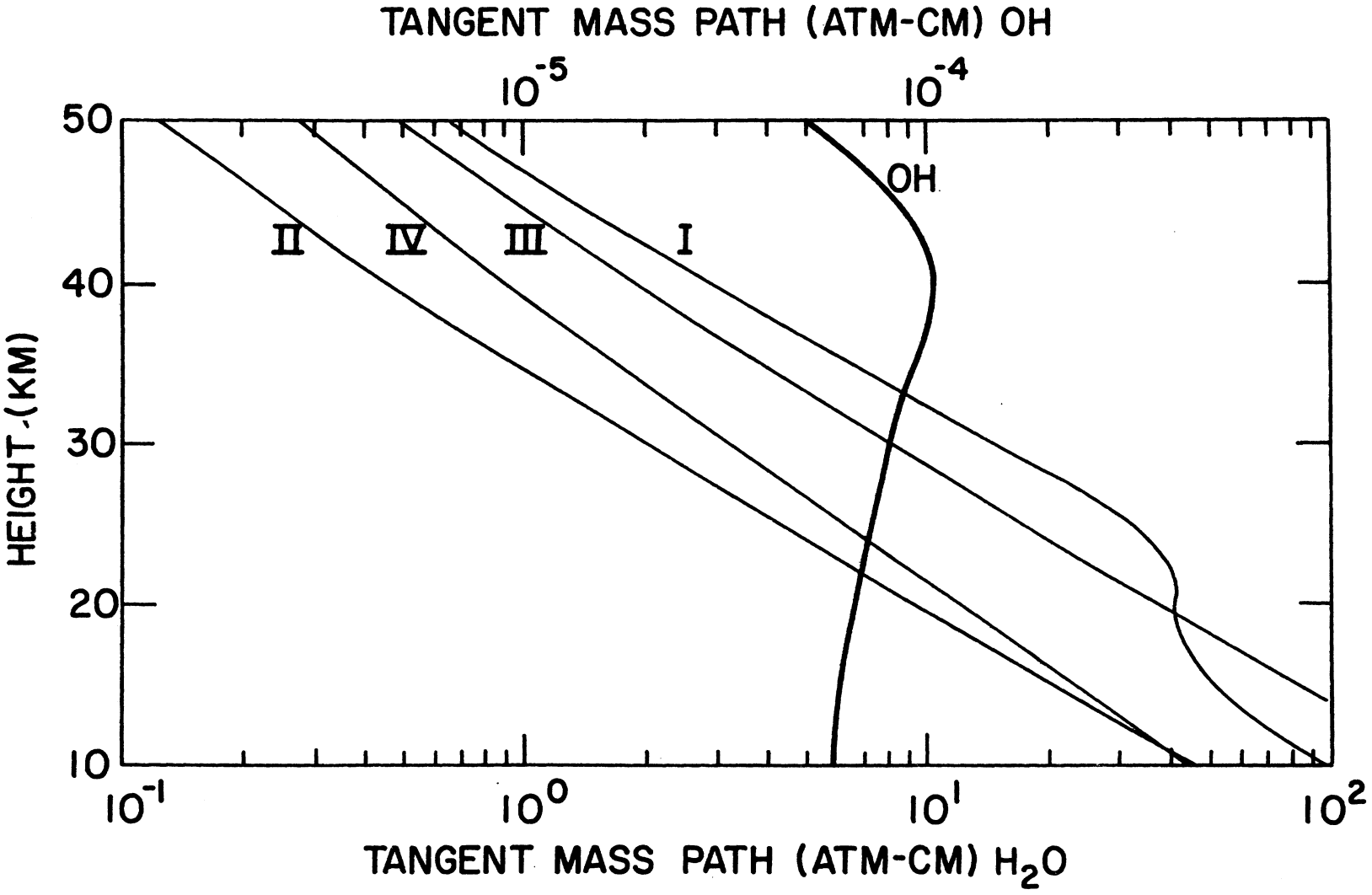

Fig. 2.2.5 Water vapor and hydroxyl tangent mass paths (atm-cm) based on model water vapor profiles from Fig. 2.2.4 and hydroxyl profile from Fig. 2.3.1.

An estimate of water vapor absorption at various heights for Profiles I and II was made for the bands at 1595 (ν_2), 5332 (the Ω bands), and the ν_3 band at 3755 cm^{-1}. These bands were chosen since absorption contours are readily available from Burch, Gryvnak, Singleton, France, and Williams (1962). As was the case for the ozone profiles the maximum percent absorption from each profile was used. Unfortunately, their choice of pressure and mass path do not, in general, coincide with our tangent path pressures and mass paths, so that only a very approximate maximum absorption estimate is possible. As in the case of the ozone results, the water vapor contours also apply to room temperature, while our tangent path stratospheric temperatures are much lower.

For Profile I, corresponding to maximum water vapor, the 5332 cm^{-1} band gives appreciable absorption at least to 19 km, but certainly not to 38 km. For example, at 19 km, the tangent path pressure is 36. 7 mb while the path is 41 atm cm. From Burch et. al 's absorption profile, for a pressure of 36 mb, and a mass path of only 4. 12 atm cm, the maximum absorption is about 5%. On the other hand, at 38 km, the tangent mass path is about 4 atm cm, but the pressure is only 2. 7 mb, which would make the tangent path absorption much less than 5% at this elevation. A comparison for the 14 km height (pressure of 77 mb and mass path 56 atm-cm as opposed to Burch et al's contour for a pressure and mass path of 66 mb and 58 atm-cm respectively) indicates that the absorption is 27%, while at the tropopause, it is somewhat less than 55%. For Profile II, the 5332 cm^{-1} band will have a small absorption above about 20 km; at this elevation the tangent pressure and mass path are about 36. 7 mb and 9. 5 atm cm respectively, and as indicated above, for this same pressure but 4.12 atm cm, the maximum absorption is only 5%.

The same reasoning can be applied to the 3700 cm^{-1} band as was done above for the 5332 cm^{-1} band, except that the 3700 cm^{-1} band is stronger and will have appreciable absorption above 19 km, but certainly not extending to 38 km. For Profile II, e. g., rather than an absorption of 5% for a pressure of 36 mb and a mass path of 4. 12 atm cm, the maximum absorption is 20%.

An analysis for the ν_2 band cannot be made above a height of 25 km, since here the tangent pressure is 18 mb, representing the smallest pressures used by Burch et. al. along with a mass path of 2. 12 atm cm; these parameters yield a maximum absorption of 12%; however the mass path associated with the 25 km level is about 33 atm cm for Profile I and 4. 3 atm cm for Profile II. Thus there will be significant absorption for both profiles at least to 25 km. The absorption is certainly very small at the 42 km height, since here the tangent path for Profile I is 2. 12 atm cm, the same as Burch et. al., but the pressure is only 1. 6 mb; thus the maximum absorption would be much less than 12%. At 17 km, for Profile I, the maximum absorption is about 65% for a pressure of 50 mb and mass path of 45 atm cm (Burch et al's contour is for a pressure and mass path of 50 mb and 44 atm cm respectively). Profile II, at 19 km, yields an absorption of 35 % for a pressure of 45 mb and 11 atm cm while Burch et al's contour has values of 45 mb and 10. 1 atm cm.

2.3 Hydroxyl Radical

2.3.1 Distribution

The hydroxyl radical is significant in the stratosphere, primarily because of its influence on concentrations of other minor constituents. Much of the literature is concerned with carbon monoxide (primarily troposphere) and ozone (stratosphere and mesosphere), for which the hydroxyl is an important controlling mechanism, and relatively few papers are available which give explicit estimates of hydroxyl concentrations. These are theoretical or model studies; the authors are unaware of any observational results for the troposphere and mid stratosphere.

Tropospheric models for which estimates of hydroxyl concentrations were calculated are those of Levy (1971); McConnell, McElroy and Wofsy (1971) and Weinstock and Niki (1971). They find tropospheric concentrations of approximately $2 \times 10^{6}/cm^{3}$ (see Fig. 2.3.1). Levy constructed a steady state model for large radical and formaldehyde concentrations for which the hydroxyl concentration can be estimated at $1.2 \times 10^{6}/cm^{3}$. Both McConnell et. al., and Weinstock and Niki were primarily concerned with the sources and removal mechanisms for carbon monoxide, the former showing that an important source for carbon monoxide below 30 km is the reaction, $OH + CH_4 \rightarrow H_2O + CH_3$, while the latter demonstrated that the major removal mechanism is $CO + OH \rightarrow CO_2 + H$. Weinstock and Niki find that the average concentration of hydroxyl in the troposphere required to maintain a carbon monoxide balance is 2.3×10^{6} molecules/cm^{3}, with daylight values being approximately twice as large. McConnell et. al. present a vertical profile, with a hydroxyl concentration of $3 \times 10^{6}/cm^{3}$ up to 5 km and then decreasing to about about $9 \times 10^{5}/cm^{3}$ at about 12 km. One should keep in mind that the

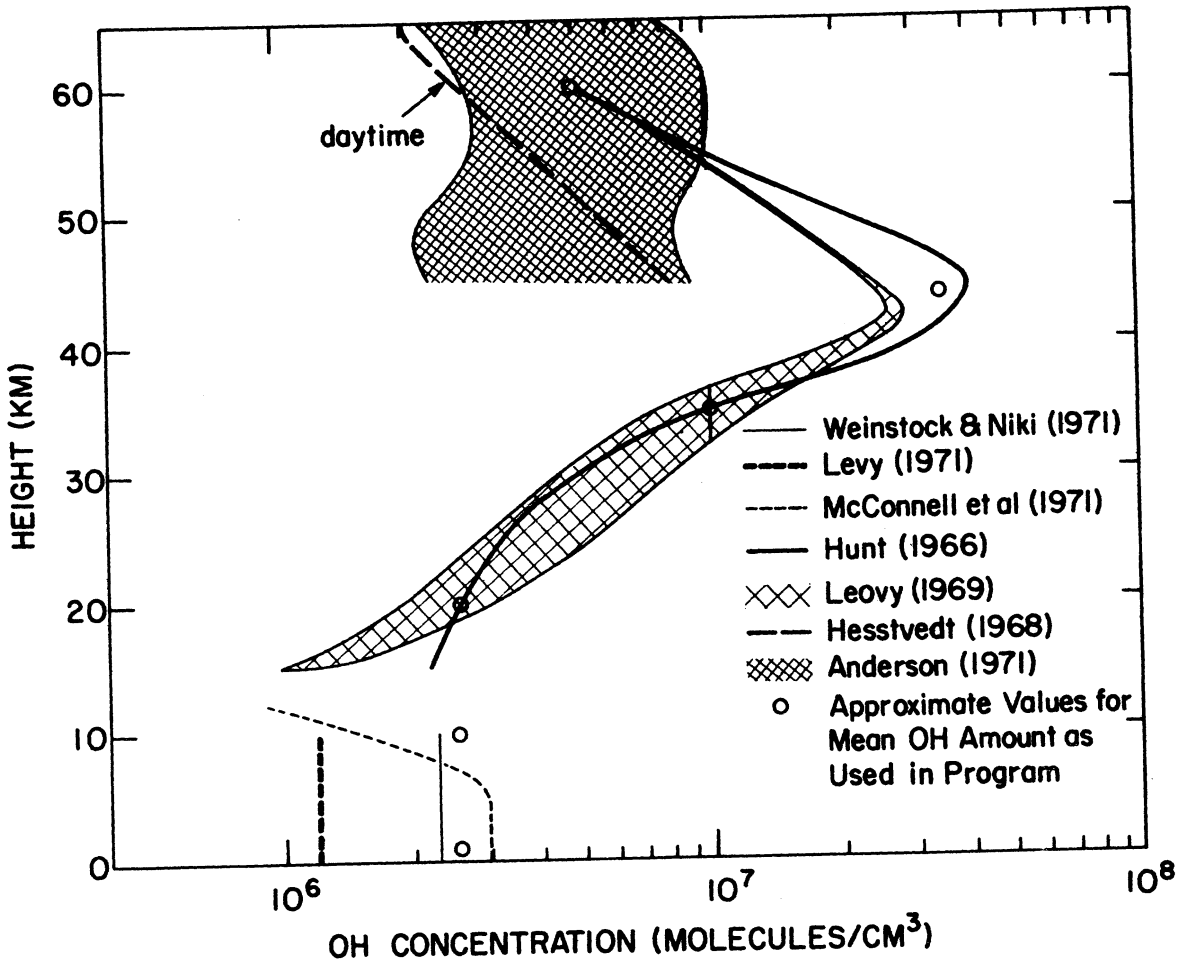

Fig. 2.3.1 Comparisons of hydroxyl distributions in the troposphere and stratosphere.

hydroxyl concentration depends on the assumed ozone and water vapor concentrations. In constructing their height profile, McConnell et. al. used a typical mid latitude ozone distribution, a stratospheric water vapor concentration of 3×10^{-6} by volume, and tropospheric water vapor densities equal to half the dew point values.

Numerous photochemical studies for an "oxygen-hydrogen atmosphere" have been made (see, e. g., Hunt (1966)) and the significance of the hydrogen-oxygen compounds in reducing the ozone amount to values smaller than given by the pure oxygen atmosphere is well known. In such a study the hydroxyl radical is an important constituent and its variation with height has been estimated by Leovy (1969), who developed an analytic model for the photochemistry to a height of 60 km (see Fig. 2. 3. 1). The earlier, more detailed study of Hunt (1966) is also given. The shaded ragion refers to uncertainty due to the different ways of treating the H_2O_2 reactions. The maximum hydroxyl concentration occurs at a height of about 40 km with a value of $2\text{-}3 \times 10^7/cm^3$. These results should only be viewed as very approximate since it was pointed out (see discussion, Leovy, 1969) that the reaction, $CO + OH \rightarrow CO_2 + H$, was not included in Leovy's treatment of the problem. Results for hydroxyl for Hesstvedt's (1968) oxygen-hydrogen model are also shown in Fig. 2. 3. 1. His results only extended to 45 km since he was primarily concerned with the mesosphere and lower thermosphere. His concentration is nearly two orders of magnitude larger during the daytime than at night. It should also be indicated that the calculations presented in Fig. 2. 3. 1 do not include vertical eddy transport, which is quite significant.

The theoretical studies shown in Fig. 2. 3. 1 are in reasonable agreement near the stratopause with the experimental results of Anderson (1971)

who made rocket-borne observations of an electronic transition in the hydroxyl molecule, and computed number densities in the height range of 45 to 70 km. The shaded area indicates the range of uncertainty. There appears to be no other measurements for hydroxyl concentrations in the stratosphere.

2.3.2 Spectral Properties

The spectral properties of the hydroxyl radical have been extensively studied primarily because of its importance to the airglow emission especially in the spectral region of 6700 to 8900 A at heights near the mesopause level (for a review, see Wallace, 1969 or Chamberlain 1961). The upper vibrational levels are very important to studies of this emission, and consequently much of the work has been devoted to the band constants of these excited vibrational states. These states are probably not very significant to the present study, since in the stratosphere the population densities of these levels should be given by the Boltzmann distribution and the band intensities and therefore the absorption should be small.

Band constants for the lower vibrational levels have been determined from laboratory measurements by Dieke and Crosswhite (1948) and Herman and Hornbeck (1953). The former analyzed vibrational levels up to $v=4$ from high resolution data for the $A^2\Sigma - X^2\Pi$ bands, while the latter studied the emission spectra from the 4-0, 5-1, and 6-2 bands, and give band constants up to $v=7$. This work was further extended by Wallace (1960) who obtained the parameters for vibrational levels 7, 8, and 9, and Bass and Garvin (1962) for the levels 7 through 10; in this latter study, ground state wavenumbers for rotational lines in 26 bands in the visible and near infrared are given. Recently, Engleman (1972) has more accurately determined rotational

wavenumbers of the $A^2\Sigma - X^2\Pi$ (0-0) amd (1-0) bands. In the present study, we shall use the compilation of rotational line positions and relative intensities given by Chamberlain (1961). He includes the first 7 rotational levels for each of the vibrational transitions through v=9. Relative intensities have been calculated for a temperature of 225K.

Intensities of a few of the hydroxyl bands are given in Table 2. 3. 1. The 0-1 vibrational transition is much larger than the overtones or upper level transitions for a Boltzmann distribution of energy states. For comparison, we have included the band strength of the electronic transition $^2\Sigma - ^2\Pi$.

Transition (cm^{-1})	Band strength ($cm^{-2}atm^{-1}$)
3568 (0-1)	100
6971 (0-2)	4
3400 (1-2)	$3. \times 10^{-9}$
$32600\ ^2\Sigma - ^2\Pi$	29000.

Table 2. 3. 1: Band strengths ($cm^{-2}atm^{-1}$) for selected transitions in the hydroxyl molecule. From Penner (1959)

---

2. 3. 3 Preliminary results

Since the ground configuration of the hydroxyl radical gives a $^2\Pi$ state, the vibrational-rotational bands will have strong Q branches, and for the 0-1 transition, Chamberlain (1961) estimates that 0. 268 of the total band strength resides in this branch. If one assumes a band strength of 100 $cm^{-2}atm^{-1}$, and a spectral resolution δ of 5 cm^{-1}, then the absorption for a mass path u can be estimated from the parameter Su/δ . From our

approximate hydroxyl distribution (see Fig. 2.3.1) the tangent paths have been calculated and are shown in Fig. 2.2.5. Note that because the volumetric mixing ratio of OH increases, there is not a large variation in the stratospheric tangent path. If we assume a tangent path of 10^{-4} atm cm, then the above parameter has a value of approximately 5×10^{-4}. The fractional absorption can then be estimated from the weak line approximation and is about 0.05%. In order to obtain an absorption of 10%, a resolution of 0.03 cm^{-1} would be required. Thus it appears doubtful that one could measure hydroxyl concentrations in the stratosphere utilizing the vibrational bands. Possibly above the ozone layer the electronic bands could be used; this will be investigated in future studies.

References

Ozone

Breiland, J. G., (1967), Comparison of the Vertical Distribution of Thermal Stability in the Lower Stratosphere with the Vertical Distribution of Atmospheric Ozone. J. Atmos. Sci., 24, 569-576.

Clough, S. A., and F. X. Kneizys, (1965), Ozone Absorption in the 9.0 Micron Region. AFCRL Rep. No. 65-862 or Physical Sciences Research Paper No. 170, 79 pp.

Craig, R. A., (1965), The Upper Atmosphere, Meteorology and Physics. Academic Press, New York. 509 pp.

Danielsen, E. F., (1968), Stratospheric-tropospheric Exchange Based on Radioactivity, Ozone, and Potential Vorticity. J. Atmos. Sci., 25, 502-518.

Dopplick, T. G., (1970), Global Radiative Heating of the Earth's Atmosphere. MIT Rep. No. 24, Dept. of Meteorology, Planetary Circulations Project, 128pp.

Drayson, S. R. and C. Young, (1967), Private Communication.

Dutsch, H. U., (1966), Two years of Regular Ozone Soundings Over Boulder, Colorado. NCAR-TN-10, Nat. Center for Atmos. Res., Boulder. 433pp.

Dutsch, H U., (1970), Atmospheric Ozone-A Short Review. J. Geophys. Res. 75, 1707-1712.

Goldman, A. and T. G. Kyle, (1968), A Comparison Between Statistical Model and Line by Line Calculation With Application to the 9.6μ Ozone and the 2.7 water vapor bands. Applied Optics, 7, 1167-1177.

Hering, W. S., and T. R. Borden, Jr., (1965), Mean Distributions of Ozone Density Over North America, 1963-1964. Environmental Res. Papers. No. 162, AFCRL, Bedford, Mass. 19 pp.

Hilsenrath, E., (1971), Ozone Measurements in the Mesosphere and Stratosphere During Two Significant Geophysical Events. J. Atmos. Sci., 28, 295-297.

Hunt, B. G., (1966), Photochemistry of Ozone in a Moist Atmosphere. J. Geophys. Res., 71, 1385-1398.

Johnston, H., (1971), Reduction of Stratospheric Ozone by Nitrogen Oxide Catalysts from Supersonic Transport Exhaust. Science, 173, 517-522.

Kaplan, L. D., (1959), The Atmosphere and Sea in Motion, Rockefeller Inst. Press. p. 170.

Kaplan, L. D., M. V. Migeotte, and L. Neven, (1956), 9.6 Micron Band of Telluric Ozone and its Rotational Analysis. J. Chem. Phys., 24, 1183-1186.

Mateer, C. L., D. F. Heath, and A. J. Krueger, (1971), Estimation of Total Ozone from Satellite Measurements of Back Scattered Ultraviolet Earth Radiance. J. Atmos. Sci., 28, 1307-1311.

McCaa, D. J., and J. H. Shaw, (1967), The Infrared Absorption Bands of Ozone Ohio State Univ., prepared for AFCRL, Rep. No. 67-0237. 94 pp.

Prabhakara, C., V. V. Salmonson, B. J. Conrath, J. Steranda, and L. J. Allison, (1971), Nimbus 3 IRIS Ozone Measurements Over Southeast Asia and Africa During June and July 1969. J. Atmos. Sci., 28, 828-831.

Ramanathan, K. R. and R. N. Kulkarni, (1960), Mean Meridional Distributions of Ozone in Different Seasons Calculated From Umkehr Observations and Probable Vertical Transport Mechanisms. Quart. J. Roy. Meteor. Soc. 144-155.

Randhawa, J. S., (1971), The Vertical Distribution of Ozone Near the Equator. J. Geophys. Res., 76, 8139-8142.

Shah, G. M., (1967), Quasi-biennial Oscillation in Ozone. J. Atmos. Sci., 24, 396-401.

Walshaw, C. D., (1954), An Experimental Investigation of the 9.6μm Band of Ozone . Thesis, Cambridge Univ.

Walshaw, C. D., (1955), Line Widths in the 9.6μ Band of Ozone. Proc. Phys. Soc. A., 68, 530.

Walshaw, C. D., (1957), Integrated Absorption by the 9.6μ Band of Ozone. Quart. J. Roy. Meteor. Soc., 83, 315-321.

Willett, H. C., (1968), Remarks on the Seasonal Changes of Temperature and of Ozone in the Arctic and the Antarctic Stratospheres. J. Atmos. Sci., 25, 341-360.

Water Vapor

Babrov, H. J., (1967), Strength of Lines in the ν_1 and ν_3 Infrared Bands of H_2O. Warner and Swasey Co., Flushing, N. Y. Prepared for AFCRL, No. 67-0156.

Benedict, W. S., and L. D. Kaplan, (1959), Calculation of Line Widths in H_2O-N_2 Collisions. J. Chem. Phys., 30, 388.

Benedict, W. S. and L. D. Kaplan, (1964), Calculation of Line Widths in H_2O-H_2O and H_2O-O_2 Collisions. J. Quant. Spectrosc. Radiat. Transfer, 4, 453-469.

Benedict, W. S., and R. F. Calfee, (1967), Line Parameters for the 1.9 and 6.3 Micron Water Vapor Bands. ESSA Professional Paper No. 2. Washington, D. C.

Burch, D. E., D. Gryvnak, E. Singleton, W. France, and D. Williams, (1962), Infrared Absorption by Carbon Dioxide Water Vapor, and Minor Atmospheric Constituents. Ohio State Univ. Res. Rep. Optical Physics Lab. No. AFCRL-62-0156.

Crutcher, H. L. and H Van Loon, (1970), Selected Level Heights, Temperature, and Dew Points for the Northern Hemisphere, supercedes NAVAIR 50-1C-52, Asheville, N. Carolina.

Fridovich, B. and J. R. Kinard, (1972), Intensity Half Width Products for Seven Lines in the 6.3μm Water Vapor Band. J. Opt. Soc. Amer., 62, 542-544.

Gates, D. M., R. F. Calfee, D. W. Hansen, and W. S. Benedict, (1964), Line Parameters and Computed Spectra for Water Vapor Bands at 2.7μ. Nat. Bureau of Standards Monograph 71, Washington, D. C., 126 pp.

Goldman, A. and T. G. Kyle, (1968), A Comparison Between Statistical Model and Line by Line Calculations with Application to the 9.6μm Ozone and the 2.7 Water Vapor Bands. Applied Optics, 7, 1162-1177.

Goody, R. M., (1964), Atmospheric Radiation. London, Oxford Univ. Press, 436 pp.

Gutnick, M., (1962), Mean Annual Mid Latitude Moisture Profiles to 31 km. Res. Rep. No. 147. AFCRL-62-681, Air Force Cambridge Res. Lab., 30pp.

Houghton, J. T., (1963), The Absorption of Solar Infrared Radiation by the Lower Stratosphere. Quart. J. R. Meteor. Soc., 89, 319-331.

Krakow, B., and A. R. Healy, (1969), Strengths of 31 Water Vapor Lines Between 1612 and 1429 cm^{-1}. J. Opt. Soc. Amer., 59, 1490-1491.

Mastenbrook, H. J., (1968), Water Vapor Distribution In the Stratosphere and High Troposphere. J. Atmos. Sci., 25, 299-311.

Mastenbrook, H. J., (1971), The Variability of Water Vapor in the Stratosphere. J. Atmos. Sci., 28, 1495-1501.

McKinnon, D. and H. W. Morewood, (1970), Water Vapor Distribution in the Lower Stratosphere Over North and South America. J. Atmos. Sci., 27, 483-493.

Palmer, C. H., Jr., (1960), Experimental Transmission Functions for the Pure Rotational Band of Water Vapor. J. Opt. Soc. Amer., 50, 1232-1242.

Penner, S. S., (1959), Quantitative Molecular Spectroscopy and Gas Emissivities. Reading, Mass., Addison Wesley. 582 pp.

Prinz, D. K., (1968), Strength-half-width Products of Self-broadened Lines in the 6.3 Micron Band of Water Vapor. No. PB-173429, Nat. Tech. Information Service, Springfield, Va.

Scholtz, T. G., D. H. Ehhalt, L. E. Heidt, and E. A. Martell, (1970), Water Vapor, Molecular Hydrogen, Methane, and Tritium Concentrations Near the Stratopause. J. Geophys. Res., 75, 3049-3054.

Sissenwine, N., D. D. Grantham, and H. A. Samela, (1968), Mid-latitude Humidity to 32 km. J. Atmos. Sci., 25, 1128-1140.

Starr, V., J. P. Peixoto, and R. G. McKean, (1969), Pole to Pole Moisture Conditions for the IGY, 75, 300-331, Pure and Applied Geophys.

Taljaard, J. J., H. VanLoon, H. L. Crutcher, and R. L. Jenne, (1969), Climate of the Upper Air, Part I, Southern Hemisphere, Temperatures, Dew Points, and Heights at Selected Pressure Levels. NAVAIR 50-1C-55, Washington, D. C.

Williamson, E. J., and J. T. Houghton, (1965), Radiometric Measurements of Emission from Stratospheric Water Vapor. Quart. J. R. Meteor. Soc., 91, 330-338.

Hydroxyl Radical

Anderson, J. G., (1971), Rocket Measurement of OH in the Mesosphere. J. G. R., 76, 7820-7824.

Bass, A. M. and D. Garvin, (1962), Analysis of the Hydroxyl Radical Vibration Rotation Spectrum Between 3900 A and 11500 A. J. Mol. Spectrosc., 9, 114-123.

Chamberlain, J. W., (1961), Physics of the Aurora and Airglow. Academic Press, New York, 368 pp.

Dieke, G. H. and H. M. Crosswhite, (1948), The Ultraviolet Bands of OH, Bumblebee Series Rep. No. 87 (John Hopkins Univ.)

Engleman, R., Jr., (1972), Accurate Wavenumbers of the $A^2\Sigma - X^2\Pi$ (0, 0) and (1, 0) Bands of OH and OD. J. Quant. Spectrosc. Radiat. Transfer., 12, 1347-1350.

Herman, R. C. and G. A. Hornback, (1953), Vibration-rotation Bands of OH. Ap. J., 118, 214-227.

Hesstvedt, E., (1968), On the Effect of Vertical Eddy Transport on Atmospheric Composition in the Mesosphere and Lower Thermosphere. Geofysiske Publikasjoner, XXVII, 1-35.

Hunt, B. G., (1966), Photochemistry of Ozone in a Moist Atmosphere. J. G. R., 71, 1385-1398.

Leovy, C. B., (1969), An Analytical Model for Photochemistry in the Presence of Water Vapor, in Meteorological and Chemical Factors in D-Region. Aeronomy - Record of Third Aeronomy Conference, Report No. 32., Univ. of Illinois, Urbana.

Levy, H. II, (1971), Normal Atmosphere: Large Radical and Formaldehyde Concentrations Predicted. Science, 173, 141-143.

McConnell, J. C., M. B. McElroy, and S. C. Wofsy, (1971), Natural Sources of Atmospheric CO. Nature, 233, 187-188.

Penner, S. S. (1959), Quantitative Molecular Spectroscopy and Gas Emissivities. Addison Wesley, 585 pp.

Wallace, L., (1960), The Constants of the $^2\pi - {}^2\Pi$ Oh Bands. Ap. J., 132, 894-897.

Wallace, L., (1969), OH Bands in the Airglow from International Dictionary of Geophysics, England, and Kitt Peak Nat. Obs. Rep. No. 142.

Weinstock, B. and H. Niki, (1971), The Balance of Carbon Monoxide in Nature. Publication Preprint. Ford Motor Co., Scientific Res. Staff. 8pp.

Chapter 3. Molecules Containing Carbon

3.1 Carbon Dioxide

Carbon dioxide is present in the earth's atmosphere in a sufficiently large quantity and has many strong absorption bands in the infrared and hence it is a very important contributor of atmospheric radiation. Since 1909 (Gold) when the importance of atmospheric CO_2 radiation to the terrestrial heat budget was noted, a vast amount of effort to understand this radiative transfer process of CO_2 (Drayson 1966, Plass, 1956) and to measure the CO_2 content in the earth's atmosphere has been carried out by many researchers (Gluckauf 1944, Callender 1958, Bolin and Bischof 1970, Bischof 1971).

3.1.1 Atmospheric Distribution

A systematic program to measure carbon dioxide concentrations in the atmosphere was started during the International Geophysical Year (IGY) 1957-1958 and measurements were routinely made at many ground stations, from aircraft and on ship cruises on the Pacific, Atlantic and Indian Oceans. The United States program was mainly concentrated at Hawaii, Alaska and the Antarctica. It has been noticed that the global atmospheric content of carbon dioxide has been increasing since the dawn of the industrial revolution. The reason for this increase being the consumption of fossil fuels by man. The average atmospheric CO_2 concentration at present is considered to be about 320 ppm by volume (Table 3.1.1) and its estimated rate of increase is about 0.7 ppm by volume a year (Robinson and Robbins, 1969). This is an overall figure and the actual concentration of CO_2 differs from place to place and time to time. A seasonal variation of atmospheric CO_2 has been noticed (Pales and Keeling 1965, Junge and Czeplak 1968). The amplitude of these seasonal variations was found to decrease with altitude being approximately 6 ppm at

about 2 km and decreasing to about 3 ppm at 10 km altitude. In the stratosphere there is an abrupt change in that these variations are very small, about ± 1 ppm. This is due to the considerably smaller vertical mixing in the stratosphere. The maximum CO_2 content in the northern hemisphere occurs in April-May and the minimum during the months of September-October. This is due to the cycle of the growth of vegetation on the earth's surface. Close to the ground a diurnal variation of CO_2 with a maximum in the predawn hours can also be noticed due to the diurnal variation of the respiration by plants.

In the stratosphere Bischof (1965, 1971) noticed that during May, the time of tropospheric CO_2 maximum the CO_2 content in the lower stratosphere was 4 ppm lower than in the upper troposphere, while in October the time of CO_2 minimum in the troposphere, it was 3 ppm higher. The tropopause thus acts as a damping layer for vertical exchange. Hays and Olivero (1970) have considered the photochemical production and loss and diffusion of CO_2 and calculated atmospheric CO_2 profiles for model atmospheres. They show that CO_2 is well mixed throughout the lower stratosphere and troposphere, while deviations from complete mixing are possible in the upper stratosphere and mesosphere. Fig. 3.1.1 shows the average distribution of CO_2 in the atmosphere.

Carbon dioxide is produced naturally by biological decay and in respiration. Outgassing from volcanoes, and other geochemical emmisions are other natural sources. Release of CO_2 from the oceans also occurs. Man's pollution by the combustion of fuels is another major source. Estimated emission rates for natural and pollution sources is 10^{12} and 1.4×10^{10} tons/year. (Robinson and Robbins, 1970). CO_2 is removed from the atmosphere by absorption in biological processes and in photosynthesis and by absorption by the oceans. There is a continuous exchange of CO_2 between the oceans and the atmosphere

Author	Location	Altitude	Technique	Year	Conc.	Remarks
Hagemann et. al. (1959)	U. S. Panama Brazil	45000- 100000 ft	Balloon flight Air sampling	1957-58	312ppm Avg: 312ppm 310ppm	
Steinberg and Rohrbough(1962)	Texas	22 km	Balloon flight absorption on Zeolite	March 1961	323-338ppm	
Bolin and Keeling (1963)	Global esp. Pacific Ocean, Hawaii	Surface 700 mb 500 mb	Continuous infrared gas analysis flask sampling	1957-62	315±8 ppm	Seasonal and latitudinal variations noticed. Yearly increase; sources in tropical oceanic areas and industrial area in Northern Hemisphere at mid latitudes.
Brown and Keeling (1965)	Antarctica	Ground Level	Continuous infrared gas analyzer	1960-63	313. 1±3. 1 ppm	Regular seasonal variations in troposphere, decreasing amplitude with altitude
Bischof (1971) Ref. Papers (1960, 62, 70)	Sweden	Ground to lower stratosphere	Air sample collection	1963-68	Average 322. 9ppm	0. 7 ppm/year increase noted

Table 3. 1. 1: Measurements of CO_2 in the atmosphere

on a global scale (ReVelle and Suess 1957, Takahasi T. 1961). Speculation that pollution by man is possibly altering the delicate balance between atmospheric CO_2 and CO_2 in the oceans has been carried out. Eriksson (1963) discusses the effect of changes of surface temperature of the oceans on atmospheric CO_2. Photodissociation of CO_2 occurs in the thermosphere and mesosphere. The photochemistry of atmospheric CO_2 has been treated by Bates and Witherspoon (1952). CO_2 is relatively inactive chemically and has a residence time of 2-4 years in the atmosphere. This conservative character makes CO_2 suitable as a tracer for studying transport processes in the atmosphere.

3.1.2 Infrared Spectral Properties

Carbon dioxide has a complex infrared spectrum. The molecule is triatomic and linear. There are various isotopic species in the atmosphere (Keeling 1960) but the main most abundant (approximately 98.42%) is $C^{12}O_2^{16}$. The isotopic species $C^{13}O_2^{16}$ and $C^{12}O^{16}O^{18}$, form about 1.11% and 0.41% respectively and the other isotopic species are present in much smaller fractions of the total carbon dioxide.

The carbon dioxide infrared spectrum has been thoroughly studied by many authors. The $C^{12}O_2^{16}$ and $C^{13}O_2^{16}$ molecules are symmetric (O-C-O) and the infrared spectrum consists of the ν_2 (15μm) and ν_3 (4.3μm) fundamentals. The ν_3 fundamental being a parallel band consists of only P and R branch lines. In the 15μm region, besides the ν_2 fundamental, are many overtone and combination bands, the total strength of all these together being approximately one-eighth that of the ν_2 fundamental. In the 4.3μm region also there are other overtone and combination bands besides the fundamental ν_3. Besides these two regions 15μm and 4.3μm where there are strong bands, there are other regions of the spectrum where CO_2 has other overtone and combination

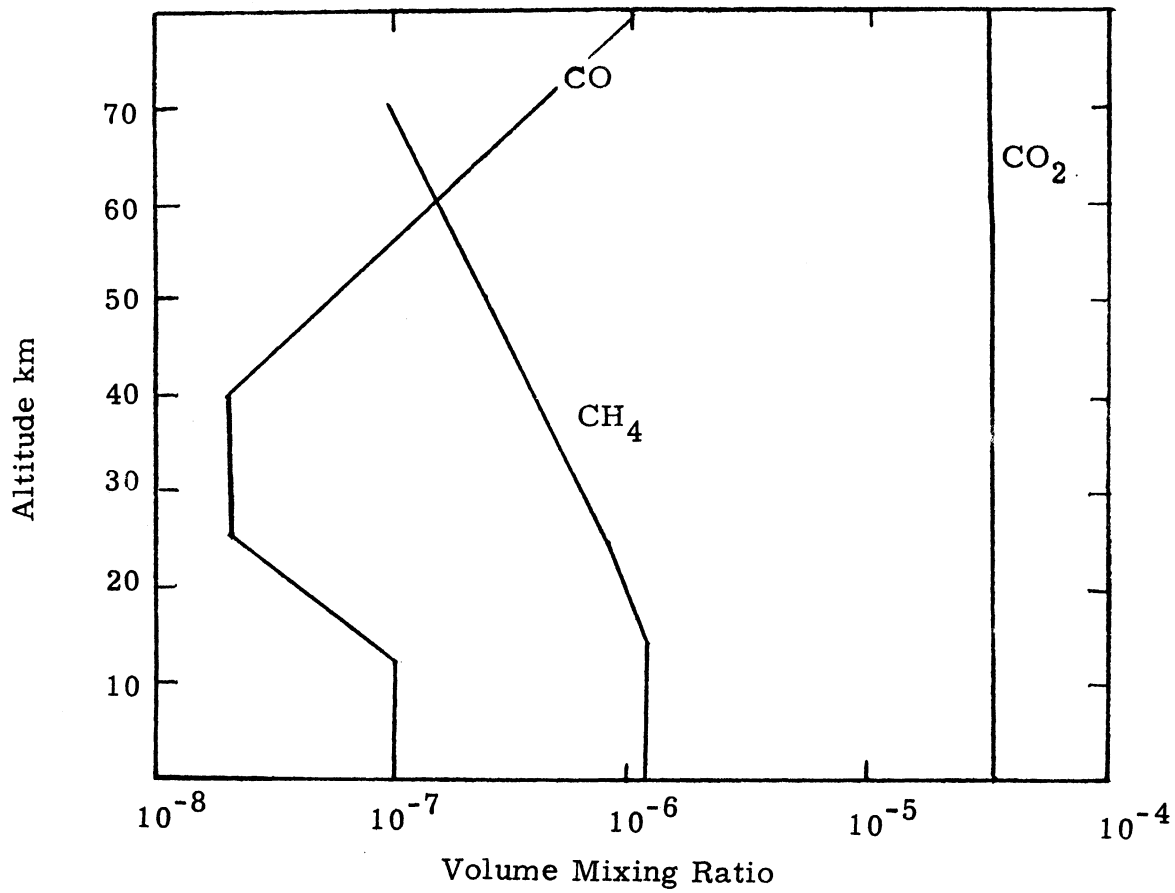

Fig. 3.1.1: Atmospheric distribution of CO_2, CO and CH_4

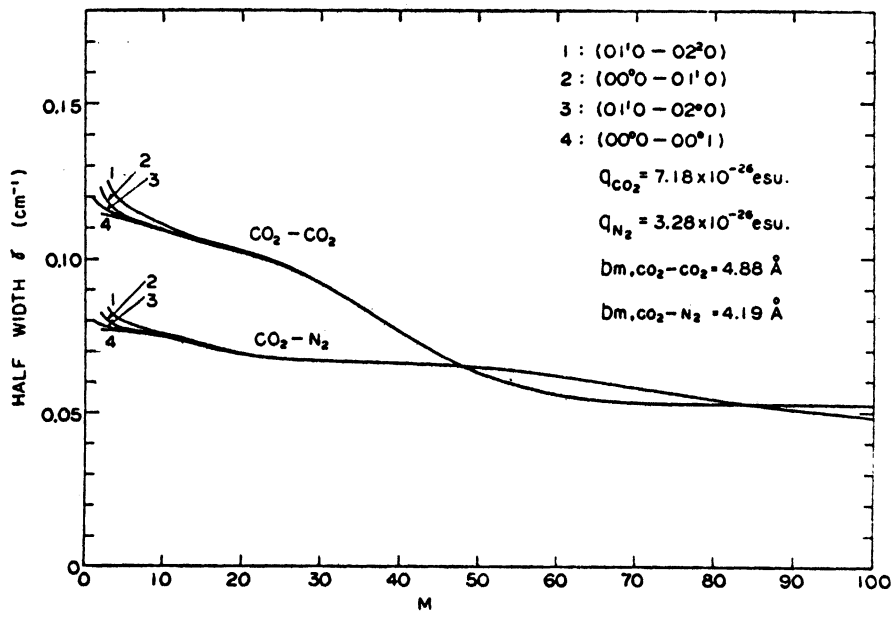

Fig. 3.1.2: Variation of self- and N_2- broadened line widths with rotational quantum index number for CO_2 bands. (from Yamamoto et. al., 1969)

Region μm	Center cm^{-1}	Upper	Lower	Intensity at $300^{o}K$ cm^{-1} $(atm\ cm)^{-1}_{STP}$	Reference
1.2	8192.6	(103:0)II	000:0	0.0012	Burch et. al. 1965
	8136.0	(113:1)II	010:1	0.0001	
	8294.0	(103:0)I	000:0	0.0017	
	8276.8	(113:1)I	010:1	0.00015	
	7593.5	(401:0)III	000:0	0.00029	Burch et. al. 1967
	7460.4	(401:0)IV	000:0	0.00011	
1.4	6972.5	003:0	000:0	0.041	Burch et. al. June 1965
	6935.0	013:1	010:1	0.0033	
	6679.7	(112:1)I	000:0	0.0001	
1.6	6503.0	(301:0)I	000:0	0.00161	Schurin & Ellis 1968
	6347.8	(301:0)II	000:0	0.0132	
	6227.9	(301:0)III	000:0	0.00137	
	6057.9	(301:0)IV	000:0	0.00145	
	5857.6	(102:0)II	000:0	0.00001	Burch et. al. Aug. 1965
	5687.0	003:0	(100:0)II	0.00002	
	5584.3	003:0	(100:0)I	0.00002	
	5349.0	(102:0)I	010:1	0.14	Burch et. al. 1964
2.0	5248.0	(102:0)II	010:1	0.33	
	5099.6	(201:0)I	000:0	0.33	
	4977.8	(201:0)II	000:0	1.05	
	4853.6	(201:0)III	000:0	0.23	
	4591.0	(301:1)III	000:0	0.42	
2.7	3723.2	(111:1)I	010:1	3.5	Burch et. al. 1969
	3714.8	(101:0)I	000:0	44.9	
	3612.8	(101:0)II	000:0	29.0	
	3580.3	(111:1)I	010:1	2.3	
4.3	2349.3	001:0	000:0	2700.0	
	2336.7	011:1	010:1	210.0	
4.8	2129.8	(200:0)I	010:1	0.01	
	2093.4	(120:2)I	010:1	0.041	
	2076.9	(110:1)I	000:0	0.66	
5.2	1932.5	(110:1)II	000:0	0.05	
9.4	1061.0	(100:0)I	001:0	0.0159	Schurin & Ellis 1970
10.4	961.0	(100:0)II	001:0	0.0199	McCubbin & Mooney 1968
15.0	828.3	(120:2)I	(110:1)II	0.00022	
	791.4	(110:1)I	(100:0)II	0.0242	
	757.5	(120:2)I	030:3	0.0099	
	741.7	(110:1)I	020:2	0.158	
	738.6	(200:0)II	(110:1)II	0.0154	
	688.7	(110:1)I	(100:0)I	0.33	Drayson 1972
	668.1	030:3	020:2	0.93	
	667.8	020:2	010:1	16.5	
	667.4	010:1	000:0	214.0	
	647.1	(110:1)II	(100:0)II	0.77	
	720.8	(100:0)I	010:1	5.5	
	618.0	(100:0)II	010:1	4.7	
	597.3	(110:1)II	020:2	0.154	
	581.7	(120:2)II	030:3	0.0092	
	544.3	(110:1)II	(100:0)I	0.011	

Table 3.1.2: Band centers and intensities of CO_2 ($C^{12}O_2^{16}$) bands.

bands. There are bands at 10μm, 5μm, 2.7μm and also some weaker bands at 2μm, 1.6μm, 1.4μm and 1.2μm regions of the electromagnetic spectrum. Many authors have carried out theoretical calculations and experimental measurements of the CO_2 bands (Boese et. al., 1966; Burch et. al., 1962; 1970; Calfee and Benedict, 1966; Drayson and Young, 1965, 1966, 1967; Drayson et. al., 1968; France and Dickey, 1955; Gryvnak et. al., 1966; Oberly et. al., 1968; Plyler et. al., 1962; Tubbs and Williams, 1972; Winters et. al., 1964; References in Table 3.1.2).

Table 3.1.2 gives a list of the important bands of carbon dioxide, the band centers and intensities. The vibrational and rotational constants for the CO_2 bands have been determined by many workers and are known fairly accurately. Detailed calculations on the relative intensities of individual lines for various bands of the CO_2 molecule have been published by Gray (1967), Gray and Young (1969), Young (1970) and Young et. al. (1970). The variation of line half-width for important bands has been calculated by Yamamoto et. al. (1969), using the Anderson theory.

3.1.3 Atmospheric Application

Transmittance calculations show that CO_2 absorption can be readily measured in all the strong band regions for all tangent heights in the stratosphere and lower mesosphere. Calculations of CO_2 absorptance at 655 cm^{-1} have been made for a model atmosphere, (Table 3.1.3) assuming a concentration distribution of CO_2 of constant mixing ratio of 320 ppm by volume.

Tangent Height (km)	Mixing Ratio (ppmv)	$\bar{u}$ $(\text{atm cm})_{300K}$	$\bar{p}$ (mb)	$\bar{T}$ (^{o}K)	Average Abs
5	320	11100.	372.	239.	1.
10	320	5760.	183.	218.4	1.
15	320	2650.	84.	217.6	1.
20	320	1210.	38.3	219.5	1.
25	320	553.	17.7	225.	1.
30	320	257.	8.3	231.6	0.84
35	320	121.	4.	242.6	0.4
40	320	59.	2.	255.	0.2
45	320	30.	1.	264.7	0.1
50	320	16.	0.56	266.1	0.05
55	320	8.5	0.3	258.7	0.03
60	320	4.5	0.16	247.4	0.02
65	320	2.3	0.08	231.5	0.01
70	320	1.1	0.04	214.4	0.0
75	320	0.46	0.02	198.3	0.

Table 3.1.3: Average absorption at 655 cm^{-1} by atmospheric CO_2

The above calculations are approximate and calculate the average absorption by CO_2 using the isolated line model. Only, Lorentz broadening of the spectral line is incorporated. No variation of the strength or the half-width with temperature has been included. For an accurate calculation of the atmospheric transmittance, the variation of line strengths and line half-width with temperature, and Doppler broadening of lines must be included.

Measurement of CO_2 absorption in the atmosphere is slightly complicated by the fact that other constituents have absorption bands close to those of CO_2. In the 15μm region there is absorption by water vapor (especially in the troposphere) and by ozone (especially in the stratosphere) and N_2O (17μm), in the 4.3μm there is absorption by water vapor, N_2O (4.5μm), CO (4.6μm), and in the 2.7μm region there is absorption by water vapor and methane. However using the ideal spectral channels for measurement, the accurate determination of atmospheric CO_2 absorption and thereby the CO_2 distribution in the atmosphere appears feasible.

3.2 Carbon Monoxide

3.2.1 Atmospheric Distribution

Carbon monoxide is one of the minor constituents in the atmosphere. Its atmospheric presence was first noticed spectroscopically by Migoette (1949) and many subsequent measurements of its atmospheric content have been made (Table 3.2.1). Recent measurements by Seiler and Junge 1969, made on airplane flights show that CO is well mixed in the troposphere. The average global concentration of CO in the atmosphere is roughly 0.12 ppm and the estimated total amount in the atmosphere is 7.4×10^4 gm. Considerable variations of the atmospheric CO content from the average value of 0.12 ppm have been noticed depending on the location of measurement. Measurements in the atmosphere over oceans far from pollution sources showed CO concentrations as low as 0.06 ppm while CO content in the atmosphere over highly polluted areas was found to be as high as 0.3 ppm. Measurements in the Southern hemisphere indicate lower concentrations of CO of 0.06 ppm. In the stratosphere Seiler and Warneck (1972) measure a rapid decrease in concentration. They noticed sudden changes from tropospheric values of 0.12 ppm

Author	Location	Altitude	Technique	Year	Conc.	Remarks
Benesch et. al. (1953)	Jungfraujoch Switzerland	total amount	Spectroscopically	1950-51	0.031-0.14 ppm	From Junge (1963)
Locke and Herzberg (1953)	Ottawa Ohio Jungfraujoch Mt. Wilson	total amount	Spectroscopically	1952	0.11-0.22 0.19 0.15 0.16 ppm	
Robbins et. al. (1968)	Greenland West U. S. Alaska N. Pacific Near coast S. Pacific	near surface	Chemical method	1965	0.2-0.8 0.8 0.09 0.1 0.03-0.06 0.05 ppm	
Seiler and Junge (1969)	Polar Frankfurt-Anchorage Tokyo flights	10 km upper troposphere and lower stratosphere	Commercial aircraft Lufthansa	1968	0.1-0.2ppm sudden decrease to 0.03ppm in stratosphere	
Seiler and Junge (1970)	Western Europe South Africa	upper troposphere lower stratosphere	Commercial aircraft flights	1967-69	0.1-0.15ppm 0.16-0.3ppm (in polluted areas)	mid tropospheric conc. show marke differences betwee hemispheres
	Atlantic Ocean $10^{o}S$ to $60^{o}N$ at $30^{o}W$	surface water	ship cruise		10 to 40 times the atmospheric equilibrium value	
Seiler and Warneck (1972)	Western Europe	upper troposphere and lower stratosphere	chartered aircraft continuous recording instrument	Jan-Mar 1971	average 0.12 in tropopause 0.4 in stratopause	

Table 3.2.1: Measurements of CO in the atmosphere

to stratospheric values of 0.03 ppm. There are not many measurements at higher altitudes because of the difficulty in measurement. The molecular weight of CO is nearly the same as N_2 and this makes identification by mass spectrometry extermely difficult.

The main sources of CO in the atmosphere are forest fires (Robinson and Robbins, 1968), release by the oceans by the photochemical oxidation of dissolved organic carbon (Wilson et. al. 1970), photochemical reactions of terpenes and other organic matter, the oxidation of atmospheric methane (Wofsy et. al., 1972), dissociation of atmospheric CO_2 by lightning (Swinnerton et. al., 1971) and of considerable importance man's contribution by the combustion of fuels. This last source has been steadily increasing since the industrial revolution, and the present estimated rate of pollution is 3.4×10^{14} gm. of CO a year. Jaffe (1968) and Grenda et. al. (1971) have given a detailed listing of the various sources of atmospheric CO.

Recent measurements (Lamontagne et. al., 1971) of CO content in surface waters of oceans show very high concentrations (15 to 75 times that of the equilibrium value in the atmosphere) with a diurnal cycle showing a maximum during daylight hours. This seems to indicate a very large production of CO in the surface layers of the oceans. Thus release of CO by the oceans could be a very important source of atmospheric carbon monoxide.

The processes by which CO is being removed from the atmosphere are still only slightly understood. It is accepted that there must be such processes, since the atmospheric CO content has not increased considerably in spite of the huge inputs of CO. Chemical reactions in the stratosphere (Hesstvedt 1970, Pressman and Warneck 1970, Levy 1971) and at ground level (Westberg 1971) and biological actions on the ground and in the sea are some

of the sinks of atmospheric CO. Plant life absorbs CO from the atmosphere and this is thought to be an important sink for CO (Douglas, 1967). A recent review of the sources and sinks of atmospheric CO has been presented by Bortner et. al. (1972).

Wofsy et. al. (1972) have calculated CO concentration profiles in model atmospheres. In the stratosphere the dominant sink mechanism is the reaction $CO + OH \rightarrow CO_2 + H$. Junge et. al. (1971) have calculated CO residence times and vertical fluxes in the troposphere and at the tropopause. In the upper stratosphere and the mesosphere the photodissociation of CO_2 is responsible for the increase in mixing ratio of CO. Fig. 3. 1. 1 shows the average distribution of atmospheric CO.

Carbon monoxide is toxic and at high concentrations is fatal to human and animal life (Stern 1968). CO has been listed as a possible serious health hazard by the National Air Pollution Control Administration and is one of the gasses measured in the U. S. Public Health Service Continuous Air Monitoring program as an air quality indicator in cities. CO has absorption bands in the infrared region of the electromagnetic spectrum and hence it contributes to a small extent to the earth's long wave radiative transfer and heat budget. Also the overall CO balance is interrelated to the CO_2 balance and the photochemistry of the two are interdependent (Kummler et. al., 1969). Hence a detailed knowledge of the radiative properties and the distribution in the atmosphere of CO are important.

3. 2. 2 Infrared Spectral Properties

The infrared spectrum of CO has been extensively studied because of its great simplicity. CO is a diatomic molecule and there are many isotopic species in the atmosphere, but approximately 98. 7% of total CO is $C^{12}O^{16}$. The fundamental 0-1 band of CO is at 4. 6μm and the first and

second overtone bands 0-2 at 2.7μm and 0-3 at 1.57μm. Theoretical calculations of line strengths and line half-widths have been carried out by Kunde (1967). Experimental studies in the 0-1 bands (Benedict et. al. 1962) 0-2 bands (Kostkowski and Bass 1961, Korb et. al. 1968, Hunt et. al. 1968) and 0-3 bands (Plyler and Thibault 1963, Burch and Gryvnak 1967, Bouanich and Haeusler 1972) have been reported. For remote sensing applications these CO bands have some disadvantage in that there is overlapping by absorption lines of other constituents. There is overlapping by CO_2, N_2O, O_3 and H_2O absorption bands in the 4.6μm band of CO and the 2.3μm band is strongly overlapped by water vapor and methane absorption bands. Table 3.2.2 lists the strengths of the important bands of CO. Fig. 3.2.1 gives the variation of half width with rotational quantum number for CO bands.

Region μm	Center cm^{-1}	Transition	Intensity at $300^{o}K$ in $cm^{-1}(atm\ cm)^{-1}_{STP}$
1.57	6350.5	3-0	0.0130
2.7	4260.0	2-0	2.06
4.6	2143.2	1-0	261.0

Table 3.2.2: Band centers and intensities of CO ($C^{12}O^{16}$) bands

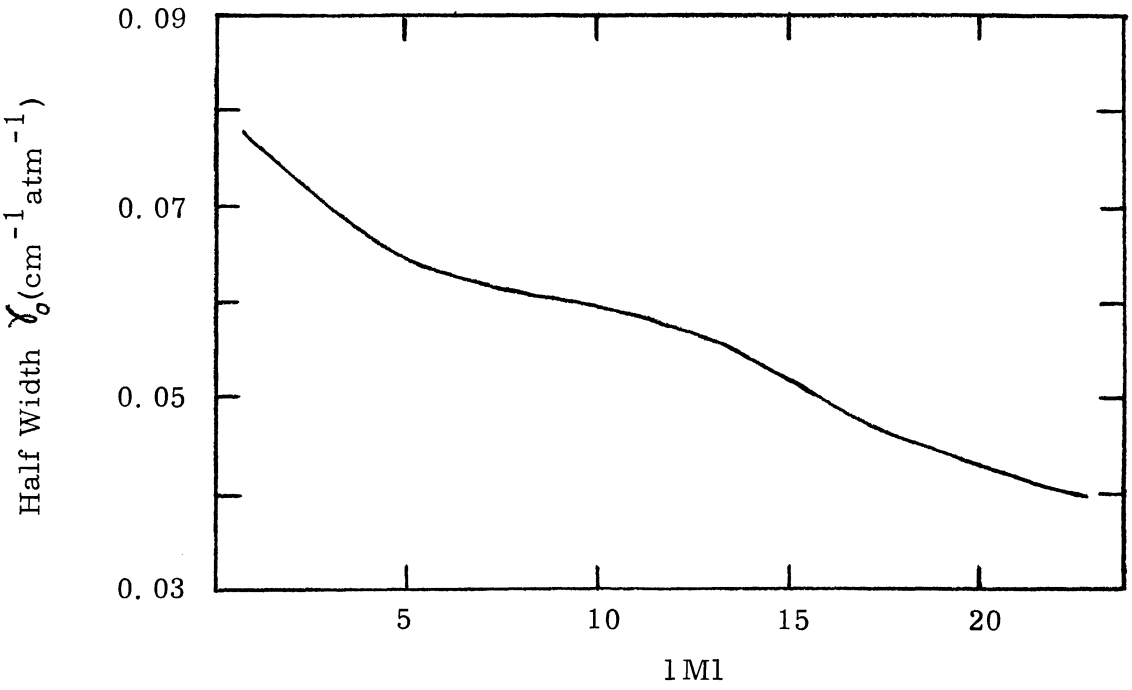

Fig. 3. 2. 1: Variation of N_2-broadened line half-width with rotational quantum index number for CO bands (from Bouanich and Hauesler, 1972)

3. 2. 3 Atmospheric Application

Calculations of average absorptance at 2173 cm^{-1} have been made for a model atmosphere (Appendix) assuming a concentration distribution for CO (Fig. 3. 1. 1). Mixing ratio 0. 1 ppm from 0-12 km, 12-25 km varying linearly, 25-40 km constant 0. 02 ppm, 40-79 km varying linearly 79 km 1 ppm. The calculations are similar to those described for CO_2 in section 3. 1. 3.

Tangent Height (km)	Mixing Ratio (ppmv)	$\bar{u}$ $(atm\ cm)_{300K}$	$\bar{p}$ (mb)	$\bar{T}$ (^oK)	Average Abs
5	0. 1	3. 3	387	240	0. 52
10	0. 1	1. 6	197	218	0. 26
15	0, 08	0. 54	92	218	0, 1
20	0. 05	0. 15	40	221	0. 036
25	0. 02	0. 045	14	233	0. 012
30	0. 02	0. 028	5. 2	243	0. 006
35	0. 02	0. 021	2.	253	0. 003
40	0. 02	0. 022	1. 2	258	
45	0. 14	0. 023	0. 84	262	
50	0. 27	0. 018	0. 49	263	

Table 3. 2. 3: Average absorption at 2173 cm^{-1} by atmospheric CO

There is measurable absorption in the stratosphere, and by the suitable choice of spectral channels the measurement of atmospheric CO from a satellite appears feasible.

3.3 Methane

3.3.1 Atmospheric Distribution

Methane is present in the earth's atmosphere in a considerable amount, being the eighth most abundant gas in the earth's atmosphere. The main sources of atmospheric methane are the decomposition of organic matter (Koyama 1963, Ehhalt 1967) and the emissions from coal and natural gas fields and petroleum industries. No known sources of methane exist in the atmosphere. The total estimated global emission rate is approximately 8×10^{14} gm./year. The major sink for atmospheric methane is thought to be the oxidation to H_2O and CO_2 in the stratosphere. Migoette (1948) made the first measurements of atmospheric CH_4 content and later measurements followed (Table 3.3.1). Most of the measurements have been the determination of total amount of methane in the atmosphere or the determination of methane content of ground level air. Measurements of methane content higher in the atmosphere are very very few, and of doubtful accuracy. The measurements indicate that methane is well mixed up to the tropopause with a mixing ratio varying from 0.6 to 1.6 ppm by volume and that the mixing ratio decreases above the tropopause to about 65% of its tropospheric average value at 25 km and to 20% of its tropospheric average value at the stratopause (Ehhalt et. al., 1972). Crutzen (1971) has calculated theoretical distributions of atmospheric methane showing a rapid decrease of methane above 25 km to nearly zero value at 50 km. The variation 0.6 to 1.6 ppm of the mixing ratio of methane could be latitude, seasonal or proximity to a source or sink variation. However the widely differing techniques, and the inherent difficulty of measurements could be the reason for the uncertainty. Calculations of methane content are also rough because of the limited knowledge of the sources and sinks of methane. More detailed measurements are required for the

Author	Location	Altitude	Technique	Year	Conc.	Remarks
Goldberg (1951)	Michigan Mt. Wilson	Total amount	Spectroscopic 1.67μ measurement	1950	1.2 $(\text{atm cm})_{STP}$	
Bowman and Shaw (1963)	Columbus Ohio	ground level	Spectroscopic 3.3μ measurement	1963	1.7±0.3ppm	
Fink et. al. (1964)	Pennsyl-vania	total amount	Spectroscopic 1.67μ measurement	1963	1.11 $(\text{atm cm})_{STP}$	
Bainbridge and Heidt (1966)	Southern U. S. A. East Texas and West Louisiana	0-23 km	Air sampling balloon and aircraft flights	March-July 1965	1.4-1.6ppm in troposphere rapidly decreases in stratosphere 1.1-1.3ppm at 24 km.	
Kyle et. al. (1969)	U. S. Holloman Air Base	0-30 km	Balloon flight absorption at 1300 cm^{-1} vertical amount in atmosphere	Dec. 1967	total vertical amount 1.2 atm cm decreases above tropopause to 0.3 atm cm at 24 km	
Scholz et. al. (1970)	White Sands New Mexico	44-62 km	Air sampling with cryocon-denser on rocket flight	Sept. 1968	Stratopause average 0.25±0.01 ppm between 44 and 62 km	

Table 3.3.1: Measurements of CH_4 in the atmosphere

determination of atmospheric methane distribution. Fig. 3.1.1 shows the approximate distribution of methane in the atmosphere.

3.3.2 Infrared Spectral Properties

Methane has a very complex infrared spectrum characteristic of a tetrahedral molecule. Many theoretical and experimental studies have appeared in the literature (Plyler et. al. 1960, Barnes et. al. 1972, Kyle 1968, Margolis and Fox 1968, Hecht 1960, Henry et. al. 1970, Varanasi and Tejwani 1972, McMahon et. al. 1972). More laboratory measurements in the area of determination of line strengths and half-widths of methane bands for atmospheric application are useful. The ν_3 (3.3μm) and ν_4 (7.7μm) fundamentals are active in the infrared. Besides these two bands there are many overtone and combination bands at 1.1μm, 1.7μm, 2.3μm, 3.3μm, 3.6μm, 3.9μm, 7.7μm and other regions of the spectrum. Table 3.3.2 gives a few important bands and the band strengths.

Region μm	Band Center cm^{-1}	Intensity at 300°K in cm^{-1} (atm cm)$^{-1}_{STP}$
1.67	6005	1.6
3.31	3019	370.0
3.85	2600	307.0
7.66	1306	204.0

Table 3.3.2: Band centers and intensities of CH_4 bands
Adapted from Goody (1964)

3.3.3 Atmospheric Application

The absorbpion by atmospheric methane is estimated from Burch et al (1962) and is shown in Table 3.3.3. Optical masses were calculated by the method described in the appendix. The methane distribution assumed (Fig. 3.1.1.) is mixing ratio 1.2 ppm from 0-14 km varying linearly to 0.8 ppm at 24 km and decreasing to 0.25 ppm at 50 km.

Tangent Height (km)	Mixing Ratio (ppmv)	$\bar{u}$ $(\text{atm cm})_{300K}$	$\bar{p}$ (mb)	$\bar{T}$ (^{o}K)	Absorption
5	1.2	40.3	382	240	.7
10	1.2	20.	191	218	.45
15	1.04	7.8	87.6	217	.37
20	0.88	3.	40	219	.30
25	0.74	1.2	18.5	224	.22
30	0.64	0.46	8.8	230	.12
35	0.54	0.18	4.3	241	.08
40	0.45	0.07	2.2	254	.03
45	0.35	0.025	1.2	266	.01
50	0.25	0.009	0.65	270	.0

Table 3.3.3: Average absorption at 3020 cm^{-1} by atmospheric CH_4

The accurate measurement of absorption by atmospheric methane from a satellite appears feasible.

References

Bainbridge, A. E. and L. E. Heidt, (1966), Measurements of Methane in the Troposphere and Lower Stratosphere. Tellus, 18, 221.

Barnes, W. L., J. Susskind, R. H. Hunt and E. K. Plyler, (1972), Measurement and Analysis of the ν_3 Band of Methane. J. Chem. Phys., 56, 5160.

Bates, D. R. and A. E. Witherspoon, (1952), The Photochemistry of Some Minor Constituents of the Earth's Atmosphere (CO_2, CO, CH_4, N_2O). Mon. Not. Roy. Astron. Soc., 112, 101.

Benedict, W. S., R. Herman, G. E. Moore and S. Silverman, (1962), The Strengths, Widths and Shapes of Lines in the Vibration-Rotation Bands of CO. Astrophys. Jour., 135, 277.

Benesch, W. M. Migeotte, and L. Nevan, (1953), Investigation of Atmospheric CO at the Jungfraujoch, J. Opt. Soc. of Am., 43, 1119.

Bischof, W., (1960), Periodic Variations of the Atmospheric CO_2 Content in Scandinavie. Tellus, 12, 216.

Bischof, W., (1962), Variations in Concentration of Carbon Dioxide in the Free Atmosphere. Tellus, 14, 67.

Bischof, W., (1965), Carbon Dioxide Concentrations in the Upper Troposphere and Lower Stratosphere I. Tellus, 17, 398.

Bischof, W., (1970), Carbon Dioxide Measurements from Aircraft. Tellus, 22, 545.

Bischof, W., (1971), Carbon Dioxide Concentration in the Upper Troposphere and Lower Stratosphere II. Tellus, 23, 558

Bischof, W., and B Bolin, (1966), Space and Time Variations of the CO_2 Content of the Troposphere and Lower Stratosphere. Tellus, 18, 155.

Boese, R. W., J. H. Miller, and E. C. Y. Inn, (1966), Intensity Measurements of the 1μm CO_2 Bands. J. Q S. R. T., 6, 717.

Bolin, B., and W. Bischof, (1970), Variations of the Carbon Dioxide Content of the Atmosphere in the Northern Hemisphere. Tellus, 22, 431.

Bolin, B., and C. D. Keeling, (1963), Large Scale Atmospheric Mixing as Deduced from Seasonal and Meridional Variations of Carbon Dioxide. J. G. R., 68, 3899.

Bouanich, J. P. and C. Hauesler, (1972), Linewidths of Carbon Monixide Self-broadening and Broadened by Argon and Nitrogen, J. Q. S. R. T., 12, 695.

Bortner, M. H., R. H. Kummler, and L. S. Jaffe, (1972), A Review of Carbon Monoxide Sources, Sinks and Concentrations in the Earth's Atmosphere. NASA-CR-2081.

Bowman, R. L., and J. H. Shaw, (1963), The Abundance of Nitrous Oxide, Methane and Carbon Monoxide in Ground Level Air. App. Optics, 2, 176.

Brown, C. W., and C. D. Keeling, (1965), The Concentration of Atmospheric Carbon Dioxide in Antarctica. J. G. R., 70, 6077.

Burch, D. E., and D. A. Gryvnak, (1967), Strengths, Widths, and Shapes of the Lines of the 3ν CO Band. Philco-Ford Corp. Aeronutronic Div. Publ. U-3972.

Burch, D. E., D. A. Gryvnak, and R. R. Patty, (1964), Absorption by CO_2 between 4500 and 5400 cm^{-1} Philco (Ford Motor Co.) Aeronutronic Div. Publ. No. U-2955.

Burch, D. E., D. A. Gryvnak, and R. R. Patty, (1965), Absorption by CO_2 between 8000 and 10,000 cm^{-1} (1-1.25 micron region) Aeronutronic Div. Philco Corp. Publ. No. U-3200.

Burch, D. E., D. A. Gryvnak, and R. R. Patty, (June, 1965), Absorption by CO_2 between 6600 and 7125 cm^{-1} (1.4 micron region). Aeronutronic Div. Philco Corp. Scientific Report Publ. No. U-3127.

Burch, D. E., D. A. Gryvnak, and R. R. Patty, (Aug., 1965), Absorption by CO_2 between 5400 and 6600 cm^{-1} (1.6 micron region). Aeronutronic Div. Philco Corp. Ford Motor Co. Publ. No. U-3201.

Burch, D. E., D. A. Gryvnak, and R. R. Patty, (1967), Absorption by CO_2 between 7125 and 8000 cm^{-1} (1.25-1.40 microns) Philco-Ford Corp., Aeronutronic Div. Publ. No. U-3930

Burch, D. E., D. A. Gryvnak, R. R. Patty, and C. E. Bartky, (1969), Absorption of Infrared Radiant Energy by CO_2 and H_2O. IV. Shapes of Collision Broadened CO_2 Lines. J. Opt. Soc. of Am., 59, 267.

Burch, D. E., D. A. Gryvnak, and J. D. Pembrook, (1970), Investigation of the Absorption of Infrared Radiation by Atmospheric Gases, AFCRL-70-0373. Air Force Cambridge Res. Labs.

Burch, D. E., D. A. Gryvnak, E. B. Singleton, W. L. France, and D. William, (1962), Infrared Absorption by CO_2, Water Vapor, and Minor Atmospheric Constituents. AFCRL-62-698 Air Force Cambridge Res. Labs.

Calfee, R. F., and W. S. Benedict, (1966), Carbon Dioxide Spectral Line Positions and Intensities Calculated for the 2.05 and 2.7 micron regions. Nat. Bur. Std. Tech. Note: 332.

Callendar, G. S., (1958), On the Amount of Carbon Dioxide in the Atmosphere. Tellus, 10, 243.

Crutzen, P. J., (1971), Ozone Production Rates in an Oxygen- Hydrogen-Nitrogen Oxide Atmosphere, J. G. R., 76, 7311.

Douglas, E., (1967), Carbon Monixide Solubilities in SeaWater, J. Phys. Chem., 71, 1931.

Drayson, S. R., (1966), Atmospheric Transmission in the CO_2 Bands between 12μ and 18μ. App. Optics, 5, 385.

Drayson, S. R., (1972), Atmospheric Radiative Transfer by Carbon Dioxide, Conference on Atmospheric Radiation, Aug. 1972, AMS, Fort Collins, Colorado.

Drayson, S. R., and C. Young, (1965), Band Strength and Line Half-width of the 10.4μ CO_2 Band. J. Q. S. R. T., 7, 993.

Drayson, S. R., and C. Young, (1966), Theoretical Investigations of Carbon Dioxide Radiative Transfer. Rep. No. 07349-1-F, Coll. of Eng., Univ. of Michigan.

Drayson, S. R., and C. Young, (1967), The Frequencies and Intensities of Carbon Dioxide Absorption Lines between 12 and 18 microns. Rep. No. 08183-1-T, Coll. of Eng., Univ. of Michigan.

Drayson, S. R., S. Y. Li, and C. Young, (1968), Atmospheric Absorption by Carbon Dioxide, Water Vapor, and Oxygen. Final Report No. 08183-2-F, Coll. of Eng., Univ. of Michigan.

Ehhalt, D. H., (1967), Methane in the Atmosphere. J. Air. Pollution. Cont., 17, 518.

Ehhalt, D. H., L. E. Heidt, and E. A. Martell, (1972), The Concentration of Atmospheric Methane between 44 and 62 km Altitude. J. G. R., 77, 2193.

Erikson, E., (1963), Possible Fluctuations in Atmospheric Carbon Dioxide Due to Changes in the Properties of the Sea. J. G. R., 68, 3871.

Fink, U., D. H. Rank, and T. A. Wiggins, (1964), Abundance of Methane in the Earth's Atmosphere. J. Opt. Soc. of Am., 54, 572.

France, W. L., and F. P. Dickey, (1955), Fine Structure of the 2.7 micron Carbon Dioxide Rotation-Vibration Band. J. Chem. Phys., 23, 471.

Gluckauf, E., (1944), Carbon Dioxide Content of Atmospheric Air. Nature, 153, 620.

Gold, E., (1909), The Isothermal Layer of the Atmosphere and Atmospheric Radiation. Proc. Roy. Soc. Lond. A 82, 43.

Goldberg, L., (1951), The Abundance and Vertical Distribution of Methane in the Earth's Atmosphere. Astrophys. Jour., 113, 567.

Goody, R. M., (1964), Atmospheric Radiation I - Theoretical Basis. Oxford at the Clarendon Press.

Gray, L. D., (1967), Relative Intensity Calculations for Carbon Dioxide III, Relative Line Intensities of Transitions from the Vibrational Ground State for Temperatures from 160° to 280° K. J. Q. S. R. T., 7, 795.

Gray, L. D., and A. T. Young, (1969), Relative Intensity Calculations for Carbon Dioxide IV. Calculations of the Partition Function for Isotopes of CO_2. J. Q. S. R. T., 9, 569.

Grenda, R. N., M. H. Bortner, P. J. LeBel, J. H. Davis, and R. Dick, (1971), Carbon Monixide - Pollution Experiment I. A Solution to the Carbon Monoxide Sink Anomaly. AIAA Paper No. 71-1120. Joint Conference on Sensing of Environmental Pollutants, Palo Alto, California.

Gryvnak, D. A., R. R. Patty, D. E. Burch, and E. E. Miller, (1966), Absorption by CO_2 between 1800 and 2850 cm^{-1} (3.5 - 5.6 micron). Philco-Ford Corp. Aeronutronic Div. Publ. No. U-3857.

Hagemann, F., J. Gray, Jr., L. Machta, and A. Turkevich, (1959), Stratospheric Carbon-14, Carbon Dioxide, and Tritium. Science, 130, 542.

Hays, P. B., and J. J. Olivero, (1970), Carbon Dioxide and Monoxide above the Troposphere. Planetary and Space Sci., 18, 1729.

Hecht, K. T., (1960), Vibration-Rotation Energies of Tetrahedral XY_4 Part II - The Fundamental $\nu 3$ of CH_4 J. Mol. Spectry., 5, 390.

Henry, L., N. Husson, R. Andia, and A. Valentin, (1970), Infrared Absorption Spectrum of Methane from 2884 to 3141 cm^{-1}. J. Mol. Spectry., 36, 511.

Hesstvedt, E., (1970), Vertical Distribution of CO Near the Tropopause. Nature, 225, 50.

Hunt, R. H., R. A. Toth, and E. K. Plyler, (1968), High Resolution Determination of the Widths of Self Broadened Lines of Carbon Monoxide. J. Chem. Phys., 49, 3909.

Jaffe, L. S., (1968), Ambient Carbon Monoxide and its Fate in the Atmosphere. J. Air Pollution Cont. Assoc., 18, 534.

Junge, C. E., (1963), Air Chemistry and Radioactivity. New York, Academic Press, New York.

Junge, C. E., and G. Czeplak, (1968), Some Aspects of the Seasonal Variation of Carbon Dioxide and Ozone. Tellus, 20, 422.

Junge, C. E., W. Seiler, and P. Warneck, (1971), The Atmospheric ^{12}CO and ^{14}CO Budget. J. G. R., 76, 2866.

Keeling, C. D., (1960), The Concentration and Isotopic Abundances of Carbon Dioxide in the Atmosphere. Tellus, 12, 200.

Keeling, C. D , T. B. Harris, and E. M. Wilkins, (1968), The Concentration of Atmospheric Carbon Dioxide at 500 and 700 millibars. J. G. R., 73, 4511.

Korb, C. L , R. H. Hunt, and E. K. Plyler, (1968), Measurement of Line Strengths at Low Pressures - Application to the 2-0 Band of CO. J. Chem. Phys., 48, 4252.

Kostkowski, H. J., and A M. Bass, (1961), Direct Measurement of Line Intensities and Widths in the First Overtone Band of CO. J. Q. S. R T., 1, 177.

Koyama, T., (1963), Gaseous Metabolism in Lake Sediments and Paddy Soils and the Production of Atmospheric Methane and Hydrogen. J. G. R., 68, 3971.

Kummler, R. H., R. N. Grenda, T. Baurer, M. H. Bortner, J. H. Davies, and J. MacDonald, (1969), Satellite Solution of the Carbon Monoxide Sink Anamoly. Trans. Amer. Geophys. Union, 50, 174.

Kunde, V. G., (1967), Tables of Theoretical Line Positions and Intensities for the V=1, V=2, and V=3 Vibration Rotation Bands of $C^{12}O^{16}$ and $C^{13}O^{16}$. NASA X-622-67-248 Goddard Space Flight Center.

Kyle, T. G., (1968), Line Parameters of the Infrared Methand Bands. Sci. Rep. No 1. Air Force Contract AF 19(628)-5706. Dept. of Physics, Univ. of Denver

Kyle, T. G., D. G. Murcray, F. H. Murcray, and W. J. Williams, (1969), Abundance of Methane in the Atmosphere Above 20 km. J G. R., 74, 3421.

Lamontagne, R. A., J. W. Swinnerton and V. J Linnenbom, (1971), Non-equilibrium of Carbon Monoxide and Methane at the Air-Sea Interface J. G. R , 76, 5117.

Levy, H., (1971), Normal Atmosphere-Large Radical and Formaldehyde Concentrations Predicted. Science, 173, 141.

Locke, J. L., and L. Herzberg, (1953), The Absorption Due to Carbon Monoxide in the Infrared Solar Spectrum. Canad. J. Phys., 31, 504.

Ludwig, C. B., R. Bartle, and M. Griggs, (1969), Study of Air Pollutant Detection by Remote Sensors. NASA CR-1308. General Dynamics Rep. No. GDC-DBE 68-011. Convair, San Diego, Calif.

Margolis, J. S. and K. Fox, (1968), Infrared Absorption Spectrum of CH_4 at 9050 cm^{-1}. J. Chem. Phys., 49, 2451.

McCubbin, T. K., Jr., and T. R. Mooney, (1968), A Study of the Strengths and Widths of Lines in the 9.4 and 10.4m CO_2 Bands.

McMahon, J., G. J. Troup, and G. Hubbert, (1972), The Effect of Pressure and Temperature on the Half-Width of the Methane Absorption at 3.39m.

Migoette, M., (1949), The Fundamental Band of CO at 4.7m in the Solar Spectrum. Phys. Rev., 76, 1108.

Migoette, M. V., (1948), Spectroscopic Evidence of Methane in the Earth's Atmosphere. Phys., 73, 1948.

Oberly, R., K. N. Rao, Y. H. Hahn, and T. K. McCubbin, Jr., (1968), Bands of Carbon Dioxide in the Region of 4.3 microns. J. Mol. Spectry., 25, 138.

Pales, J. C., and R. D. Keeling, (1965), The Concentration of Atmospheric Carbon Dioxide in Hawaii. J. G. R., 70, 6053.

Plass, G. N., (1956), The Influence of the 15μ Carbon Dioxide Band on the Atmospheric Infrared Cooling. Quart. J. R. Met. Soc., 82, 310.

Plyler, E. K., and R. J. Thibault, (1963), Self Broadening of Carbon Monoxide in the 2v and 3v Bands. J. Res. Nat. Bur. Std., 67A, 201

Plyler, E. K., E. D. Tidwell, and L. R. Blaine, (1960), Infrared Absorption Spectrum of Methane from 2470 to 3200 cm^{-1}. J. Res. Nat. Bur. Std. 64A, 201.

Plyler, E. K., E. D. Tidwell, and W. S. Benedict, (1962), Absorption Bands of Carbon Dioxide from 2.8-4.2μ. J. Opt. Soc. of Am., 52, 1017.

Pressman, J. and P. Warneck, (1970), The Stratosphere as a Chemical Sink for Carbon Monoxide. J. Atmo. Sc., 27, 155.

Revelle, R., and H. Suess, (1957), Carbon Dioxide Exchange Between Atmosphere and Ocean and the Question of an Increase of Atmospheric CO_2 During Past Decades. Tellus, 9, 18.

Robbins, R. C., K. M. Borg, and E. Robinson, (1968), Carbon Monoxide in the Atmosphere. J. Air. Poll. Control Assoc., 18, 106.

Robinson, E., and R. C. Robbins, (1968), Sources, Abundance and Fate of Gaseous Atmospheric Pollutants. Final Rep. SRI. Project Pr-6755. Amer. Petr. Inst. Washington, D. C.

Robinson, E. and R. C. Robbins, (1970), Global Effects of Environmental Pollution. Ed. S. F. Singer, Springer Verlag, N. Y.

Scholz, T. G., D. H. Ehhalt, L. E. Heidt, and E. A. Martell, (1970), Water Vapor, Molecular Hydrogen, Methane and Tritium Concentration Near the Stratopause. J. G. R., 75, 3049.

Schurin, B. D., and R. E. Ellis, (1968), Integrated Intensity Measurements of Carbon Dioxide in the 2.0μ, 1.6μ, and 1.43μ regions. App. Optics., 7, 467.

Schurin, B. D., R. E. Ellis, (1970), Total Intensity Measurements for the CO_2 Bands in the 961 cm^{-1} and 1061 cm^{-1} regions. App. Optics, 9, 223.

Seiler, W. and C. Junge, (1969), Decrease of Carbon Monoxide Mixing Ratio Above the Polar Tropopause. Tellus, 21, 447.

Seiler, W. and C. Junge, (1970), Carbon Monoxide in the Atmosphere. J. G. R., 75, 2217.

Seiler, W. and P. Warneck, (1972), Decrease of the Carbon Monoxide Mixing Ratio at the Tropopause. J. G. R., 77, 3204.

Steinberg, S. and S. F. Rohrbough, (1962), The Collection and Measurement of Carbon Dioxide and Water Vapor in the Upper Atmosphere. J. Appl. Meteor., 1, 418.

Stern, A. C., (1968), Air Pollution Vol. 1. Second Ed. Academic Press, N. Y.

Swinnerton, J. W., V. J. Linnenbom, and R. A. Lamontagne, (1971), Carbon Monoxide in Rainwater. Science, 172, 943.

Takahashi, T., (1961), Carbon Dioxide in the Atmosphere and in Atlantic Ocean Water. J. G. R., 66, 477.

Tubbs, L. D., and D. Williams, (1972), Broadening of Infrared Absorption Lines at Reduced Temperatures: Carbon Dioxide. J. Opt. Soc. of Am., 62, 284.

Varanasi, P. and G. D. T. Tejwani, (1972), Experimental and Theoretical Studies on Collision Broadened Lines in the v4 Fundamental of Methane. J. Q. S. R. T., 12, 849.

Westburg, K., N. Cohen, and K. W. Wilson, (1971), Carbon Monoxide. Its Role in Photochemical Smog formation. Science, 171, 1013.

Wilson, D. F., J. W. Swinnerton, and R. A. Lamontagne, (1970), Production of Carbon Monoxide and Gaseous Hydrocarbons in Sea Water. Relation to Dissolved Organic Carbon. Science, 168, 1577.

Winters, B., S. Silverman, and W. Benedict, (1964), Line Shape in the Wing Beyond the Band Head of the 4.3m band of CO_2. J. Q. S. R. T., 4, 527.

Wofsy, S. C., J. C McConnell, and M. B. McElroy, (1972), Atmospheric CH_4, CO and CO_2. J. G. R., 77, 4477.

Yamamoto, G., M. Tanaka, and T. Aoki, (1969), Estimation of Rotational Line Widths of Carbon Dioxide Bands. J. Q. S. R. T., 9, 371.

Young, L. D. G., (1970), Relative Intensity Calculations for Carbon Dioxide V., Relative Intensities of the More Abundant Isotopes. J. Q. S. R. T., 10, 99.

Young, L. D. G., A. T. Young, and R. A. Schorn, (1970), Improved Constants for the 7820 A and 7883 A Bands of CO_2 . J. Q. S. R. T., 10, 1291.

Chapter 4. Molecules Containing Nitrogen

4.1 Nitrous oxide (N_2O)

4.1.1 Atmospheric Distribution

The first positive identification of nitrous oxide in the atmosphere was reported by Adel (1938) who recognized its absorption bands in the solar spectrum near 7.8μm. Since that time atmospheric absorption spectra of N_2O have been detected in other spectral regions and measurements of distribution have been made using spectral techniques and also a variety of other methods. The measurements prior to 1966 have been summarized by Bates and Hays (1967) and more recently a comprehensive discussion by Schütz et. al. (1970) has appeared.

As is the case with many minor constituents, few measurements of concentration in the stratosphere have been made for N_2O. These measurements, inherently less reliable than those made near the surface, must be supplemented by estimates based on theoretical consideration involving photochemistry and transport phenonoma. Thus it is important to examine closely the distribution in the troposphere since the stratospheric N_2O is transported from below.

Measured concentrations are in the range 0.12 (Seely and Houghton, 1961) to 1.25 (Shaw et. al., 1948) parts per million by volume. This order of magnitude variation appears not to be a real effect but is probably due to errors and uncertainties in the measurement techniques. There are variations both with time and geographical location but they appear to be much smaller than the extreme figures would indicate. Fig. 4.1.1 (from Schütz et. al. 1970) shows typical variations in the troposphere. These authors measurements at Mainz show an increase for the time period from late 1966 to mid 1968

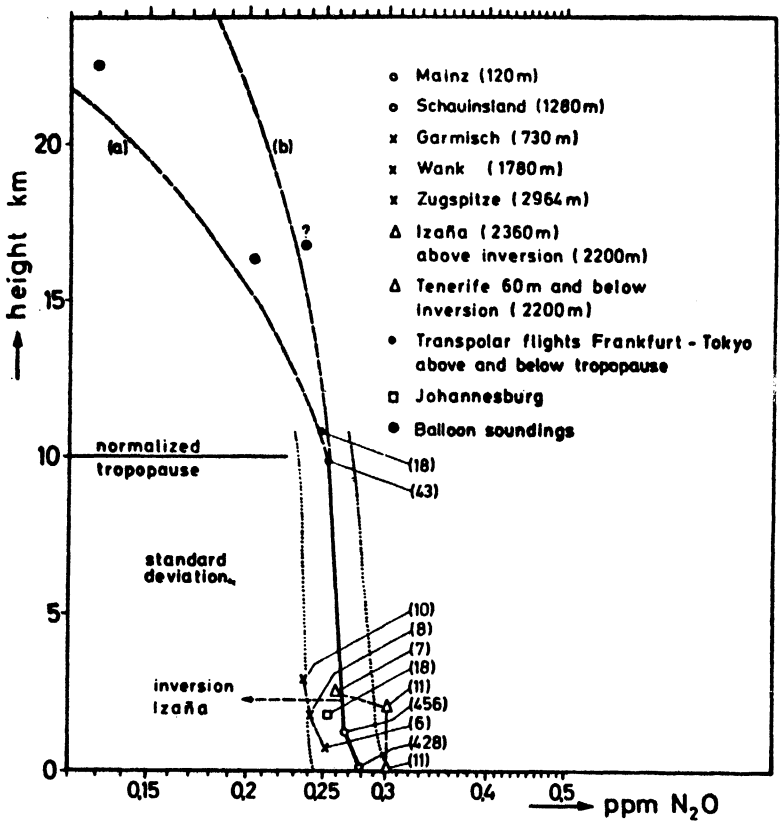

Fig. 4.1.1 Atmospheric N_2O concentrations (from Schütz et. al., 1970)

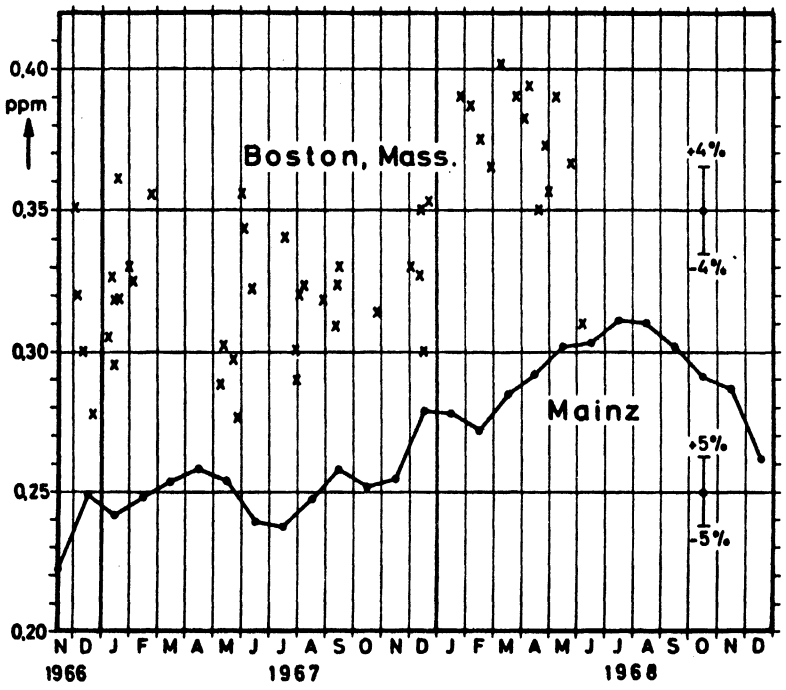

Fig. 4.1.2 Atmospheric N_2O concentrations at Mainz, Germany and Boston, Mass. (from Schutz et. al., 1970).

which is also suggested by the data of Goody (1969) taken at Boston, Mass. (Fig. 4. 1. 2). Goody's concentrations are consistently higher by at least 0. 05 ppmv (20%). It is not clear how much of this difference is in measurement techniques which might lead to a systematic error.

The data also indicate that seasonal effects are not marked and that industrial pollution does not contribute significantly to the N_2O concentration. Measurements in the tropics show similar results to those made in temperate zones (Lahue et. al., 1970).

The source of atmospheric N_2O is nitrate reduction due to bacterial activities and apparently is operative in the ocean as well as in soils (Junge and Hahn, 1971). An atmospheric residence time of 10 years or less is indicated. The major known atmospheric sink of N_2O is by photodissociation which gives a residence time of about 70 years. Clearly there must be some additional mechanism to destroy N_2O. Junge and Hahn suggest that arid regions, e. g., the Sahara Desert region, may be sinks since air from these regions has a lower N_2O content. No mechanism to accomplish this reduction has yet been advanced.

The sink of N_2O in the stratosphere has been examined by Bates and Hays (1967). The main mechanism is the photodissociation of N_2O.

$$N_2O + h\nu \longrightarrow N_2 + O \qquad \lambda < 3370\text{Å}$$

At shorter wavelengths the production of NO and N is also possible

$$N_2O + h\nu \longrightarrow NO + N \qquad \lambda < 2500\text{Å}$$

More recent data seems to exclude this as an important process.
In the troposphere the photodissociation is small and the atmospheric mixing is good, so that the concentration stays relatively uniform. In the stratosphere photodissociation becomes more important and at the same time the vertical mixing becomes much less in this stable environment. Thus the vertical

profile of N_2O depends critically on the mixing in the lower stratosphere, a quantity which is not accurately determined. Following the usual procedures Bates and Hays characterize the vertical mixing by a vertical exchange coefficient K_z and calculate for a range of values (10^2 to 10^5 cm^2 sec^{-1}). The results for 10^3 and 10^4 $cm^2 sec^{-1}$ are shown in Fig. 4. 1. 1 as the dashed lines. As can be seen the balloon soundings of Schutz et. al. fall between these curves which correspond roughly to the best estimates of vertical eddy mixing. The values are shown in Table 4. 1. 1a.

Information on stratospheric N_2O has also been obtained by Goldman et. al. (1970) from solar absorption measurements in the 4. 5μm spectral region (Table 4. 1. 1b). The measurements within the troposphere show much lower mixing ratios than reported by Schutz et. al. and by most of the more recent measurements. There is an indication of a reduction in the mixing ratio at the highest level but it may not be significant in view of the errors in making the measurement and the interpretation of the spectra.

Stratospheric N_2O concentrations have not yet been determined with sufficient accuracy or frequency to give a comprehensive picture of its stratospheric distribution. The scant measurements that do exist support the general conclusions of the theoretical study by Bates and Hays. Their calculations are of a simple nature involving photodissociation and vertical eddy diffusion, but leave out other influential factors. In particular the role of meridional and vertical transport is completely neglected. The importance of the atmospheric circulation in determining the ozone concentration in the stratosphere is well known, even if the details are as yet imperfectly understood. We should, for example, expect smaller concentrations of N_2O at high latitudes in the winter because of the subsidence of air depleted of N_2O

at higher levels. If the stratospheric distributions could be measured comprehensively, then N_2O could be used as a tracer to determine atmospheric transport. Global satellite measurements would be particularly suitable.

Date	Altitude (km)	N_2O Mixing Ratio ppm volume
June 1967	17.3	0.229*
July 1968	18.0	0.204
October 1968	23.0	0.103

* possible contamination

Table 4.4.1a: Stratospheric mixing ratios (Schütz et. al. (1970)

Date	Altitude (km)	N_2O Mixing Ratio ppm volume
	5.03	0.14
March 1968	8.08	0.17
	9.84	0.15
	10.3	0.15
	13.3	0.11

Table 4.4.1b: Stratospheric mixing ratios (Goldman et. al., 1970)

4.1.2 Infrared Spectral Properties

Nitrous oxide is a linear asymmetric molecule (N-N-O) whose chemical properties make it almost inert and easy to handle in the laboratory. These factors have contributed to its popularity with experimental and theoretical spectroscopists, so that many experimental and theoretical studies have been made of its spectral properties. Next to carbon dioxide it is the most

intensively studied linear triatomic molecule and resembles CO_2 in many ways, e. g., laser transitions in the same spectral regions between the same energy levels. The analogy with CO_2 becomes almost complete for the less abundant asymmetric isotopic molecules such as $^{12}C^{16}O^{18}O$.

Transition	Band Center (cm^{-1})	Band Intensity $cm^{-1}(atm\ cm)^{-1}_{300k}$
$01^{1}0 - 00^{0}0$	588. 8	35
$02^{0}0 - 00^{0}0$	1168. 1	10
$10^{0}0 - 00^{0}0$	1284. 9	230
$11^{1}0 - 00^{0}0$	1880. 3	0. 37
$00^{0}1 - 00^{0}0$	2223. 8	1600
$12^{0}0 - 00^{0}0$	2462. 0	10
$20^{0}0 - 00^{0}0$	2563. 3	40
$01^{1}1 - 00^{0}0$	2798. 3	2. 2
$02^{0}1 - 00^{0}0$	3364. 0	1. 7
$11^{1}1 - 01^{1}0$	3473. 2	4. 3
$10^{0}1 - 00^{0}0$	3480. 8	40
$00^{0}2 - 00^{0}0$	4417. 4	1. 6

Table 4. 1. 2: Infrared bands of N_2O
(Adapted from Gray Young, 1972)

Table 4. 1. 2 shows the more important bands together with estimates of their intensities. For the stronger bands, which are of most interest for remote sensing applications, the intensities are probably known with sufficient accuracy. Laboratory measurements could easily be made on those for which this conclusion does not hold. The intensities in Table 4. 1. 2

are the total intensities in the spectral regions indicated. The listed transitions dominate the absorption spectrum but the hot bands frequently contribute to about 10% of the intensity at room temperature. The exact intensities of these weaker bands are not always well known and would thus contribute to the difficulty in the interpretation of atmospheric spectra. In addition to the hot bands, the isotopic molecules, e. g., $^{14}N^{14}N^{18}O$, should be considered in very accurate calculations of atmospheric absorption.

In order to compute the absorption of N_2O under the varying conditions of pressure, temperature etc. found in the atmosphere it is desirable to have available a listing of line parameters, that is the wavenumber, intensity and Lorentz half-width of each line. The parameters needed to calculate the energy levels have been tabulated by Pliva (1968) and these have been used by Gray Young (1971) to compute the partition function for $^{14}N_2{}^{16}O$. This may be used to calculate the relative intensities of various transitions (Gray Young, 1972) and the absolute intensities provided that the band inteisities are known.

The Lorentz half-widths of N_2O are not well known, either for the self-broadened or air-broadened case. The large variation of estimates based on measurements in the laboratory has been discussed by Tejwani and Varanasi (1971). The values vary from 0. 157 to 0. 05 cm^{-1} at 1 atmosphere. These authors have calculated the half-widths, including the variation with rotational quantum number J, using the Anderson theory, giving a mean value of 0. 06 cm^{-1} at 1 atmosphere pressure for air-broadened N_2O. However experience with other molecules has shown that the Anderson theory gives satisfactory results only when the parameters needed by the theory (e. g., the quadrupole moments of the molecules involved) are adjusted to give

agreement with the measured values of half-width. This situation remains unsatisfactory until such time as reliable and consistent measurements of half-width are obtained.

Difficulties such as those discussed in the last paragraph make the interpretation of atmospheric spectra hazardous. Part of the disagreement between Goldman et. al., (1970), Goody (1969) and Schütz et. al. (1970) might be explained in terms of the infrared properties of N_2O. The infrared technique is a promising one and should be capable of high reliability once the minor difficulties have been resolved.

4.1.3 Atmospheric Application

A calculation has been made to determine the optical mass of N_2O for several tangent heights in the stratosphere using the technique described in the appendix. The mixing ratio profile used in the computation is shown in Table 4.1.3. It was obtained by upward extrapolation from Fig. 4.1.1 based on the values of mixing ratio calculated by Bates and Hays. It is also close to the curve given by Crutzen (1971) for a vertical eddy diffusion coefficient of 10^3 cm sec^{-1}.

Only a few laboratory measurements were available under the conditions corresponding to these tangent paths, but at the 10 km level almost complete absorption takes place in several spectral regions. It would therefore appear to be feasible to make solar occutation measurements from a satellite to determine N_2O concentrations. Essentially the same procedure has already been used from a balloon.

The choice of an optimum spectral region has not yet been determined. The 17μm band may have some advantage; although it is not the

strongest of the bands it does have an intense Q-branch which gives considerable absorption even under a resolution of a few wavenumbers so that a comparitively simple instrument could be employed.

Tangent Altitude (km)	Mixing Ratio (ppmv)	$\bar{u}$ $(\text{atm cm})_{300K}$	$\bar{p}$ (mb)	$\bar{T}$ (°K)
40	0.0	0.0		
35	.01	.002	5.0	237
30	.04	.020	10.0	227
25	.10	.118	20.7	222
20	.16	.466	43.1	218
15	.22	.150	91.8	217
10	.25	4.03	195	218

Table 4.1.3: Optical mass path parameters for N_2O tangent paths.

4.2 Odd Nitrogen Oxides

4.2.1 Atmospheric Distribution

This group of nitrogen compounds includes NO, NO_2, NO_3 and N_2O_5. All occur naturally in the stratosphere and have recently been studied in detail as they are thought to play an important role in the ozone photochemistry. Concern has been expressed that the SST would increase concentration of odd nitrogen in the lower stratosphere, leading to a decrease in the ozone concentration.

A natural source of odd nitrogen in the stratosphere is the downward flux of nitric oxide (NO) which is formed by a number of photochemical reactions in the thermosphere (see, e. g., Strobel, 1971; Norton and Barth, 1970; Nicolet, 1970). In the upper mesosphere nearly all the odd nitrogen is in the form of nitric oxide but in the stratosphere substantial amounts are in the other oxides NO_2, NO_3 and N_2O_5 as well as nitrous acid HNO_2 and nitric acid HNO_3. These components tend to dissociate during the day and also take part in reactions with hydrogen and oxygen compounds (O, O_3, OH, H_2O_2, etc.). Calculation of the stratospheric photochemistry of these nitrogen compounds have been made by Johnson (1971) and Crutzen (1971). Such calculations are complex and contain many reactions whose rates are not accurately known. Unfortunately there are few measurements of stratospheric concentrations which can be used to verify the calculated distributions. When Crutzen's values of the nitric acid concentrations are compared with the measurements of Murcray et. al. (1969) or Lazrus et. al. (1972) it is found that the theoretical concentrations are at least an order of magnitude too small (see Section 4. 3. 3 for details). It throws into doubt the validity of the results for any odd nitrogen molecules, although it is possible that the HNO_3 number densities are the only ones that are seriously in error and the predicted distributions of the other molecules are substantially correct. It would be extremely helpful to have more measurements, particularly of NO and NO_2 concentrations, in the lower stratosphere.

The agreement between the calculations of Johnston(1971) and Crutzen (1971) is reasonable. Usually the number densities agree to within a factor of two or three, which can be easily explained by the differences between the models and by the reaction rates and other parameters included in the calculations. The computations of Strobel (1971) extend down only to 30 km but again are close in the region of overlap.

Number density measurements of NO in the upper stratosphere and lower mesosphere (40 to 60 km) have been reported by Pontano and Hale (1970). Between 40 and 50 km the average value is close to 10^9 cm^{-3} but decreases almost an order of magnitude near 60 km. The measurements were made about a half hour after sunset in September and December 1968 at White Sands, N. M. At the upper level they are about an order of magnitude less than the measurement of Pierce (1969) made at twilight. Those of Meira (1971) extend only to 70 km but in this range are an order of magnitude less than Pierce.

The concern over the artificial introduction of odd nitrogen into the stratosphere by the SST is prompted by its ability to catalytically convert odd oxygen into even oxygen, primarily by the following two reactions:

$$NO + O_3 \longrightarrow NO_2 + O_2$$

$$NO_2 + O \longrightarrow NO + O_2$$

If sufficient quantities of odd nitrogen were introduced into the lower stratosphere it is conceivable that a marked reduction in the ozone concentration could result in the region of intensive SST flights. This would allow more ultraviolet radiation to reach the surface and possibly upset the energy balance of the stratosphere. Some calculations to determine effect of pollution by the SST have been made (for example, by Johnston, 1971) but they are inconclusive, largely because many of the parameters, such as production rates for odd nitrogen, reaction rates, horizontal and vertical diffusivity etc., are not sufficiently well known. It seems likely that the SST will not influence the ozone concentration greatly but this cannot yet be conclusively demonstrated.

From the foregoing discussions it is apparent that there is a critical need for measurements of odd nitrogen concentrations throughout the

stratosphere, but especially in the lower stratosphere. They are needed to verify the theoretical models and to encourage the development of new models with more adequate transport phenomena incorporated in them. Only then can we be confident in the reliability of predictions about the polluted stratosphere. Finally, concentrations of nitrogen oxides, ozone etc. would have to be monitored on a continuing basis to verify the predictions and to assure that there were no major modification of the stratosphere.

4. 2. 2 Infrared Spectral Properties

Nitric oxide (NO), being a diatomic molecule, has a simple infrared spectra. The fundamental (1-0) band is centered near 5. 3μm (1875 cm^{-1}), the (2-0) near 2. 6μm and the (3-0) near 1. 8μm. The band intensities, particularly that of the fundamental, have been measured by a number of workers and are summarized by King and Crawford (1972) and by Michels (1971). Michels describes a calculation of the intensities of the bands, which is in good agreement with experimental values for the fundamental. The averages of the measured intensities for the (1-0), (2-0) and (3-0) bands are 130, 2. 5 and 0. 1 cm^{-1} (atm cm^{-1}) respectively.

The Lorentz half-width have been measured by Abels and Shaw (1966) (mean value 0. 055 cm^{-1} at 1 atmosphere and 300K) and the positions of the lines in the fundamental measured by James and Thilbault (1964). The parameters required to make accurate atmospheric transmittance calculations appear to be known.

The survey of the spectral properties of the remaining nitrogen oxides has not yet been completed.

4.3 Nitric Acid Vapor HNO_3

4.3.1 Atmospheric Distribution

Nitric acid vapor was first detected as a stratospheric constituent by Murcray et. al. (1969) who recorded solar absorption spectra with a balloon-borne infrared spectrometer. This constituent has not been observed in the troposphere partly because of interference by other molecules (e. g., water vapor) and partly due to the lower concentrations in the troposphere. Even in the stratosphere the long paths associated with zenith angles slightly in excess of 90^{o} were required, because of the low mixing ratio. The data of Murcray et. al. was rendered somewhat difficult to interpret because of lack of suitable laboratory spectral data, although this situation has now been largely rectified.

The quantitative reduction of the balloon data by Rhine et. al. (1969) showed amounts of nitric acid vapor varying between 2. 0 and 23 x 10^{-3} atm cm, along a line of sight and corresponds to a mean value of 4. 41 (± 0. 75) x 10^{-3} (atm cm) per air mass, slightly lower than the value of Murcray et. al. This can be converted to a volume mixing ratio of approximately 5 x 10^{-9} which applies to the 20-25 km region

A confirmation of the presence of nitric acid has been provided by Lazrus et. al. (1972) who based their conclusion on the analyses of filter samples obtained during stratospheric balloon flights (21 to 27 km) and aircraft flights (17 to 19 km). The balloon data yield mixing ratios ranging from 1 to 5. 5 x 10^{-9} by volume i. e., comparable to those of Murcray et. al. at about the same altitude. The lower altitude aircraft measurements gave lower mixing ratios, ranging from zero to 0. 7 x 10^{-9} by volume

These changes of concentration with altitude are in accordance with the theory of the formation of HNO_3 . It can be produced by the reactions (see, for example, Johnson, 1971).

$$N_2O_5 + H_2O \longrightarrow 2HNO_3$$

and

$$NO_2 + OH + M \longrightarrow HNO_3 + M$$

According to Johnstonthe second is much more likely and the maximum production occurs between 25 and 40 km. It can also undergo photodissociation

$$HNO_3 + h\nu \rightarrow NO_2 + OH \qquad \lambda<3000\text{Å}$$

and there may be substantial diurnal variations, at least at some altitudes.

Of course, a comprehensive theory on the distribution of HNO_3 in the stratosphere should include transport by both eddy processes and by the mean circulation. This has been pointed out by Lazrus et. al. who suggest that the reason for the small concentration in the lower equitorial stratosphere is due to the fact that this air is of recent tropospheric origin

It is difficult to extrapolate upwards to estimate the nitric acid mixing ratio above the region where measurements exist. At sufficiently high levels photodissociation will predominate and daytime concentrations will be low. The calculations of Crutzen (1971) indicate the maximum mixing ratio occurs near 25 km at night and a few km lower during the day. However his calculated mixing ratios are lower than the measurements in the lower stratosphere by a factor of 5 to 10 at night and by a factor of 10 or more during the day. Crutzen discusses possible reasons for this discrepancy but does not reach any firm conclusions. There is a need for more measurements of the distribution of this interesting stratospheric constituent.

4.3.2 Spectral Properties of HNO_3

HNO_3 is a nearly planar molecule. Few studies of the quantative absorption of this molecule have been made and these have been prompted by the discovery of nitric acid in the stratosphere. The strongest bands are at 5.9μm, 7.5μm, 11.3μm and 22μm (Goldman et. al., 1971). Those at 7.5μm and 11.3μm have been investigated by Rhine et. al. and all except the 22μm band by Goldman et. al. Because of the small amounts of the absorber along an atmospheric path it is difficult to make measurements for conditions similar to those in the atmosphere.

The band intensities have been estimated by Goldman et. al. (Table 4.3.1) and the same authors have derived band parameters for the statistical band model from their data. No calculation of the wavenumbers and intensities of the individual lines have been reported. High resolution spectral studies would presumably be required to give the necessary input parameters.

Potentially the most useful feature of the HNO_3 bands is the intense Q-branches which give considerable atmospheric absorption for even a low resolution measurement. Band models are not usually very successful in Q-branch regions so that further measurements and development of the theory are required to extend our ability to predict atmospheric absorption at lower pressure and smaller absorber amounts.

Band	Intensity at 313K $(cm^{-1}/(atm\ cm)_{313K})$
11.3μm	600
7.5μm	1150
5.9μm	1250

Table 4.3.1: Band intensities of HNO_3 (adapted from Goldman et. al. (1971)

4. 3. 3 Atmospheric Application

Since nitric acid vapor has been detected from IR solar absorption by balloon-borne spectrometers, there is no reason why the same measurement cannot be made form a satellite. The height to which such a measurement can be extended is uncertain, reflecting our lack of knowledge of its distribution above the level of the present measurements. Absorption by a Q-branch would be the best choice in any spectral region. The result of a calculation using the day and night number densities tabulated by Crutzen (1971) are shown in Tables 4. 3. 2 (night) and 4. 3. 3 (day). These should be lower limits for the optical masses of HNO_3 along a tangent path and should be increased by about an order of magnitude to agree with the measured concentrations in the lower stratospheres. This is illustrated in Table 4. 3. 4, which compares the optical mass of HNO_3 calculated from Crutzen's day and night profiles with the measured amounts (Rhine et. al.) at the experimental tangent heights.

Tangent Height (km)	Number Density (cm^{-3})	Optical Mass $(atm\ cm)_{300K}$	$\bar{p}$ (mb)	$\bar{T}$ (^oK)
50	1.8 (3)			
45	7.0 (5)	9.4 (-7)	1.3	269
40	5.0 (6)	7.6 (-6)	2.4	252
35	8.0 (6)	1.7 (-5)	4.3	241
30	9.5 (7)	1.4 (-4)	9.7	228
25	3.9 (8)	6.5 (-4)	20	223
20	1.7 (9)	2.8 (-3)	43	218
15	2.0 (9)	5.0 (-3)	83	217
10	0.0	3.9 (-3)	108	217

Table 4.3.2: Optical parameters calculated from Crutzen (1971). Night profile of HNO_3

Tangent Height (km)	Number Density (cm^{-3})	Optical Mass $(atm\ cm)_{300K}$	$\bar{p}$ (mb)	$\bar{T}$ (^oK)
50	1.0 (1)			
45	1.0 (2)	1.4 (-10)	1.3	265
40	2.1 (3)	2.9 (-9)	2.4	251
35	8.0 (4)	1.1 (-7)	4.9	237
30	5.0 (6)	6.8 (-6)	10	227
25	4.0 (7)	6.0 (-5)	21	222
20	1.1 (9)	1.5 (-3)	46	217
15	1.9 (9)	3.9 (-3)	89	217
10	0.0	3.1 (-3)	120	217

Table 4.3.3: Optical parameters calculated from Crutzen (1971) Day profile of HNO_3

Tangent Height (km)	Calculated Optical Mass day	night	$(atm\ cm)_{300K}$ measured
29.7	8.3 (-6)	1.6 (-4)	2.2 (-3)
28.6	1.6 (-5)	2.4 (-4)	3.5 (-3)
24.6	1.0 (-4)	7.4 (-4)	1.1 (-2)
24.6	1.0 (-4)	7.4 (-4)	1.0 (-2)
18.8	2.1 (-3)	3.5 (-3)	2.5 (-2)

Table 4.3.4: Comparison of optical masses of HNO_3 calculated from the profiles of Crutzen (1971) with the experimental stratospheric values (Rhine et. al., 1969)

References

Abels, L. L. and J. H. Shaw, (1966), Widths and Strengths of Vibration-Rotation Lines in the Fundamental Band of Nitric Oxide. J. Molecular Spectros., 20, 11.

Adel, A., (1938), Further Detail in the Rock-Salt Prismatic Solar Spectrum Astrophys J., 88, 186.

Bates, D. R. and P B. Hays, (1967), Atmospheric Nitrous Oxide. Planet. Space Sci , 15, 189.

Crutzen, P. J., (1971), Ozone Production Rates in an Oxygen-Hydrogen-Nitrogen Oxide Atmosphere. J. Geophys. Res., 30, 7311.

Goldman, A., D. G. Murcray, F. H Murcray, W. J. Williams, T. G. Kyle, and J. N. Brooks, (1970), Abundance of N_2O in the Atmosphere between 4.5 and 13.5 km. J. Opt. Soc. Am., 60, 1466.

Goldman, A., T. G. Kyle, and F. S. Bonomo, (1971), Statistical Band Model Parameters and Integrated Intensities for the 5.9μ, 7.5μ and 11.3μ Bands of HNO_3 Vapor. App. Optics, 10, 65.

Goody, R., (1969), Time Variations in Atmospheric N_2O in Eastern Massachusetts. Planet. Space. Sci., 17, 1319.

Gray Young, L. D., (1971), Calculations of the Partition Function for $^{14}N_2{}^{16}O$. J. Quant. Spectros. Radiat. Transfer, 11, 1265.

Gray Young, L. D., (1972), Relative Intensity Calculations for Nitrous Oxide. J. Quant. Spectros. Radiat. Transfer, 12, 307.

James, T. C. and R. J. Thibault, (1964), Spin-Orbit Coupling Constant of Nitric Oxide. Determination from Fundamental and Satellite Band Origins. J. Chem. Phys., 41, 2806.

Johnston H., (1971), Reduction of Stratospheric Ozone by Nitrogen Oxide Catalysts from Supersonic Transport Exhaust. Science, 173, 517.

Junge, C. and J. Hahn, (1971), N_2O Measurements in the North Atlantic. J. Geophys. Res., 76, 8143.

King, W. T. and B. Crawford, (1972), The Integrated Intensity of the Nitric Oxide Fundamental Band. J. Quant. Spectrosc. Radiat. Transfer, 12, 443.

LaHue, M. D., J. B. Pate and J. P. Lodge, (1970), Atmospheric Nitrous Oxide in the Humid Tropics. J. Grophys. Res., 75, 2922.

Lazrus, A. L., B. Gandrud and R. D. Cadle, (1972), Nitric Acid Vapor in the Stratosphere. J. Appl. Meteor., 11, 389.

Meira, L. G., (1971), Rocket Measurements of Upper Atmospheric Nitric Oxide and their Consequence in the Lower Ionosphere. J. Geophys. Res., 76, 202.

Michels, H. H., (1971), Calculation of the Integrated Band Intensities of NO. J. Quant. Spectros. Radiat. Transfer, 11, 1735.

Murcray, D. G., T. G. Kyle, F. H. Murcray and W. J. Williams, (1969), Presence of HNO_3 in the Upper Atmosphere, J. Opt. Soc. Am., 59, 1131.

Nicolet, M., (1970), The Origin of Nitric Oxide in the Terrestrial Atmosphere. Planet. Space Sci., 18, 1111.

Norton, R. B. and C. A. Barth, (1970), Theory of Nitric Oxide in the Earth's Atmosphere. J. Geophys. Res., 75, 3903.

Pierce, J. B., (1969), Rocket Measurement of Nitric Oxide between 60 and 96 Kilometers. J. Geophys. Res., 74, 853.

Pliva, J., (1968), Molecular Constants of Nitrous Oxide, $^{14}N_2{}^{16}O$. J. Mol. Spectros, 27, 461.

Pontano, B. A., and L. C. Hale, (1970), Measurement of an Ionizable Constituent of the Lower Ionosphere Using a Lyman-Alpha Source and Blunt Probe. Space Research, 10, 208.

Rhine, P. E., L. D. Tubbs and D. Williams, (1969), Nitric Acid Vapor Above 19 km in the Earth's Atmosphere. Appl. Optics, 8, 1500.

Schütz, K., C. Junge, R. Beck and B. Albrecht, (1970), Studies of Atmospheric N_2O. J. Geophys. Res., 75, 2230.

Seeley, J. S., and J. T. Houghton, (1961), Spectroscopic Observations of the Vertical Distributions of Some Minor Constituents in the Atmosphere. Infrared Phys., 1, 116.

Shaw, J. H., G. B. B. Sutherland and T. W. Wormell, (1948), Nitrous Oxide in the Earth's Atmosphere. Phys. Rev., 74, 978.

Strobel, D. F., (1979), Odd Nitrogen in the Mesosphere. J. Geophys. Res., 76, 8384.

Tejwari, G. D. T. and P. Veranasi, (1971), Theoretical Line Widths for N_2O-N_2O and N_2O-Air Collisions. J Quant. Spectrosc. Radiat. Transfer, 11, 1659.

Chapter 5. Atmospheric Aerosols

5.1 Introduction

This initial study of the feasibility of determining the characteristics of atmospheric aerosols by satellite remote sensing techniques suffers from our lack of knowledge of the physical (including optical) characteristics of aerosols, from some imperfections in theories of atmospheric radiation processes and from a lack of precision in possible methods of inversion of radiation measurements to aerosol parameters. Nevertheless, the existing data and theories are reviewed in an attempt to indicate spectral regions and techniques which may possibly be used to determine atmospheric aerosol characteristics.

Our knowledge of physical and optical properties of aerosols are reviewed in the next section. Some remote sensing techniques that have already been used are then briefly described. Finally two techniques for the remote sensing of stratospheric aerosols from satellites are considered and their feasibility and practicability are discussed.

5.2 Survey of Experimental Data on Atmospheric Aerosols

The fundamental parameters needed for a study of remote sensing of atmospheric aerosols are the physical characteristics of size distribution, number density and index of refraction. This survey is an attempt to provide a suitable but not exhaustive summary of information on these parameters.

5. 2. 1 Sources of Atmospheric Aerosols

Atmospheric aerosols are both man made and formed by natural processes, i. e. :

a) Mechanical processes (including winds) disrupt and disperse matter from the earth's surface.

b) Trace gases react chemically in the atmosphere producing aerosol particles.

c) Smoke formed by industrial and agricultural combustion conveys aerosols into the atmosphere.

d) Vapors produced by condensation and sublimation rise into the atmosphere.

e) Extra terrestrial matter falls into the atmosphere.

Fig. 5. 1 (Hidy and Brock, 1970) is an interesting summary indicating the origin and nature of particles of various sizes. Fig. 5. 2 (Junge, 1963) indicates nomenclature often used to describe atmospheric aerosols. The smallest particles (Aitken particles), of size $r < 0.1\mu m$, are not very different from molecules in their optical properties. The "large particles", from $0.1\mu m$ to $1\mu m$ in radius have optical properties which show strong dependence on size and shape (Rozenberg, 1966). The giant particles, with $r > 1\mu$, consists mainly of cloud and fog particles and mineral dust.

The form of the atmospheric aerosol is modified considerably with the passage of time. Absorption of water vapour, coagulation, sedimentation, rainout, washout, attachment and chemical reactions tend to reduce the number of very small and very large particles. Distribution processes (transport and diffusion) transfer particles from place to place until removal from the atmosphere. Fig. 5. 3 (Junge, 1963) shows theoretical changes in size and volume distribution of continental aerosols due to coagulation.

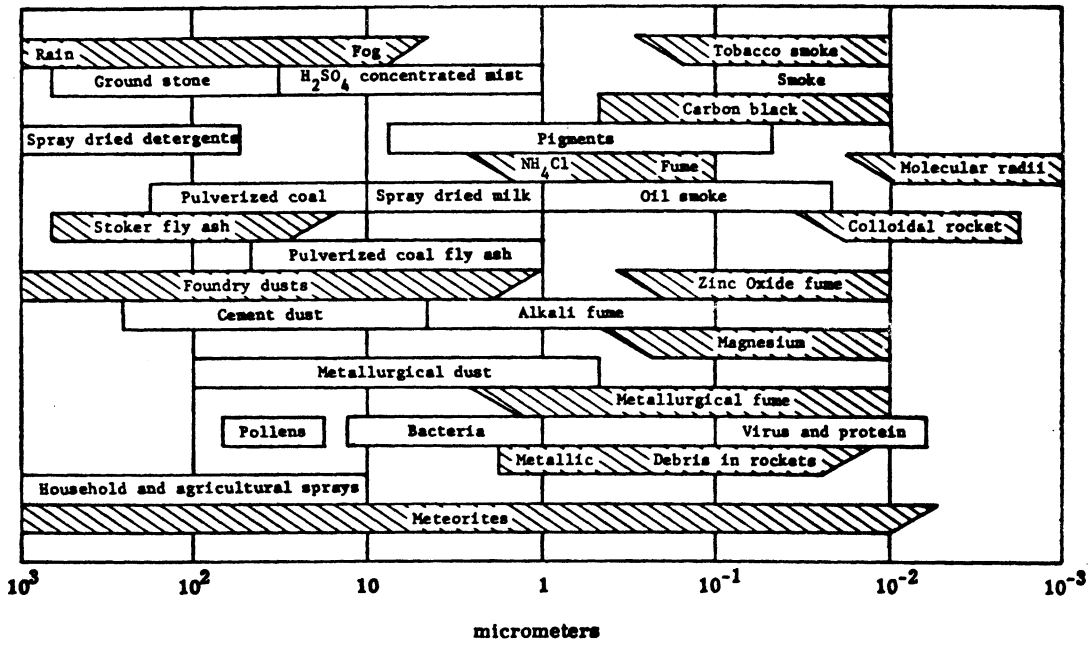

Fig. 5.1 Size range of atmospheric particles. (From Hidy and Brock, 1970).

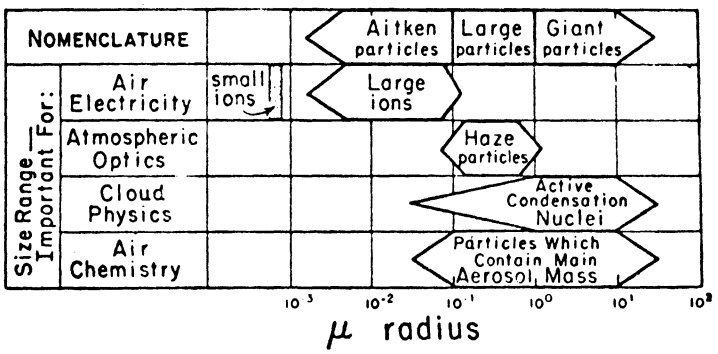

Fig. 5.2 Nomenelature of nautral acrosols and the improtance of particle sizes for various fields of meteorology (from Junge, 1963).

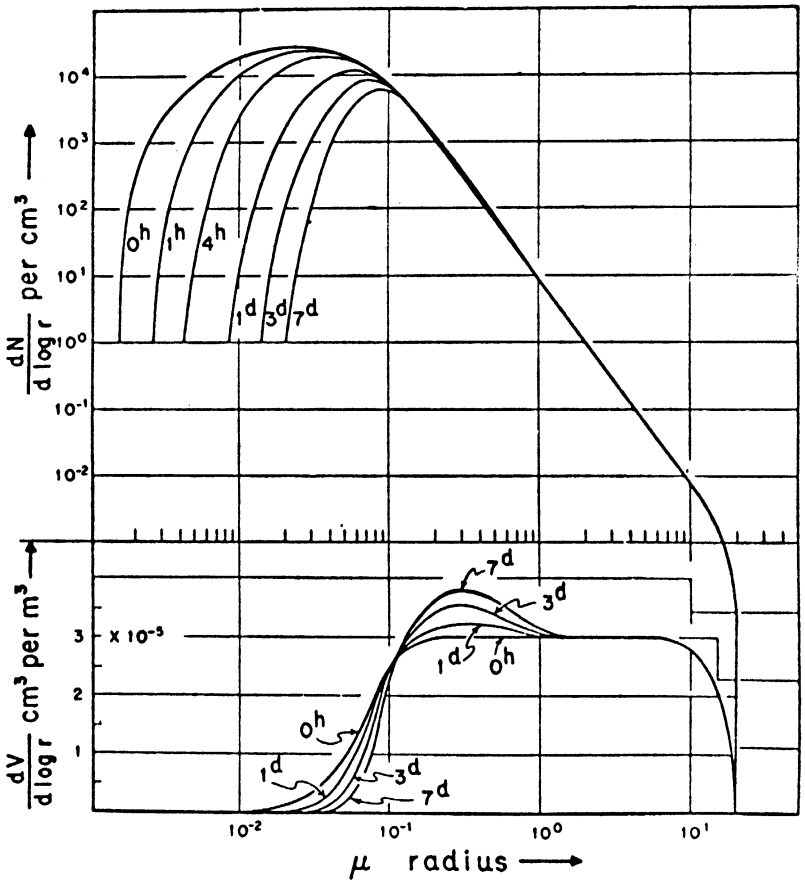

Fig. 5.3 Calculated change in the size and volume distribution of continental acrosols due to coagulation. h=hours, d=days (from Junge, 1963).

5. 2. 2 Number Densities

Surface number densities of aerosols are highly variable and usually in the range of 100 to 500 particles per cm^3. Concentrations as high as 20, 000/cm^3 may be found in industrial areas. Concentrations are assumed to diminish approximately exponentially with height for the first few kilometers. At the tropopause (at mid latitudes) number densities of a few particles per cm^3 are generally found. In the lower stratosphere (at about 20 km) there is a maximum in the aerosol particle distribution. Fig. 5. 4 (Chagnon and Junge, 1961) shows this increase for particles larger than about 0. 1μm radius. This stratospheric aerosol layer has a latitude dependent number density as indicated in Table 5. 1 from Rosen (1968).

Number Density	Location
25 cm^{-3}	Panama
8	Minneapolis
2	Ft. Churchill

Table 5. 1: Latitude dependence of stratospheric number densities (Rosen, 1968).

Since the altitude of the altitude of the tropopause decreases with latitude, the altitude of the aerosol layers decreases accordingly as shown in Fig. 5. 5 (Newell and Gray, 1972).

Additional well defined layers exist at the level of about 25 km (nacreous clouds) and at the 80 km level (noctilucent clouds). Aerosol layers have been observed near the 40-50 km level also. They often form within temperature inversions.

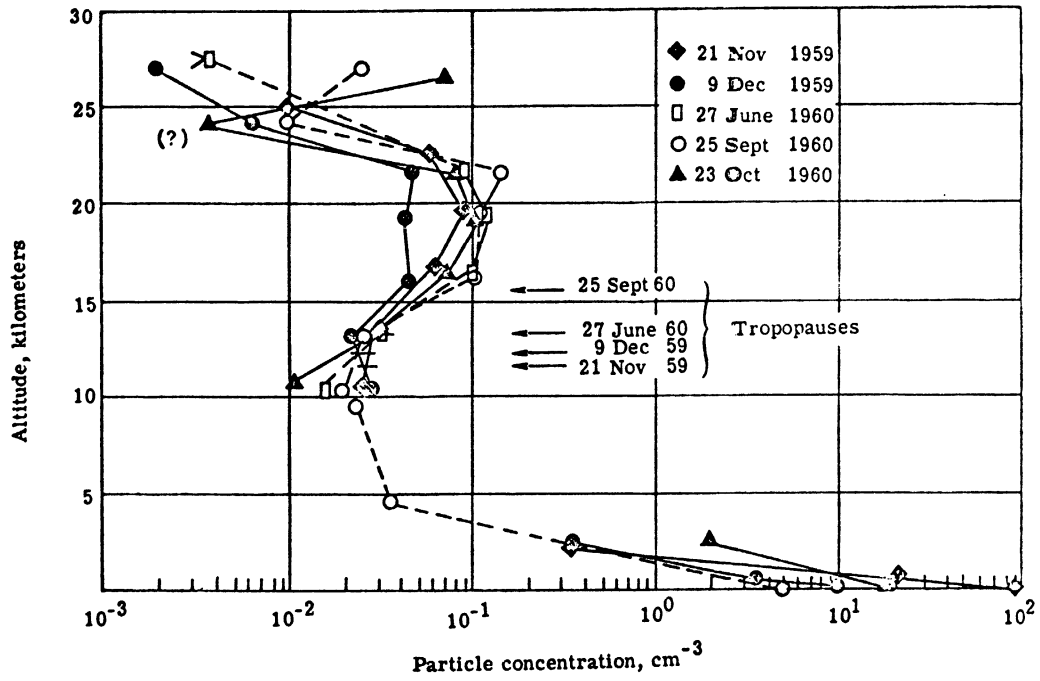

Fig. 5.4 Vertical distribution of stratospheric particles collected by inertial impactors, according to Chagnon and Junge (1961). Tropospheric measurements of other investigators are included for comparison.

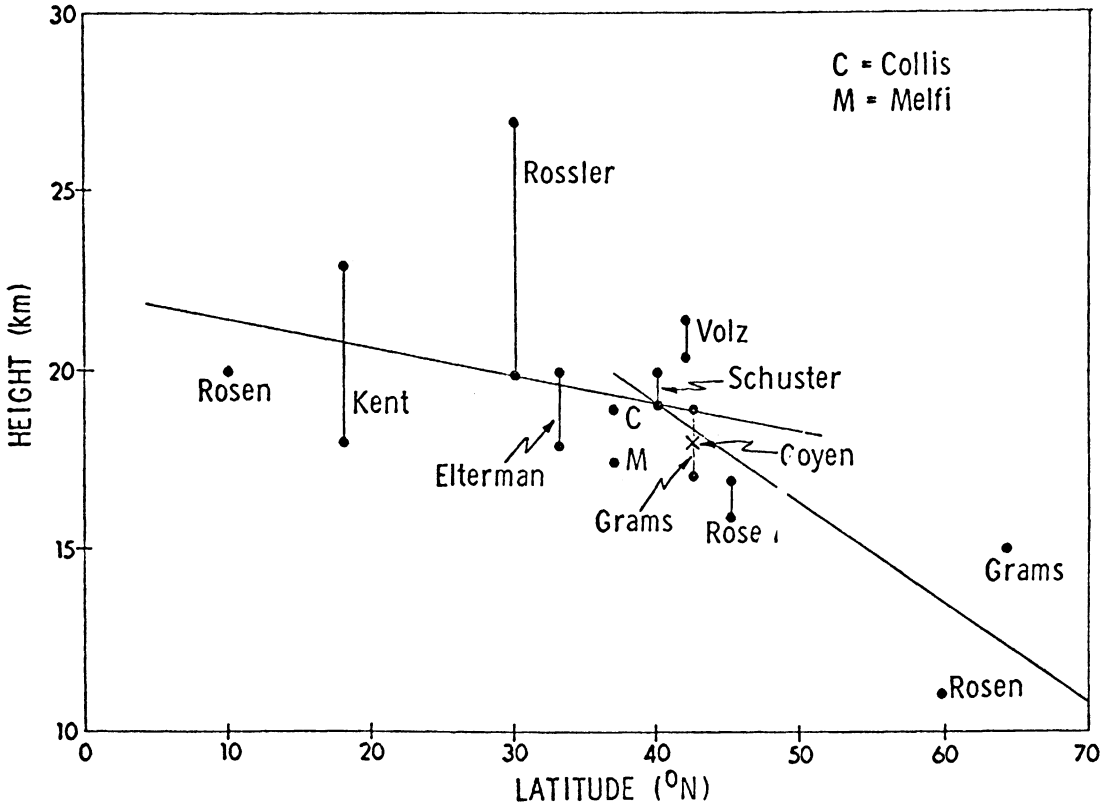

Fig. 5.5 Height variation of tropopausal aerosol layer with latitude from(Newell and Gray, 1972).

5. 2. 3 Composition of Stratospheric Aerosols

The stratospheric aerosol layer contains a large portion of sulfate particles. In addition, it contains nitric acid vapor, chlorine, bromine, silicates and other substances.

It is believed that sulfate particles are formed within the stratosphere itself by oxidation of the trace gaseous hydrogen sulfide (H_2S) and sulfur dioxide (SO_2) that enter the atmosphere by vertical mixing.

During volcanic eruptions gaseous and solid material is thrown up into the atmosphere, sometimes as high as the stratosphere. Some of this material is sulfurous.

The following summary (Table 5. 2) of possible stratospheric aerosol constituents is taken from Remsberg (1971).

$(NH_4)_2SO_4$	A	H_2O(ice)	B
H_2O_2	A	Na_2SO_4	B
H_2SO_4	A	$NaHSO_4$	B
HNO_3	A	NH_4HSO_4	B
$NOHSO_4$	A	$NH_2SO_3NH_4$	B
HNO_3-H_2SO_4-H_2O	A	NH_2SO_3H	B
NaCl	B	SO_2	B
NH_4Cl	B	H_2S	B
H_2CO_3	B	Cl_2	B
H_2SO_3	B	NOCl	B
HCl	B	$(NH_4)_2S_2O_8$	B
HNO_2	B	SiO_2	B
NH_4OH			

A abundant or more probable constituents

B minor or unlikely constituents

Table 5. 2: Possible constituents of stratospheric aerosol (Remsberg, 1971)

5. 2. 4 Size Distribution

A variety of aerosol size distribution forms have been used in the literature. Among these are:

a) The power law distribution:

$$n(r) = ar^{-\alpha} \qquad (5\text{-}1)$$

b) The logarithmic Gaussian or log normal form:

$$\frac{dn(r)}{dr} = N_o \exp\left[- A \log \left(\frac{r}{r_o} \right)^2 \right] \qquad (5\text{-}2)$$

c) Diermendjian's (1964) modified Γ distribution:

$$n(r) = ar^{\alpha} \exp(-br^{\gamma}) \qquad (5\text{-}3)$$

where

r, r_o = particle radius, cm

$n(r), N_o$ = no/cm^3

a, A, b, α, γ = constants

A convenient summary of experimental data on aerosol size distributions is that of Newell and Gray (1972).

"Distribution types commonly found in the literature include power law, bimodal, and Gaussian logarithmic forms. The power law size distribution in the form $m(r) = cr^{-\alpha}$, where r is particle radius, is ubiquitous. Values of the exponent α range from 1. 5 (Rosen, 1968) to 7 at 51 km altitude (Elliot, 1970). More common values seen in the literature are in the 3-to-4 range, as found, for example, by Newkirk (1964), Rosen (1968) (under certain conditions), Mossop (1965), Carnuth (1970) and Pueshel (1967). It has been suggested (Newkirk, 1964) that aerosol layers actually represent the addition of large numbers of small particles to a normal background of larger particles. If this is true, one would expect to see an increase in the effective α within layers, and such an effect has been observed by Rowen (1968).

Friend (1966) and Quenzel (1970) have proposed that the log-normal distribution is more representative of true populations. Others, notably Mossop (1965), Sherwood (1967) and Pilipowskyj (1968) have found that the correct distribution form is bimodal, with one peak in the 0.01μ region and the second peak near 0.2μ. Storebo (1970) has derived such a distribution on a theoretical basis. Mean particle radius estimates for stratospheric aerosols have been made by Bigg (1970), who found $\overline{r}$ = 0.1 to 0.4μ, and Mossop (1965), who found $\overline{r}$ = 0.1μ.

The diversity of these results indicates a need for extensive further study of size distributions. Each of these measured distributions may have been representative of the aerosol population at the particular time and location of the measurement."

Recent results are those of Blifford and Ringer (1969). A total of 329 size distributions, obtained from measurements of atmospheric aerosols collected at altitudes from the surface to 9 km were considered. The authors speculate that the global aerosol may be described by three overlapping log normal distributions which have means:

a) in the submicron or pollution aerosol range
b) in the Mie scattering range where atmospheric modification processes are relatively inefficient
c) in the large particle ($r > 1.0\mu$m) range which is dominated principally by soil dust and biological particles and near the ocean surface by sea salt.

In another paper De Luisi, et. al. (1972) fitted data to Diermendjian's Γ distribution function with $\alpha = 1$. The initial data are given in Fig. 5.6. Table 5.3 contains the derived constants and Fig. 5.7 shows curves of n(r) using the constants of Table 5.3

TABLE 5.3 Constants for Deirmendjian's (1964) Modified Distribution Function (Equation 1) for a = 1.0 (from de Luisi, et. al., 1972)

Volume Concentration, cm^{-3}	γ				a				b			
	S	PO	DV	All	S	PO	DV	All	S	PO	DV	All
0.1	0.6512	0.3840	0.6289	0.4081	4.440	9.662 (+1)	2.721	8.099 (+1)	4.677	7.963	4.093	7.821
0.2	0.3432	0.3729	0.3543	0.3153	1.423 (+3)	3.118 (+2)	5.481 (+2)	2.783 (+3)	1.024 (+1)	8.499	9.125	1.090 (+1)
1.0	0.0908	0.3840	0.2393	0.2458	2.431 (+17)	1.504 (+3)	1.677 (+6)	5.488 (+5)	4.206 (+1)	8.504	1.616 (+1)	1.483 (+1)
3.0	0.0502	0.3877	0.2504	0.2346	8.271 (+32)	4.372 (+3)	4.649 (+6)	3.727 (+6)	7.688 (+1)	8.479	1.623 (+1)	1.570 (+1)
10.0	0.0501	0.3988	0.2652	0.2309	3.586 (+33)	1.153 (+4)	8.440 (+6)	1.670 (+7)	7.718 (+1)	8.235	1.568 (+1)	1.602 (+1)

The following legend defines the locations where the measurements were made: S is Scottsbluff, Nebraska (125 measurements); PO is the Pacific Ocean (82 measurements); DV is Death Valley, California (81 measurements); and All is a combination of the three locations (288 measurements). The numbers in parentheses are the powers of 10 by which the associated constants are multiplied.

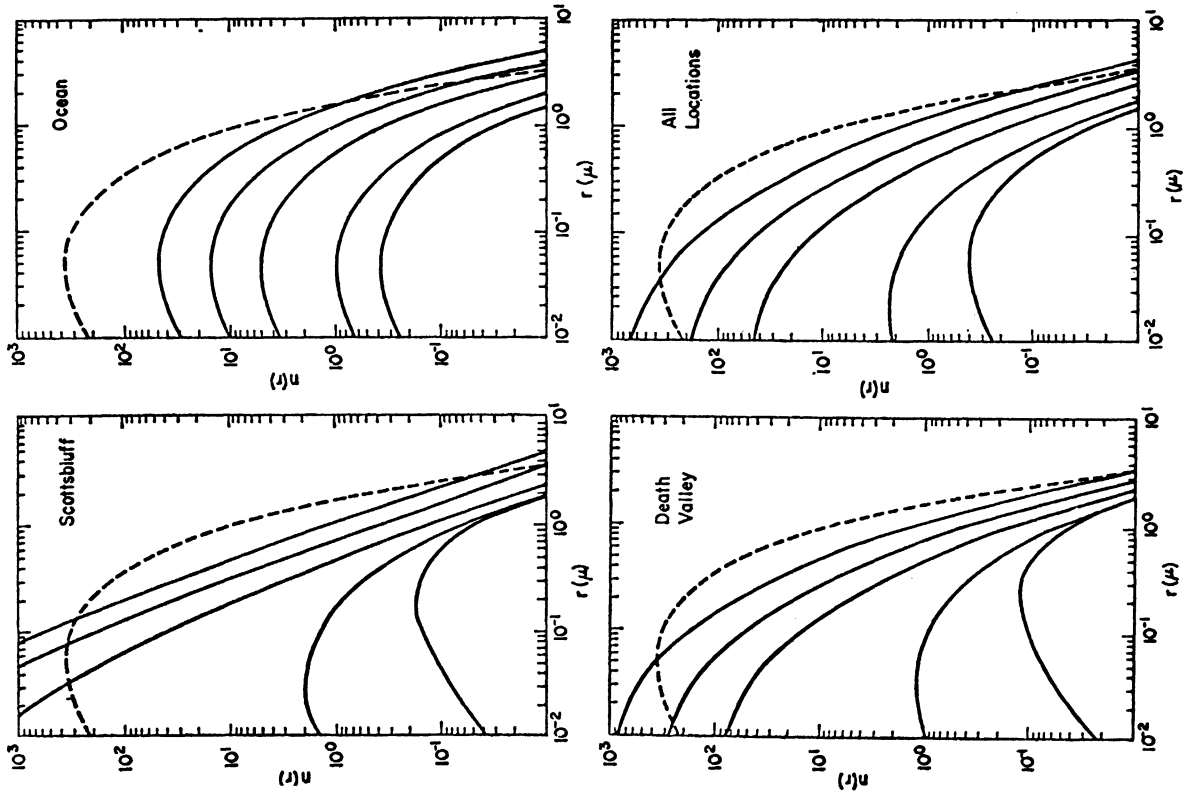

Fig. 5.7 Curves of n(r) using the constants from Table 1. The dashed curve represents Deirmendiian's haze M(a=5.333 X 104, b=8.9443, γ=1.0) (from de Luisi, et. al., 1972).

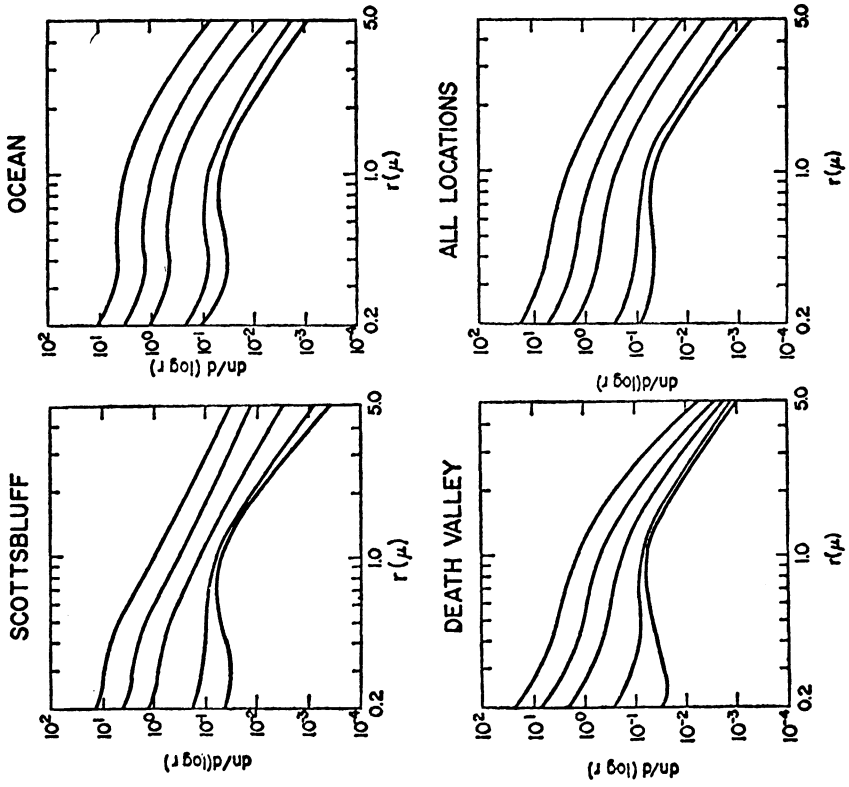

Fig. 5.6 Size distribution curves generated by linear regression for particle concentrations 0.1 (lowest curve), 0.2, 1.0, 3.0, and 10.0 cm^{-2} (from de Luisi, et. al., 1972).

Remsberg (1971) in his dissertation on the "Radiative Properties of Several Probable Constituents of Atmospheric Aerosols" used three models of aerosol distributions for stratospheric particles:

a) The bimodal size distribution used by Pilipowsky, et. al. (1968) to explain lidar and radiometersonde observations:

$$\frac{dN_1(r)}{d(\log r)} = 2.31\, \nu \bar{N}_1 \left(\frac{r}{r_{1\min}}\right)^{-\nu} \qquad 0.1 < r \leq 10\mu m \qquad (5\text{-}4)$$

where

$\nu = 2.5$

$r_{1\,\min} = 0.1\mu m$

$\bar{N}_1 = 5.2$ particles/cm^3

$$\frac{dn_2(r)}{d(\log r)} \geq 2.5 \cdot 10^8 \qquad 0.003 < r < 0.01\mu m \qquad (5\text{-}5)$$

b) The bimodal distribution that deBary and Roessler (1970) used to explain scattered radiation from a dust layer. The distribution is defined by three functions:

$$\frac{dN(r)}{d(\log r)} = 10^{-0.474}\, r^{-3.82} \qquad 0.3 < r \leq 1\mu m \qquad (5\text{-}6)$$

$$\frac{dN(r)}{d(\log r)} = 10^{+3.719}\, r^{+4.193} \qquad 0.1 < r \leq 0.3\mu m \qquad (5\text{-}7)$$

$$\frac{dN(r)}{d(\log r)} = 10^{+5} \qquad 0.03 \leq r \leq 0.05\mu m \qquad (5\text{-}8)$$

c) A modified Dermendjian "haze M" model:

$$\frac{dN(r)}{d(\log r)} = 5.63 \cdot 10^8\, r^2 e^{-22.9 r^{0.55}} \qquad (5\text{-}9)$$

The three distributions are plotted in Fig. 5.8.

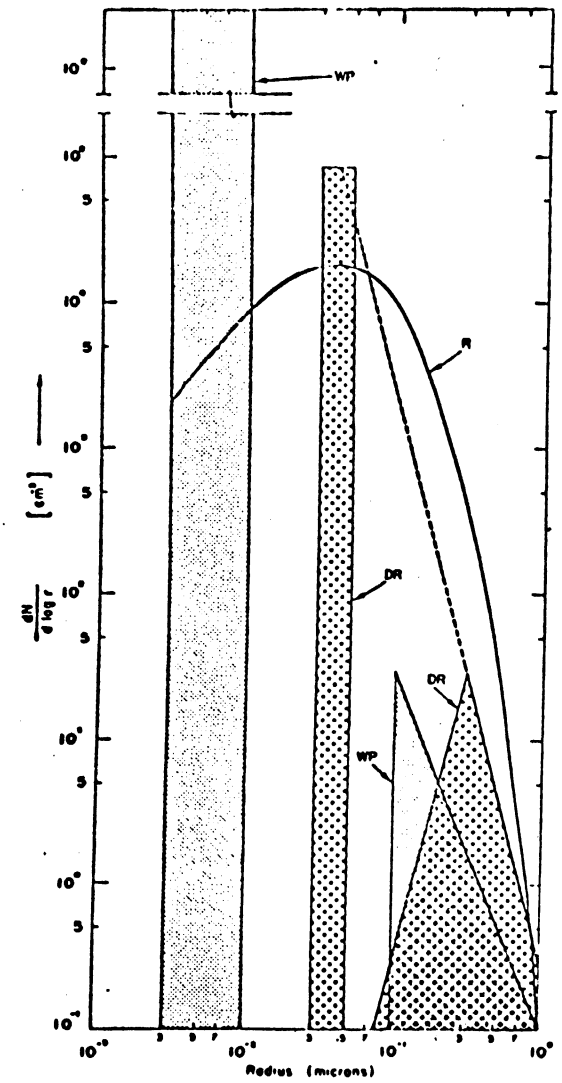

Fig. 5.8 Aerosol size distributions WP (Pilipowakyj, et. al., 1968), DR (de Bary and Roosaler, 1970). R (modified Deirmendjian haze "M" distribution) (from Remsberg, 1971).

5.2.5 Optical Characteristics of Aerosols

a) Index of Refraction of Aerosols

Knowledge of the complex index of refraction of aerosol particles is necessary for investigating the visible and near infrared radiation effects of aerosols. In the visible and near infrared investigators have usually assumed that aerosols are non absorptive and have real indices in the range of 1.33-1.5. The value of 1.33 is associated with water spheres, 1.42 is the real part of the index of refraction of hygroscopic sulfate.

The complex part of the refractive index is very important for the remote sensing of aerosols. Although, as noted above, it has generally been assumed that the absorptive part of the index is zero for aerosols in the visible and near infrared, recent measurements indicate that this may not be true. Bullrich (1969) has found a wavelength dependent absorptive index for hygroscopic sulfates, varying from 0.033 at 4000Å to 0.055 at 9200Å.

Data on the infrared refractive index of atmospheric aerosol substances have recently been presented by Volz (1972). The real part n and the imaginary (absorptive) index n' are given for dust, aerosol water solubles, sea salt and water for the wavelength range 2.5 to 40μm. The results are shown in Figs. 5.9, 5.10 and 5.11.

Remsberg (1971) has published absorption and refractive index data for aqueous solutions of ammonium sulfate and nitric acid for the spectral range of 7.5 to 14μm, within an instrument resolution of 1-3 cm^{-1}. The data are shown in Figs. 5.12, 5.13, 5.14 and 5.15. Data on crystalline ammonium sulfate are given in Figs. 5.16. (Chermack, 1970).

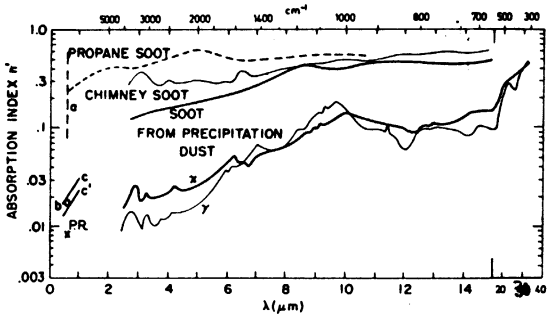

Fig. 5.9 Absorption index vs wavelength of dust and soot as calculated from transmittance measured by the potassium bromide disk technique. (from Volz, 1972)

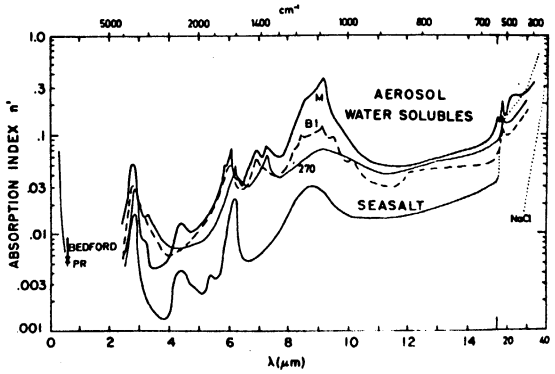

Fig. 5.10 Absorption index of water soluble aerosol substance, typical for continental rain (sample M) and continental and arctic snow as well as tropical rain (sample 270), and sea salt(from Volz, 1972)

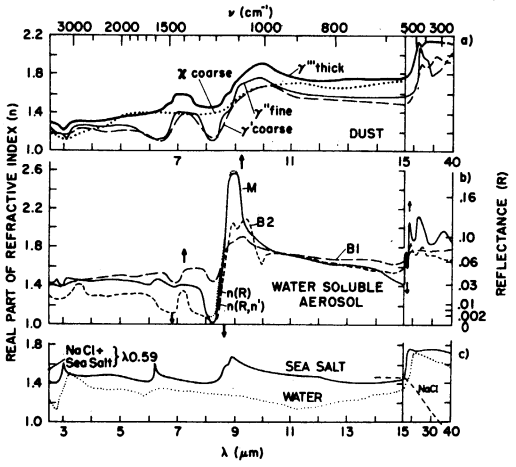

Fig. 5.11 Real part of the refractive index of dust from precititation (a), water soluble aerosol substance (b), and water and sea salt (c). Dotted line line on curve M near 9 μm: only reflection considered (from Volz, 1972).

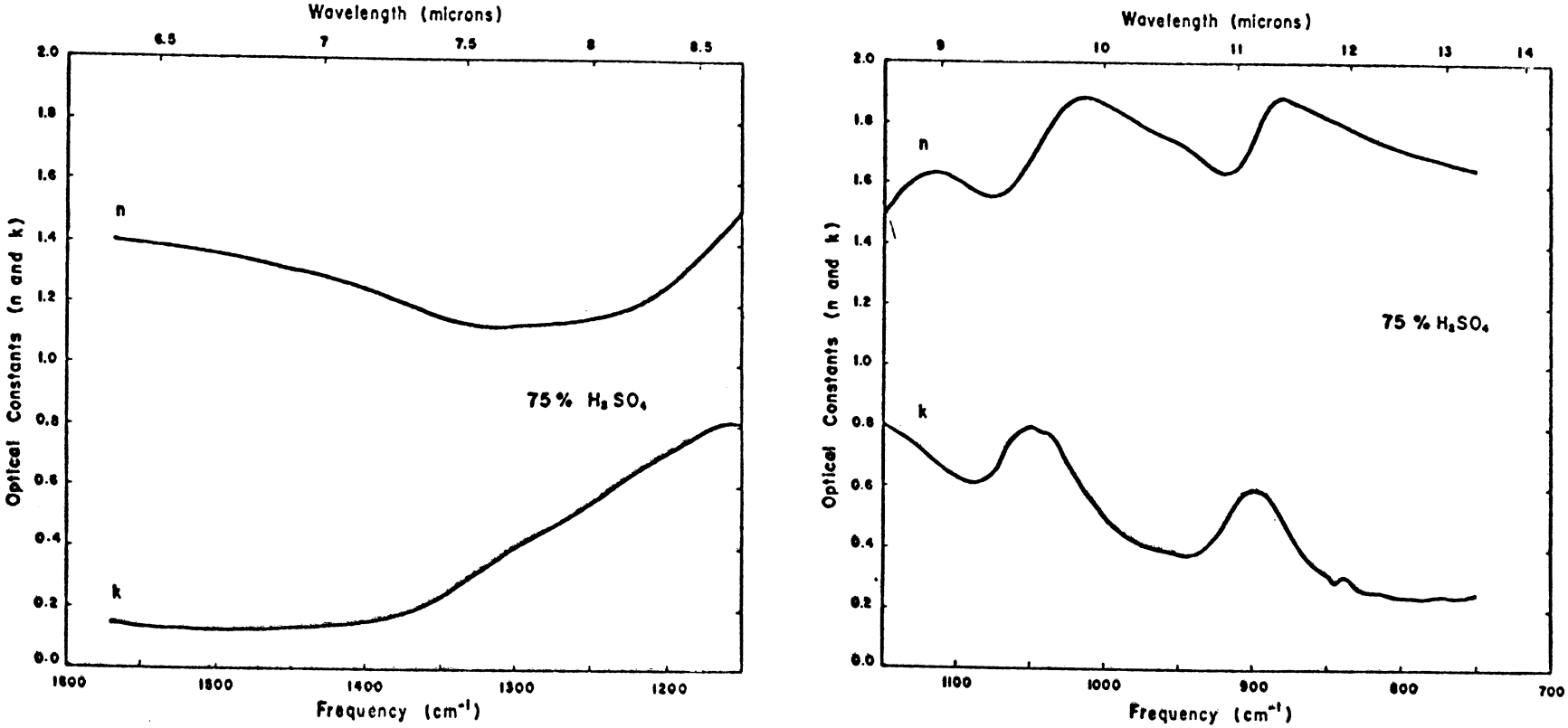

Fig. 5.12 Optical constants for 75% H_2SO_4 (Remsberg, 1971)

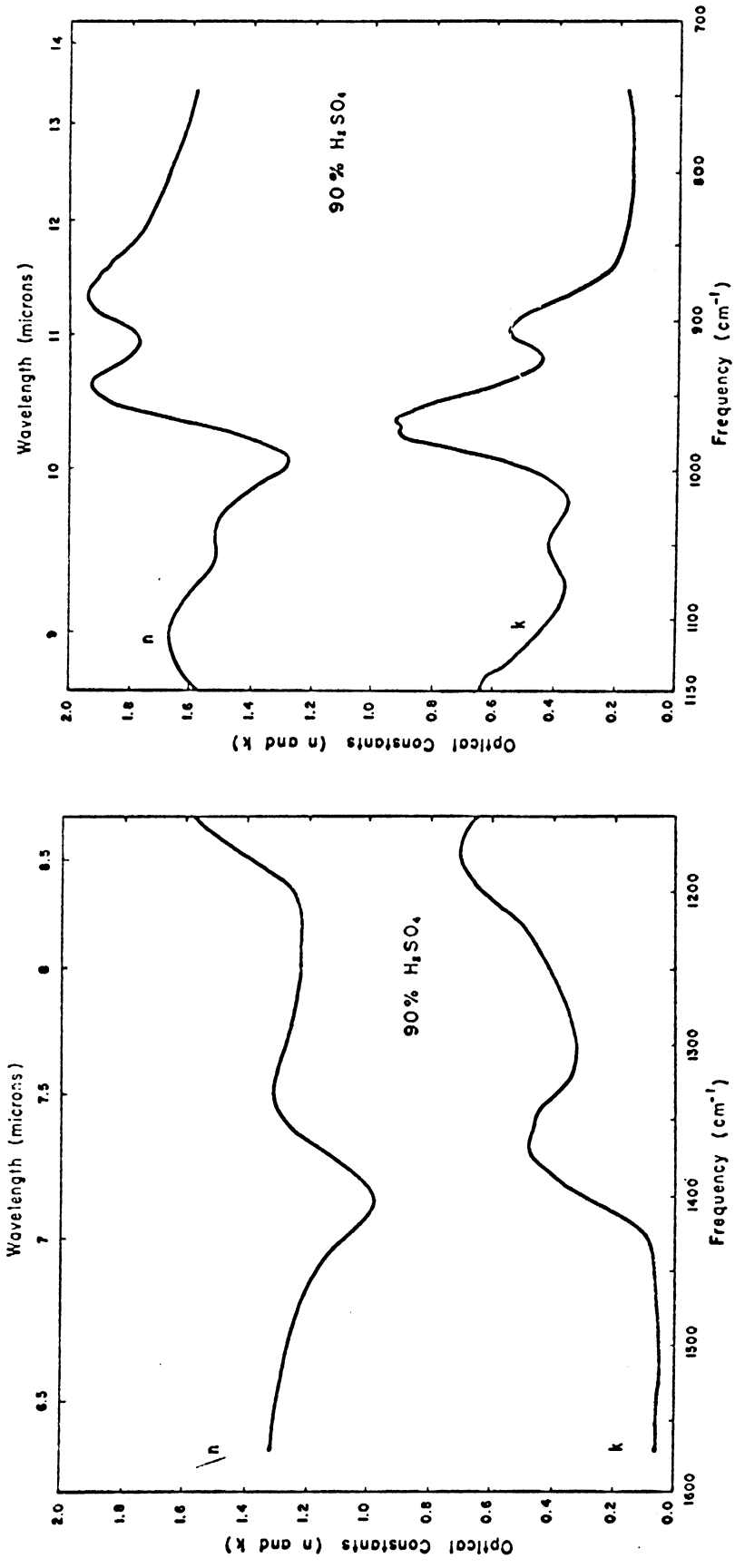

Fig. 5.13 Optical constants for 90% H_2SO_4 (from Rensberg, 1971)

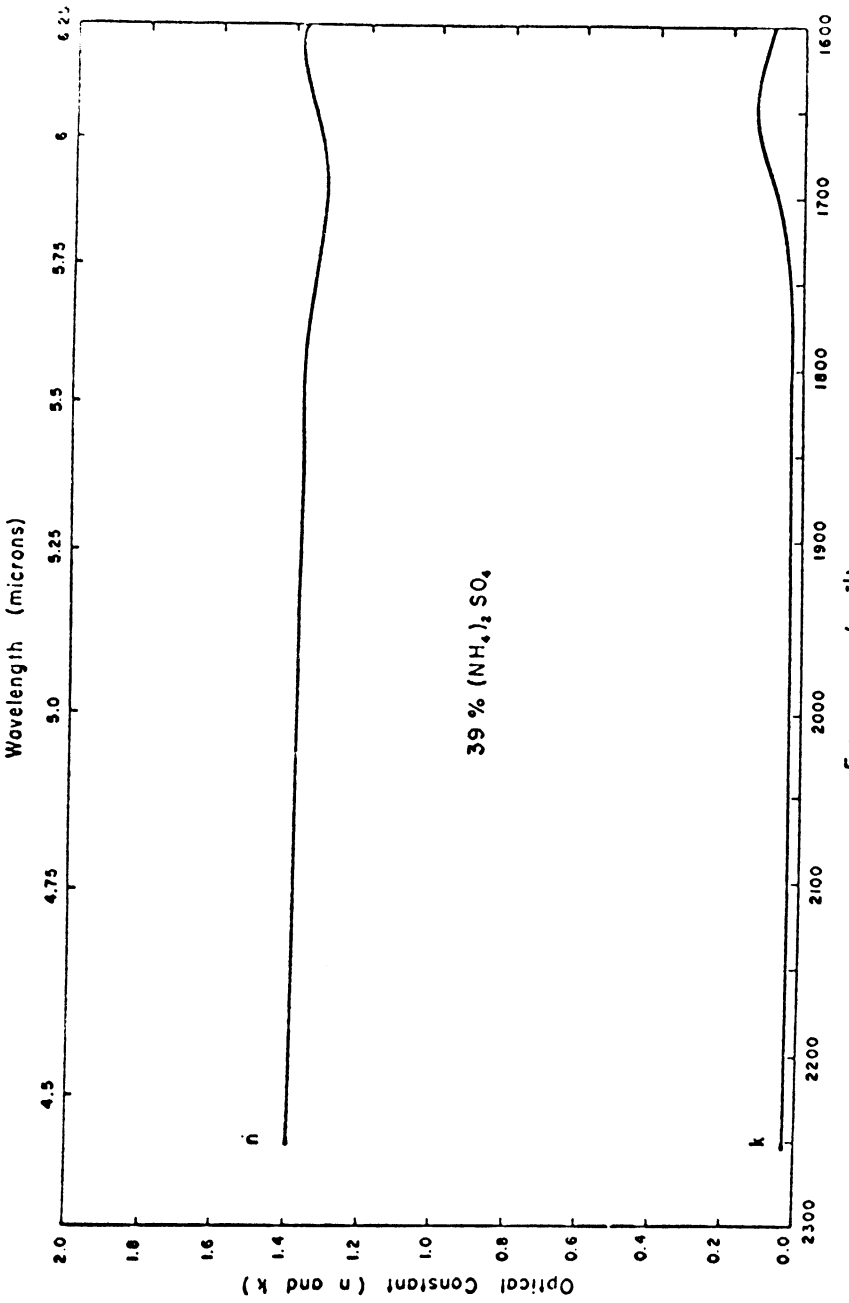

Fig. 5.14 Optical constants for 39% $(NH_4)2\ SO_4$ (from Rensberg, 1971)

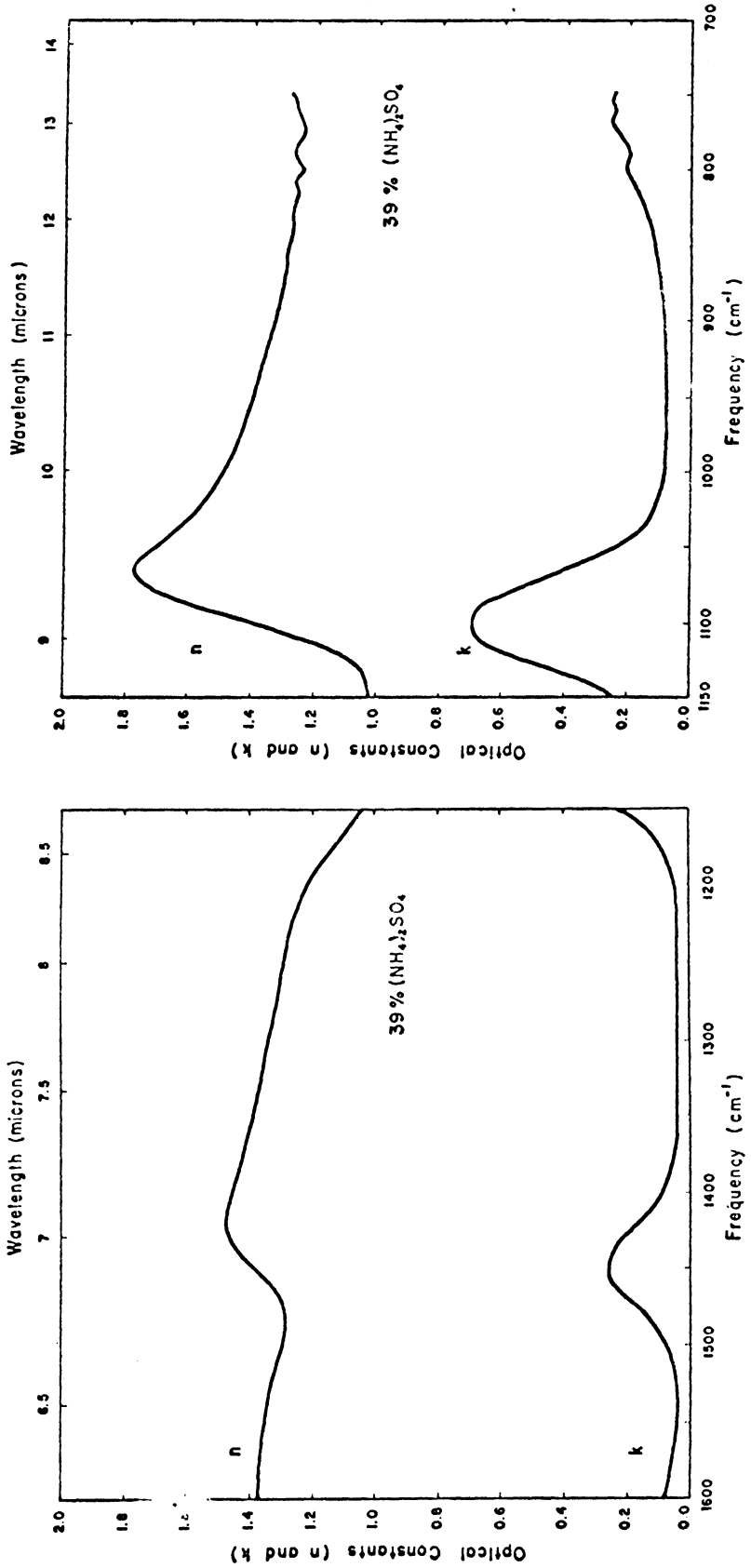

Fig. 5.14 continued.

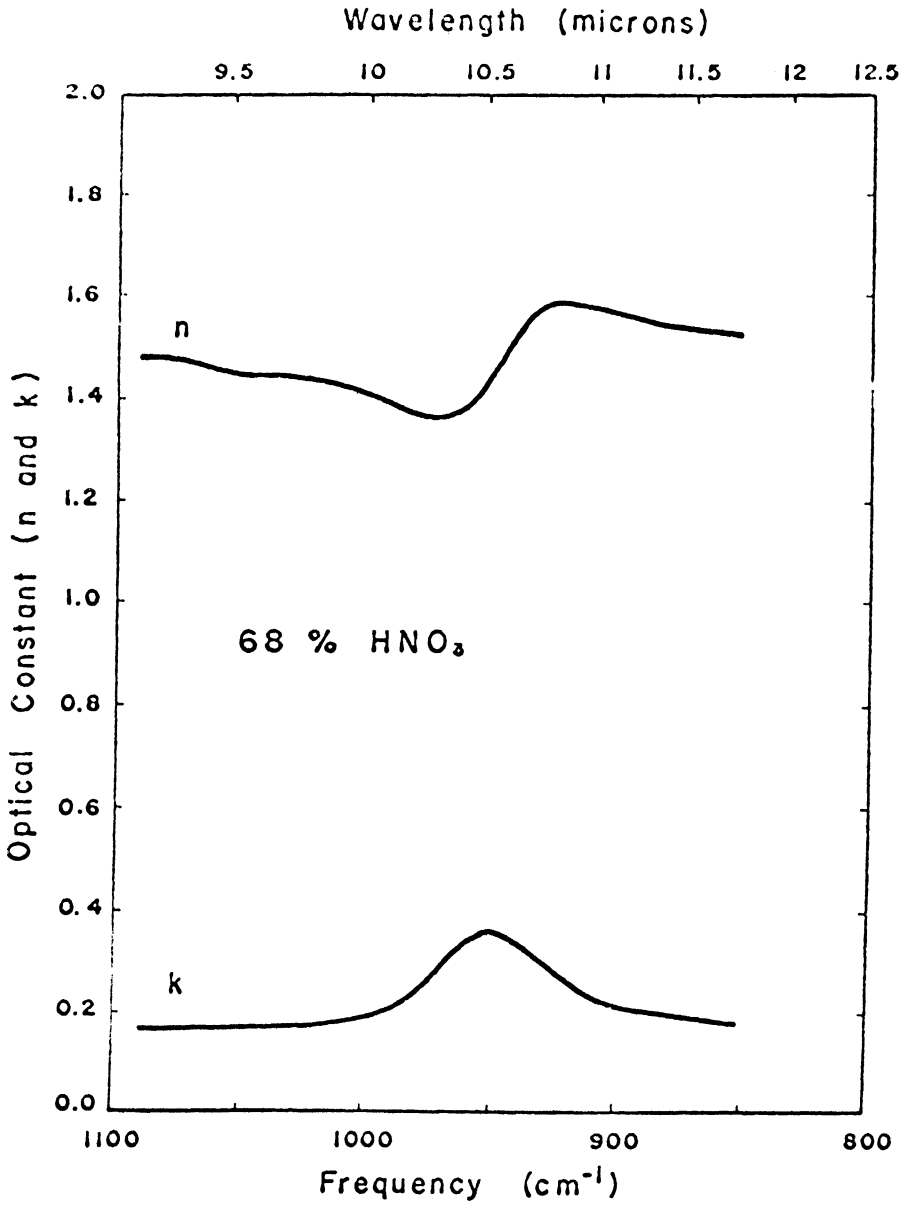

Fig. 5.15 Optical constants for 68% HNO_3 (from Remsberg, 1971)

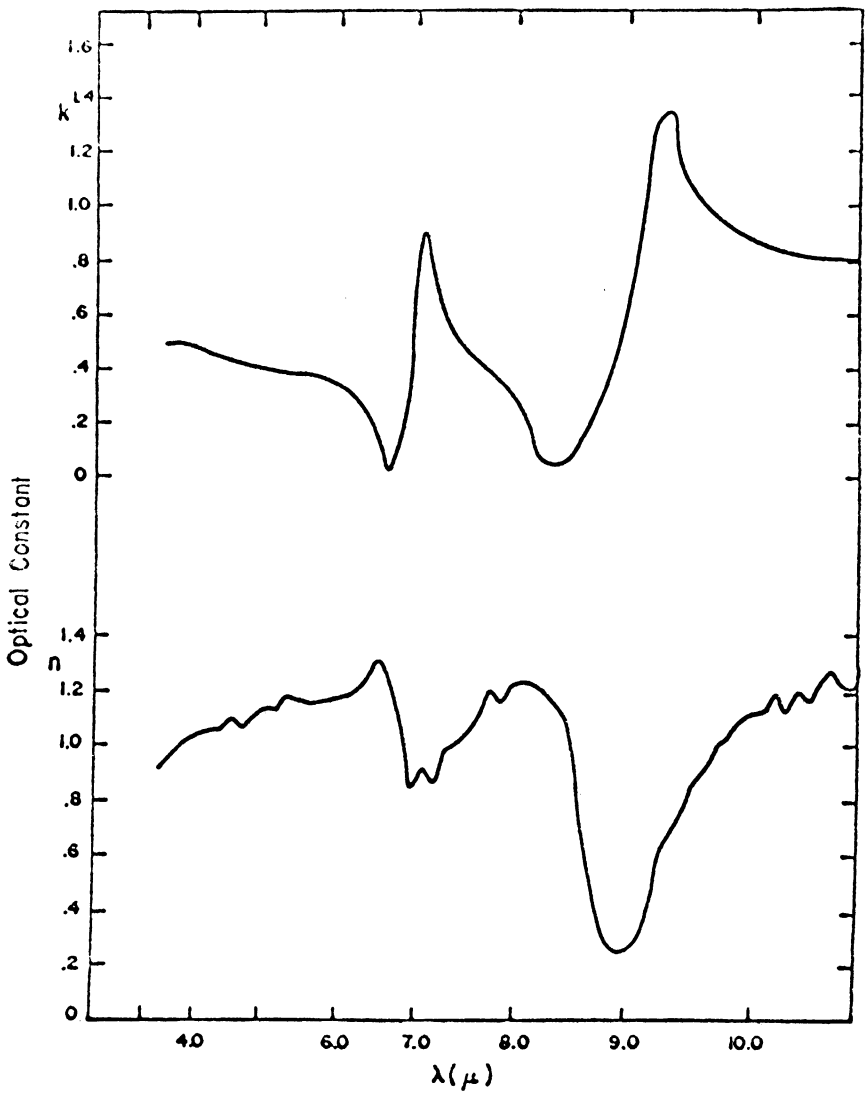

Fig. 5.16 Optical constants for crystalline ammonium sulfate, Chermack (1970).

b) Extinction Coefficients

The basic equation of radiative transfer which describes the attenuation of a beam of radiation of intensity I_λ is:

$$dI_\lambda = -I_\lambda \beta_{ext}(\lambda)\, ds \tag{5-10}$$

with

$$\beta_{ext} = \int_{r_1}^{r_2} \pi r^2 Q_{ext}(r, \lambda, \hat{n}) \frac{dn(r)}{dr} dr \tag{5-11}$$

$$Q_{ext} = Q_{sca} + Q_{abs}$$

where Q_{ext}, Q_{sca}, Q_{abs} are efficiency factors determined by Mie scattering theory as a function of particle size r, wavelength λ and complex index of refraction n. Techniques for calculating these factors are given in Deirmendjian (1961)

In the UV and visible , it is usually assumed that extinction by aerosols is only due to scattering and that absorption is negligible. However, as noted above Bullrich has found absorption effects for hygroscopic sulfates. A typical curve of aerosol extinction at 5500Å (Newell and Gray, 1972) is shown in Fig. 5.17.

In the infrared Q_{scat} is normally negligible compared to Q_{abs}. The equation for the attenuation of a beam of radiation could then be written:

$$dI_\lambda = -I_\lambda \beta_{abs}(\lambda)\, ds \tag{5-13}$$

Emitted ratiation would be given by:

$$dI_\lambda = \beta_{abs}(\lambda) \cdot B(T, \lambda)\, ds \tag{5-14}$$

where $B(T, \lambda)$ is the Planck function at temperature T. Curves of $\beta_{ext} = \beta_{abs}$ by Remsberg are shown in Figs. 5.18, 5.19, 5.20 and 5.21. His calculated emitted intensities for a 1 km path are shown in Figs. 5.22, 5.23, 5.24, 5.25 and 5.26.

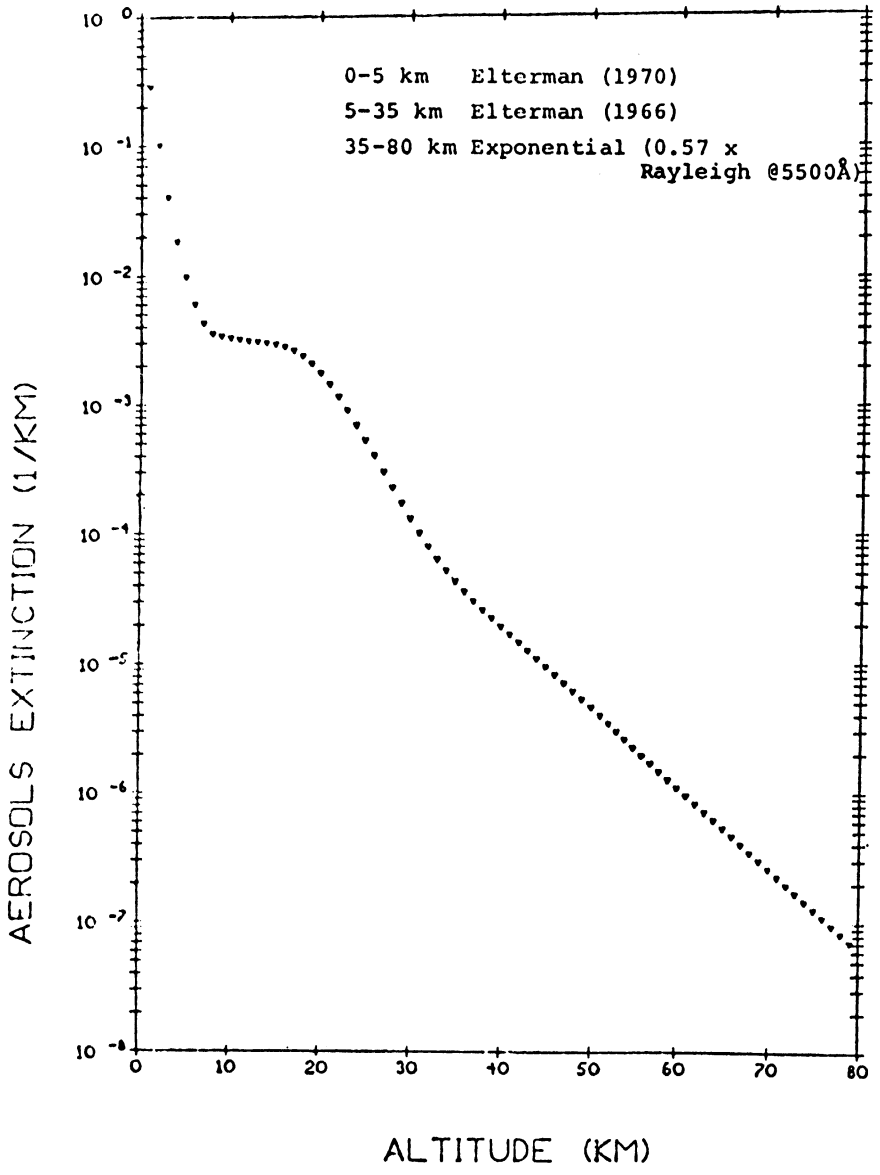

Fig. 5.17 Reference Aerosol Extinction Model λ=5500 Å (from Newell and Gray, 1972).

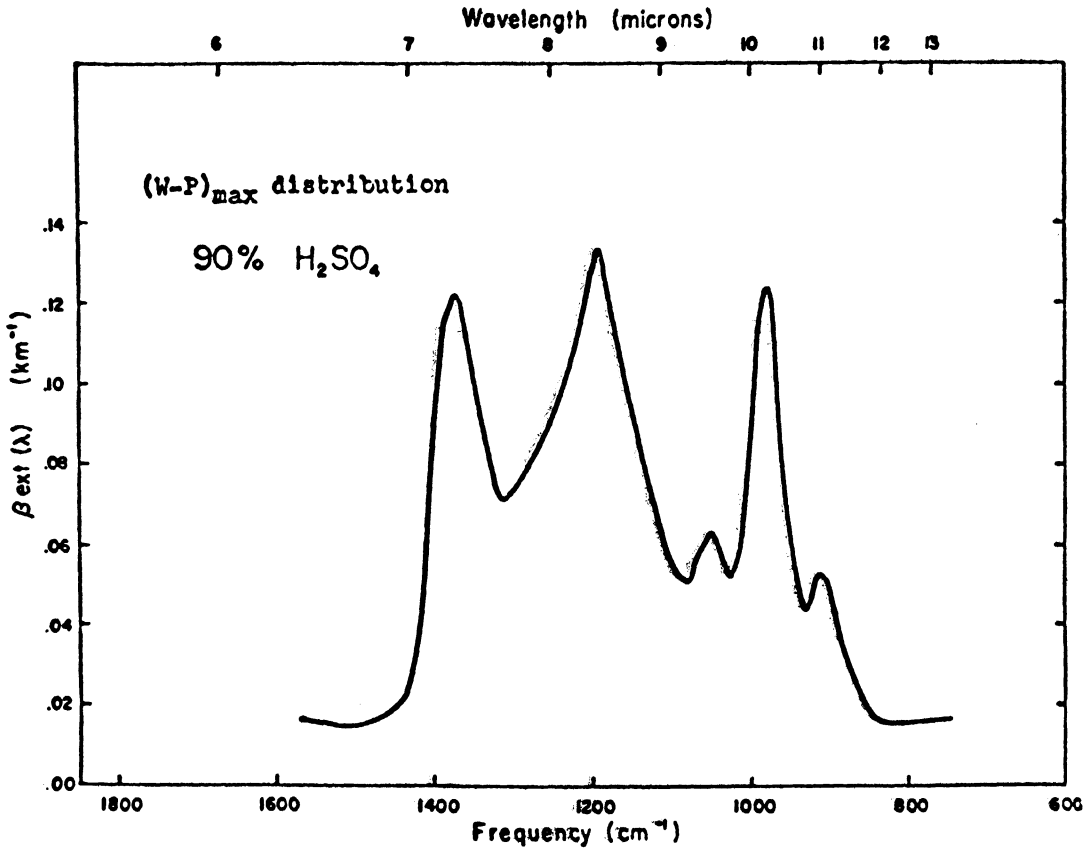

Fig. 5.18 Extinction coefficient for 75% H_2SO_4 (from Remsberg,1971)

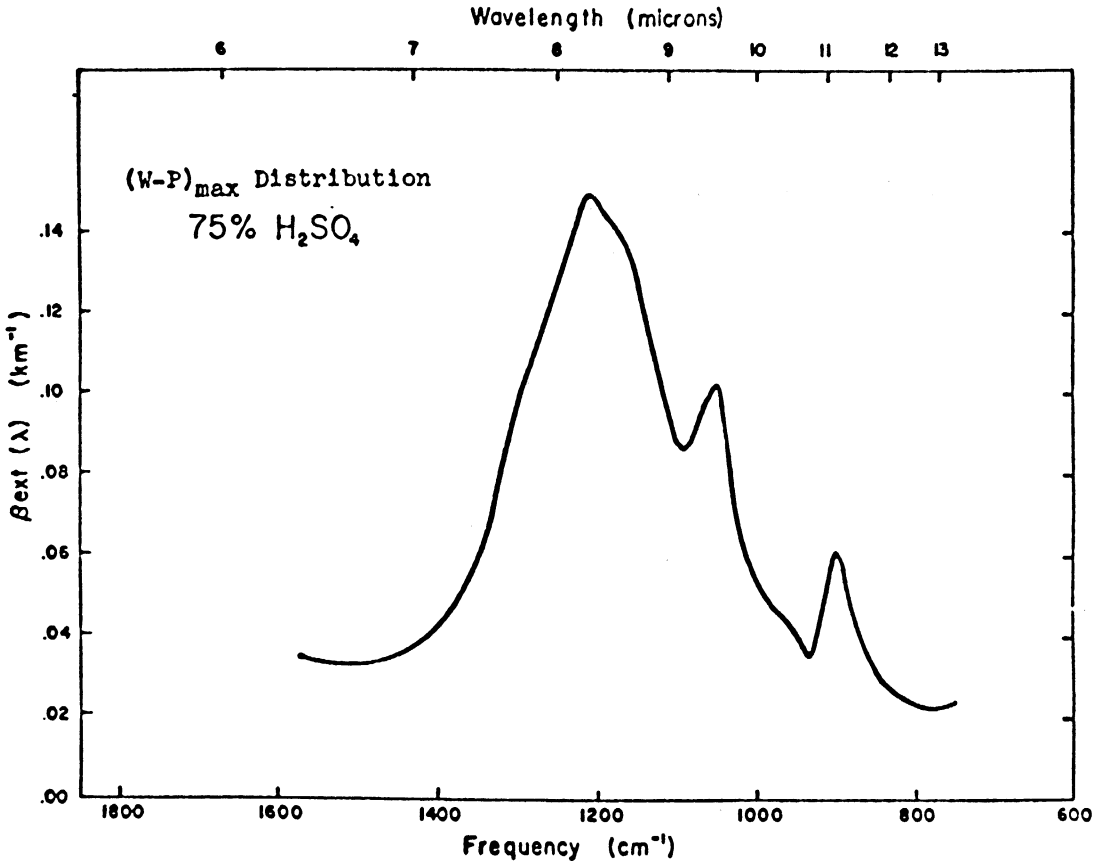

Fig. 5.19 Extinction coefficient for 90% H_2SO_4 (from Remsberg, 1971)

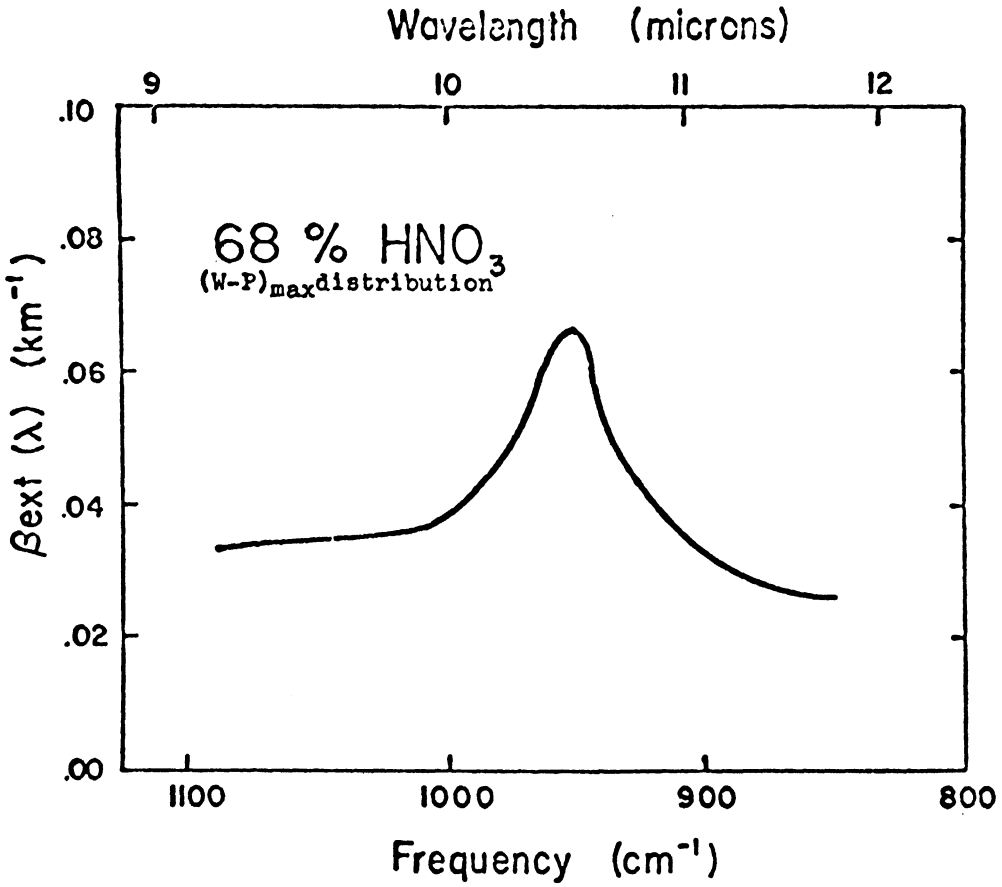

Fig. 5.20 Extinction coefficient for 68% HNO_3 (from Remsberg, 1971)

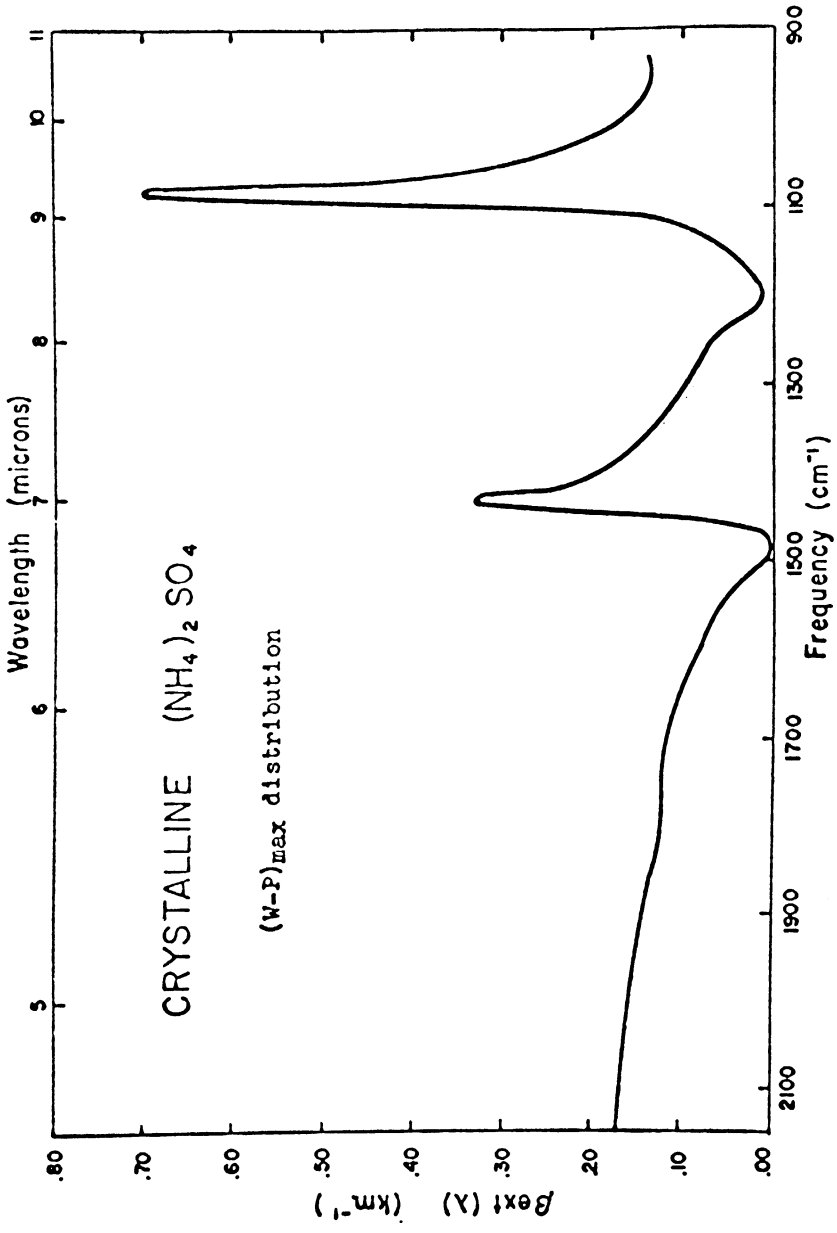

Fig. 5.21 Extinction coefficient for crystalline $(NH_4)_2\ SO_4$ (from Chermack, 1970)

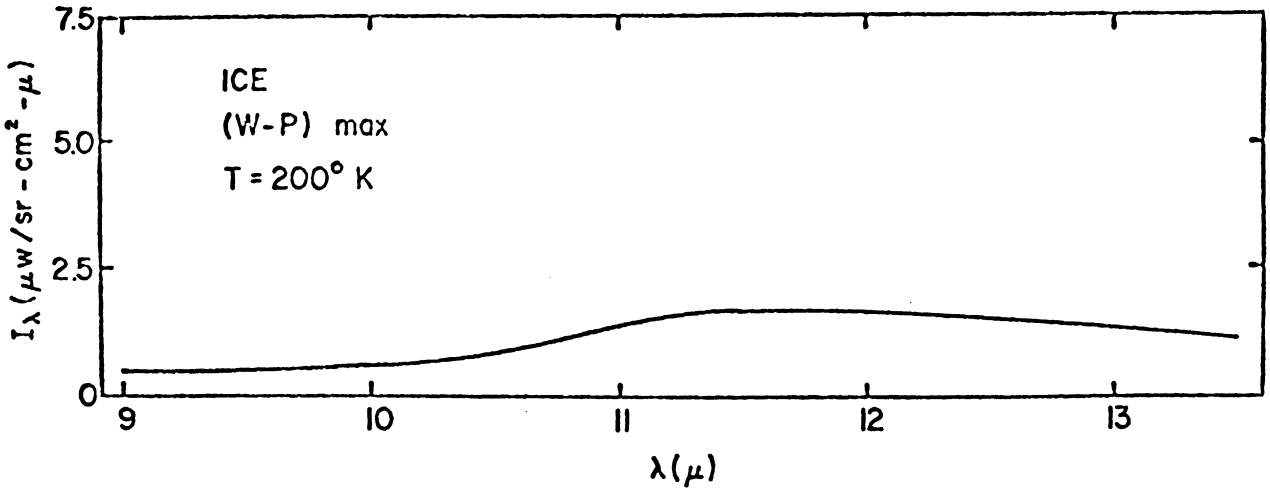

Fig. 5.22 Radiances for an ice aerosol path of one kilometer (from Remsberg, 1971)

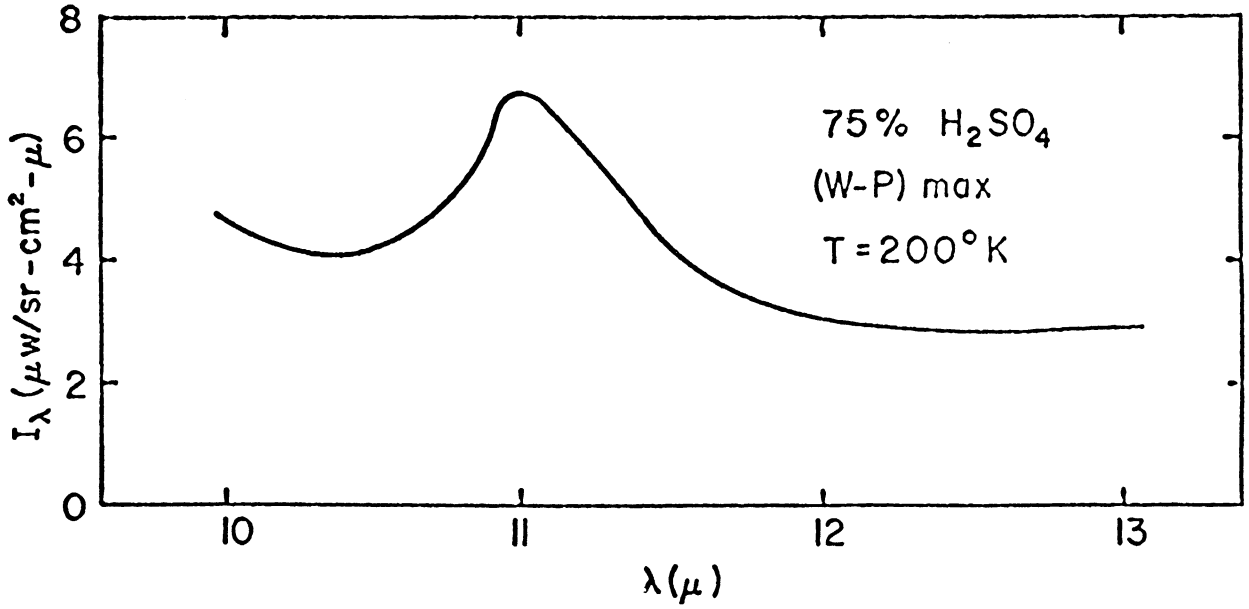

Fig. 5.23 Rediances for a 75% H_2SO_4 aerosol path of one kilometer (from Remsberg, 1971)

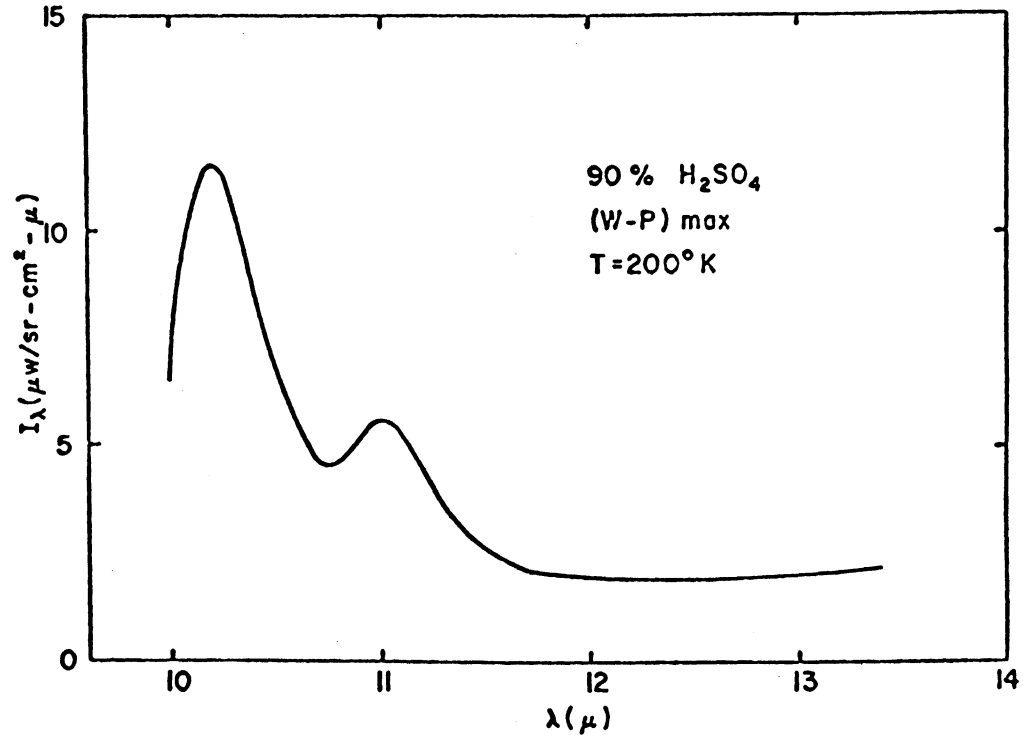

Fig. 5.24 Radiances for a 90% H_2SO_4 aerosol path of one kilometer (from Remsberg, 1971)

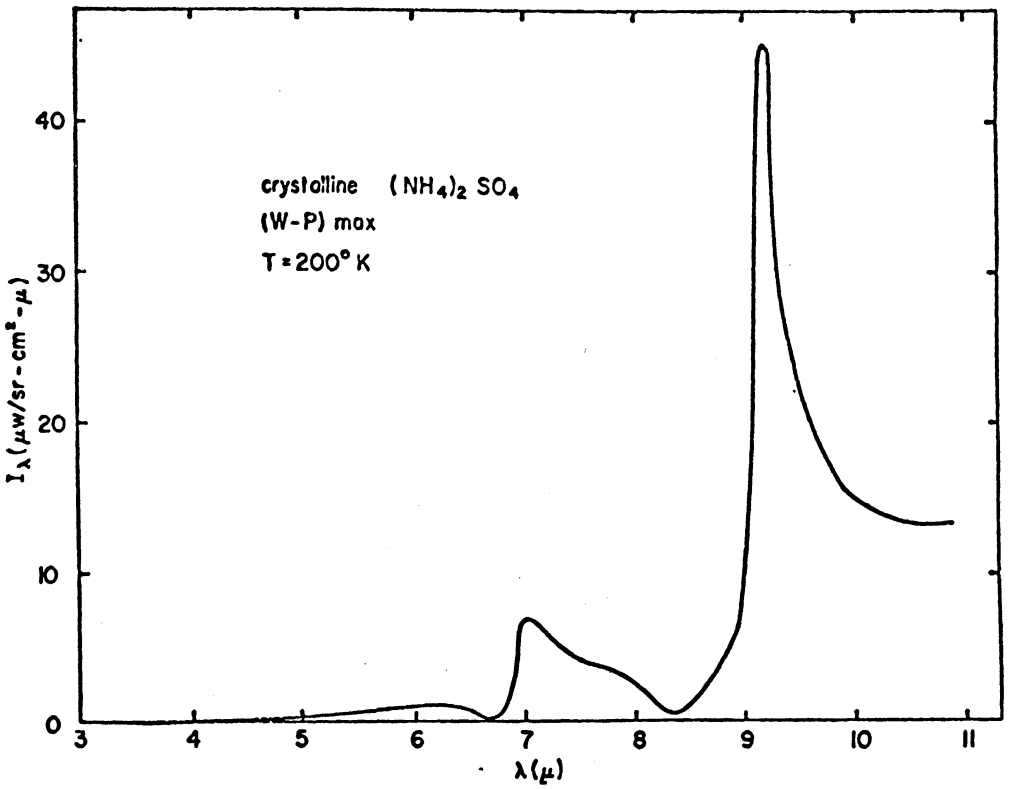

Fig. 5.25 Radiances for a crystalline $(NH_4)_2SO_4$ aerosol path of one kilometer (from Remsberg, 1971).

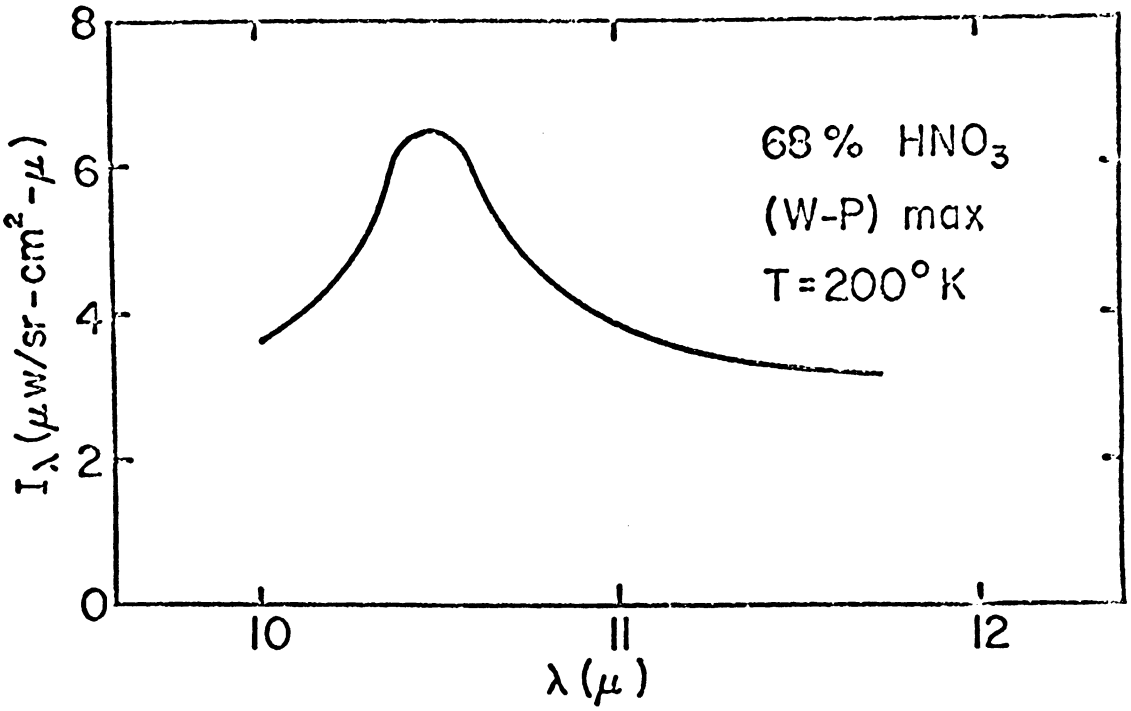

Fig. 5.26 Radiances for a 68% HNO_3 aerosol path of one kilometer (from Remsberg, 1971).

5.3 Survey of Aerosol Remote Sensing Techniques

Some information about atmospheric aerosols has already been obtained by remote sensing experiments. Generally speaking, these experiments could not provide quantitative information about particle size distributions, number density vs. altitude, or index of refraction. However qualitative information has been obtained.

5.3.1 Sunphotometer

Monochromatic solar radiation measurements can be used to determine the extinction coefficient of the vertical atmosphere due to aerosols (the atmospheric turbidity). Many years of measurements have provided a climatology of turbidity over the U. S. These data have been used to estimate particle loading in the lower atmosphere (Flowers, McCormak and Kurfis, 1969).

5.3.2 Laser Radar

Laser radars have been used to observe aerosol layer altitudes and relative scattering strength. With this technique, the intensity of the back-scattered light from a laser beam is determined as a function of range. The presence of particulate matter causes significantly different returns than a dust free atmosphere does. Aerosol particles can therefore be detected. The scattering properties of the atmosphere are determined as a function of range (altitude) with a distance resolution as low as 100 meters. Results include:

a) The determination of the dependence of the stratospheric layer on tropopause height.

b) The time variations in aerosol scattering following the Mt. Agung eruption.

5.3.3 Twilight Scattering

Measurements of twilight sky radiation yield a qualitative picture of the vertical distributions of aerosol particles (Volz, 1969, Shah, 1970). Vertical dust profiles generally agree with results by more direct methods. The effect of stratospheric dust from the Agung volcano was observed in Germany 2 months later. Highest amounts were observed about 9 months after the explosion, abnormally high amounts were observed even 5 years later.

5.3.4 Forward Scattered Sunlight

The measurement of sunlight in the sun's aureole as a function of wavelength can yield information about the altitude and size distribution of aerosols (Green, et. al., 1971). Theoretical calculations of forward scattered sunlight are carried out assuming single scattering and analytical models of the altitude-size distribution of aerosols. Optimum fits to experimental data at several wavelengths are achieved by adjusting parameters of the aerosol model.

5.4 The Remote Sensing of Aerosols from Satellites

Two experiments which have been suggested for the monitoring of aerosol layers and the possible identification of aerosol constitutions are described below. In the first (Gray, et. al., 1971), a method of determining the height of aerosol layers from the inversion of horizon-intensity profiles of the earth's sunlit horizon is described. In the second (Remsberg, 1971), the possibility of the identification of aerosol constituents from infrared emission spectra is discussed.

5. 4. 1 Aerosol Monitoring by Satellite Horizon Scanning

In the MIT experiment (Gray, et. al., 1971) the earth's horizon is scanned by a satellite multispectral sensor. The sensor signals are compared to a theoretically derived intensity profile based on a reference model of aerosol extinction vs. altitude. The computer program corrects the reference profile according to the difference between measurement and prediction considering uncertainties in the reference model and the measurements.

In the work carried out so far, simulated horizon profiles have been inverted with results shown in Figs. 5. 27 and 5. 28. Also experimental data obtained with a multispectral photometer on an x-15-1 aircraft were inverted to produce the aerosol attenuation curve shown in Fig. 5. 29. It is estimated that aerosol layers may be determined with an altitude accuracy approaching 1 km.

5. 4. 2 Identification of Aerosol Constituents Using Emitted Radiation from the Earth's Atmosphere

Remsberg has compared his calculated emitted radiation curves with data obtained by Murcray, et. al. (1969). He has computed the emitted intensity that would be obtained from a 50 km horizontal path and compared this data (Figs 5. 30, 5. 31) with Murcray's data measured at zenith angles of 80 and 85° (Fig. 5. 32). He concludes that the emission feature at 10. 8μm observed in Murcray's data can possibly be explained by the 11. 0μm feature in the H_2SO_4 data in Figs. 5. 30 and 5. 31 if a wavelength correction $\Delta\lambda = 0.2\mu m$ is applied. The wavelength correction is necessary since the index of refraction of H_2SO_4 was measured at room temperature, whereas the atmospheric aerosols are at -60 to -70°C. Such low temperatures could easily cause such a wavelength shift in the absorption coefficient and emission spectra.

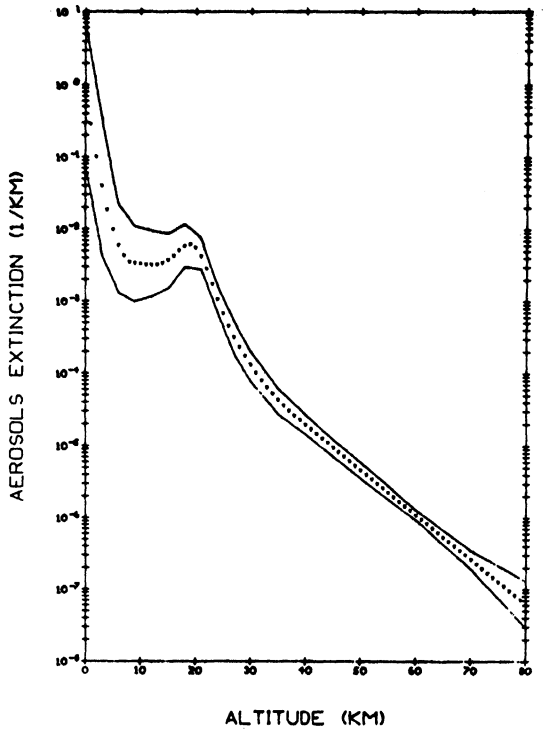

Fig. 5. 27 Simulation Results - Inversion of 20-km, γ=3 Aerosol Layer, Zenith 30^{o} (from Gray, et. al., 1971).

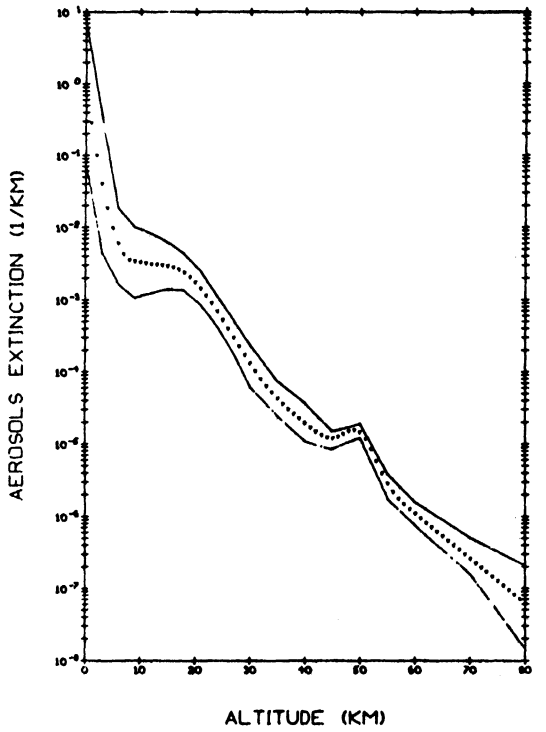

Fig. 5. 28 Simulation Results - Inversion of 50-km, γ=7 Aerosol Layer, Zenith 60^{o}(from Gray, et. al., 1971).

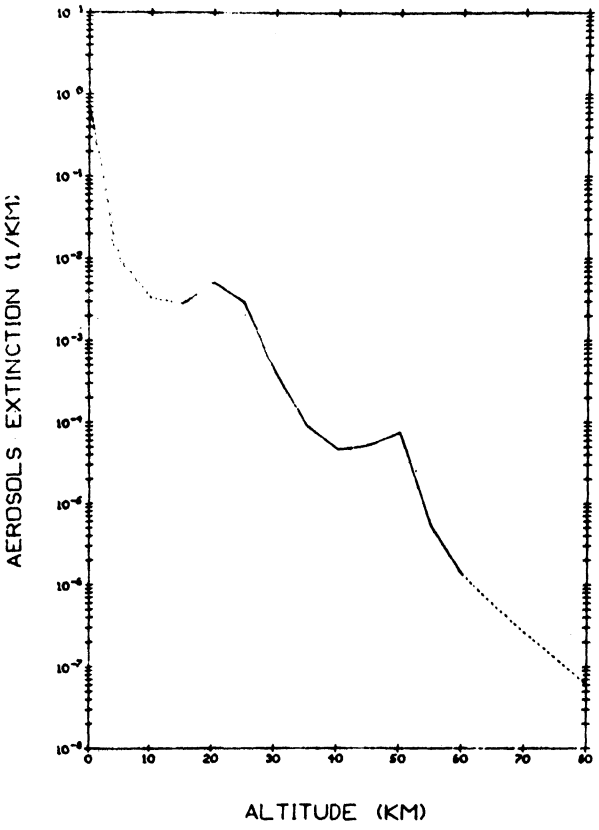

Fig. 5. 29 Experimental Results -Inversion of X-15 Data, aerosol extinction (from Gray, et. al., 1971).

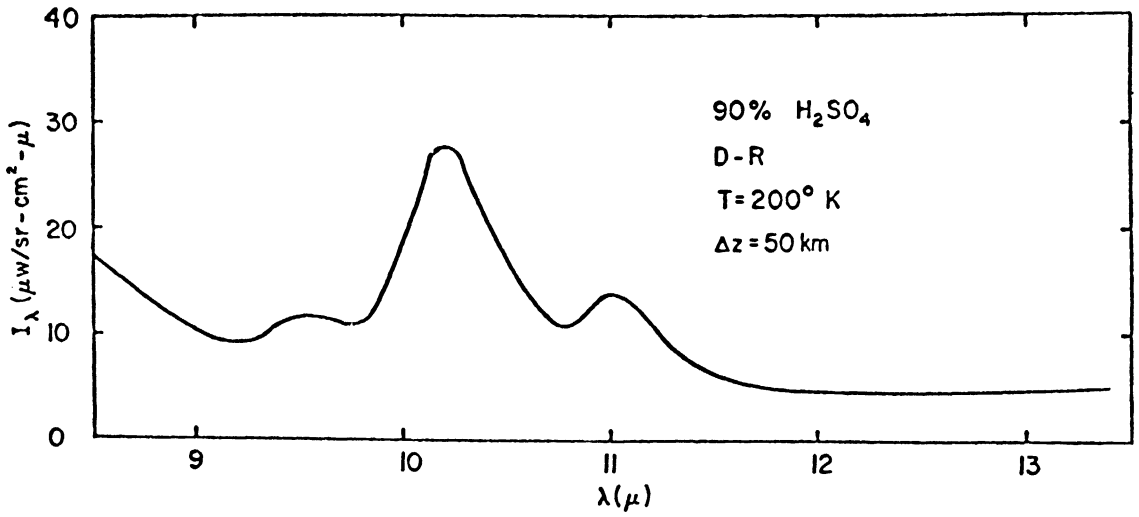

Fig. 5.30 Emitted intensigy for 90% H_2SO_4 aerosol from a 50Km horizontal path (from Remsberg, 1971).

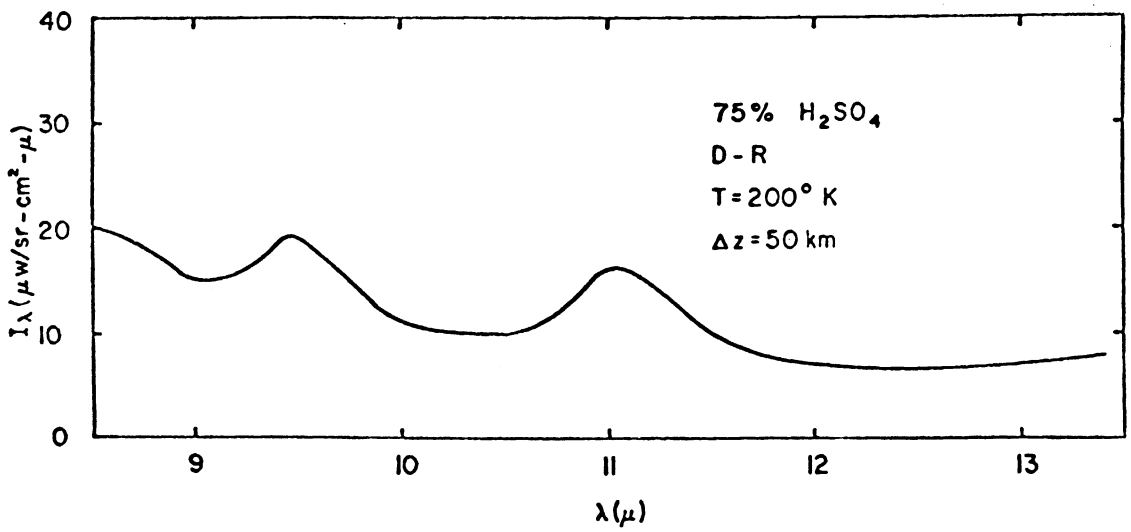

Fig. 5.31 Emitted intensity for 75% H_2SO_4 aerosol from a 50Km. horizontal path (from Remsberg, 1971).

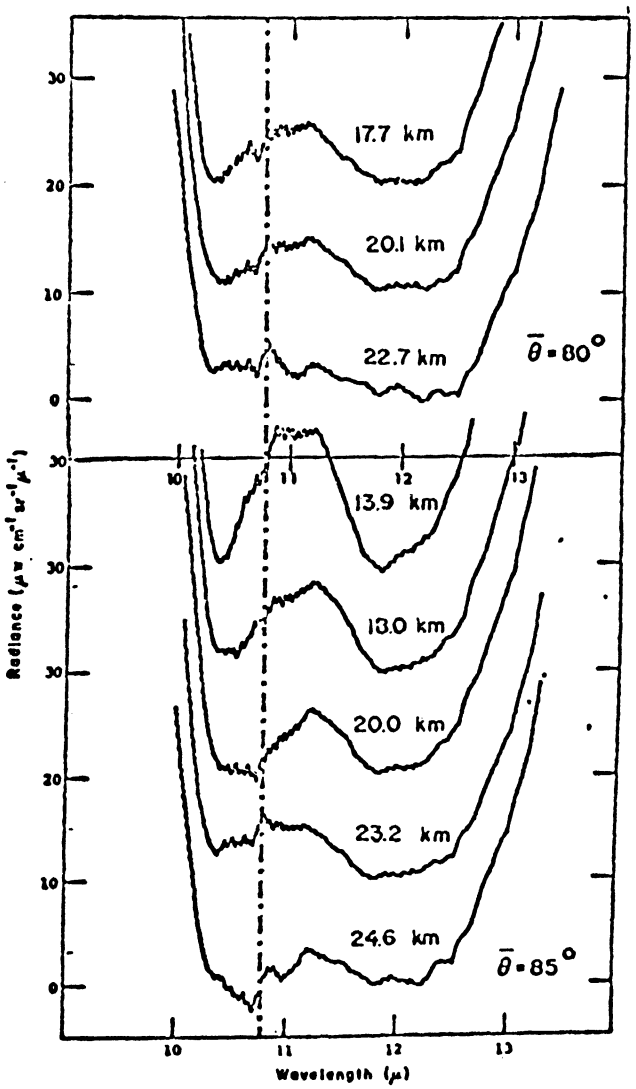

Fig. 5.32 Radiances observed at various heights and at two zenith angles for the 25 Feb. 1969 flight of Murcray (1970). Dashed line represents the position of the emission feature at 10.8μ.

5.4.3 Discussion of Satellite Measurements of Atmospheric Aerosols

The technique of horizon scanning in the visible with a multi-spectral scanner to determine the altitude of aerosol layers appears to be a feasible and practical experiment to carry out. The simulated horizon profile data already include consideration of earth albedo, sun angle and a correction factor for multiple scattering. The multiple scattering calculations will, no doubt, be improved in the near future. The reference aerosol extinction model will also be improved as our knowledge of atmospheric aerosols improves. Thus the experiment is certain to be able to determine the height of aerosol layers.

It is not certain that the visible horizon scanning data can be used to determine the physical characteristics of aerosols, however, it is possible that infrared horizon emission or absorption spectra might contain identifiable spectral features as illustrated by the work of Remsberg. Improved knowledge of the composition of aerosols and the accurate determination of the optical characteristics of aerosols at low temperatures are a necessity for the successful operation of this experiment.

Initial versions of both of these experiments can be flown on high altitude balloons to provide initial tests of their feasibility.

References

Bigg, E. K., A. Ono and W. J. Thompson, (1970), Aerosols at Altitudes between 20 and 37 Kilometers," Tellus, 22, 550-563.

Blifford, I. H., and L. D. Ringer, (1969), The Size and Number Distribution of Aerosols in the Continental Troposphere, J. Atmos. Sci , 26, no. 4, 716-726.

Bullrich, K., (1969), Determining the Vertical Distribution of Aerosol Particles in the Atmosphere with Radiative Optical Measureing Methods, Proceedings of the NATO Advanced Study Institute: Effects of Atmospheric Water on Electromagnetic Wave Propagation, D. R. May, ed. Univ. of Western Ontario, London, Canada, Aug. -Sept., 198-215.

Carnuth, W., (1970), Aerosol Size Distribution at 700, 1800 and 3000 Meter Altitudes, J. Geophys. Res., 75, No. 15, 2999-3006.

Chagnon, C. W., and C. E. Junge, (1961), The Vertical Distribution of Sub-Micron Particles in the Stratosphere, J. Meteorol., 18, 746-752.

Chermack, E., (1970), Optical Constants of Ammonium Sulfate in the Infrared, PhD. Thesis, Graduate School of Arts and Sciences, New York University at Oswego.

de Bary, E., and F. Rossler, (1966), Size Distributions of Atmospheric Aerosols Derived from Scattered Radiation Measurements Aloft, J. Geophys. Res., 71, 1011.

De Luisi, J. J., I. H. Blifford, Jr., and J. A. Takamine, (1972), Models of Tropospheric Aerosol Size Distribution Derived from Measurements at Three Locations, J. Geophys. Res., 77, No. 24, 4529-4538.

Diermendjian, D., R. Clasen, and W. Vieze, (1961), Mie Scattering with Complex Index of Refraction, J. Opt. Soc., Am., 51, 620-633.

Diermendjian, D., (1964), Scattering and Polarization Properties of Water Clouds and Hazes in the Visible and Infrared, Appl. Opt., 3, 187-196.

Elliot, D. D., (1970), Effect of a High Altitude (50 km) Aerosol Layer on Topside Ozone Sounding, Space Research XI, Proc. of the 13th Plenary Meeting of Cospar, Leningrad, 1970, Akademie-Verlag, Berlin, 1971.

Friend, J. P., (1966), Properties of the Stratospheric Aerosol, Tellus, 18, No. 2, 465-473.

Gray, C. R., H. L. Malchow, D. C. Merritt and R. E. Var, (1971), Aerosol Monitoring by Satellite Horizon Scanning, Paper presented at Joint Conference on Environmental Pollutants, Palo Alto, Calif., Nov. 8-10, 1971.

Green, A. E. S., A. Deepak and B. J. Lipofsky, (1971), Interpretation of the Sun's Aureole Based on Atmospheric Aerosol Models, Applied Optics, 10, No. 6, 1263-1279.

Hidy, G. M., and Brock, J. R., (1970), The dynamics of Aerocolloidal Systems, Pergamon Press.

Junge, C. E., (1963), Air Chemistry and Radioactivity, Academic Press.

McCormick, R. A., and K. R. Kurfis, (1966), Vertical Diffusion of Aerosols over a City, Quart, J. Roy. Meteor. Soc., 92, 392-396.

Mossop, S C., (1965), Geochimica et Cosmochimica Acta, 29, 201.

Murcray, D. G., F. H. Murcray, W. J. Williams, T. G. Kyle, and A. Goldman, (1969), Variation of the Infrared Solar Spectrum Between 700 cm^{-1} and 2240 cm^{-1} with Altitude, Appl. Opt., 8, 2519-2536.

Newell, R. E., and C. R. Gray, (1972), Meteorological and Ecological Monitoring of the Stratosphere and Mesosphere, NASA Contractor Report CR-2094, Prepared by M. I. T. for Langley Research Center.

Newkirk, G. and J. A. Eddy, (1964), Light Scattering by Particles in the Upper Atmosphere, 21, No. 1, 35-60.

Pilipowskyj, S., J. A. Weinman, B. R. Blemesha, G. S. Kent, and R. W. Wright, (1968), Investigation of the Stratospheric Aerosol by Infrared and Lidar Techniques, J. Geophys. Res., 73, 7553.

Pueschel, F. R. and K. E. Noll, (1967), Visibility and Aerosol Size Frequency Distribution, J. App. Meteor., 6, No. 6, 1045-1052.

Quenzel, H., (1970), Determination of Size Distribution of Atmospheric Aerosol Particles from Spectral Solar Radiation Measurements, J. Geophys. Res., 75, No. 15, 2915-2921.

Remsberg, E. E., (1971), Radiative Properties of Several Probable Constituents of Atmospheric Aerosols, PhD. Dissertation, University of Wisconsin, Dept. of Meteorology.

Rosen, J., (1968), Simultaneous Dust and Ozone Soundings over North and Central America, J. Geophys. Res., 73, No. 2, 479-486.

Rozenberg, G. V., (1966), Twilight, a Study in Atmospheric Optics, Plenum Press, New York.

Shah, G. M., (1970), Study of Aerosols in the Atmosphere by Twilight Scattering, Tellus, XVII, No. 1, 82-93.

Sherwood, R. D. and J. P. Friend, (1967), Project Strap Final Report, NY00-3615-1.

Volz, F. E., (1969), Stratospheric Dust Striations, Bull. Amer. Meteor. Soc., 50, 16.

Volz, F. E., (1972), Infrared Absorption by Atmospheric Aerosol Substances, J. Geophys. Res., 77, No. 6, 1017-1031.

Chapter 6. Discussion and Future Program

6.1 Summary and Conclusions

The results documented in this report have been obtained during the first six months of a study of the feasibility of determining stratospheric distributions of minor constituents and pollutants from satellite measurements of absorption during solar occultation. A major part of the effort has been expended in searching the literature and consolidating the information on the distributions and spectral properties of the molecules and aerosols. Only the infrared spectral region has been considered because absorption due to molecular oxygen and ozone in the ultraviolet is almost complete for stratospheric tangent paths. Ozone (and possibly also some other constituents) can be measured in the highest regions of the stratosphere and in the mesosphere. Such measurements using stellar occultation have already been made (Hays, et. al., 1972).

The molecules considered and discussed in this report are O_3, OH, H_2O, N_2O, NO, NO_2, N_2O_5, HNO_3, CO_2, CO and CH_4. The distribution and optical properties of stratospheric aerosols are also discussed. For some of the constituents the stratospheric distributions are well known (e. g., ozone) while for others virtually no measurements exist (e. g., oxides of nitrogen) so that estimates have to be made based on incomplete theoretical models incorporating chemical and transport effects. Despite their shortcomings, these models serve a useful purpose and provide an order of magnitude estimate of the concentrations of minor constituents. Similarly the spectral properties of some molecules are well known, particularly the diatomic and linear triatomic molecules, while for others measurements are few and the theoretical analysis is incomplete.

Having estimated the distribution of a constituent in the stratosphere the optical mass along stratospheric tangent paths was determined using

the procedure outlined in the appendix. Using low or medium resolution laboratory measurements, the absorption for different tangent heights was determined for some of the molecules. In the most strongly absorbing regions the absorption was complete before the tropopause was reached, showing that for some molecules distributional information may be obtained using a relatively simple instrument. However, other constituents absorb only to a small degree (less than one percent) and more sophisticated instrumentation would be required to detect their presence. This stage of the investigation is not complete and the reader is referred to the individual sections of the report for details on specific molecules.

The use of laboratory absorption spectra to determine atmospheric transmittance requires interpolation over pressure and optical mass, which limits its accuracy. A more serious problem is the error introduced by temperature effects. Most laboratory measurements are made at room temperature while the mean temperatures along stratospheric absorption paths are as much as $80^{o}C$ or more lower. The intensities of lines, particularly those of 'hot' bands or with high rotational quantum numbers, may change radically and thus change the absorption considerably. The values of absorption given in the tables are not highly accurate but are sufficiently good for their intended purpose, to examine the feasibility of determining concentrations from solar occultation measurements.

For the reduction of satellite data more accurate absorptions would be required. These could be obtained by the 'line-by-line' technique or perhaps by band models, provided the relevant parameters, line wavenumbers, intensity and half-width, are known. This information is not yet available for all molecules. Even for the better studied molecules the temperature dependence of Lorentz half-width is uncertain, as recent low temperature measurements

indicated variations which are not in accord with either the Anderson theory or the classical inverse square root temperature dependence. The effect on atmospheric transmittances has been discussed by Drayson (1972). Further low temperature absorption measurements are required.

6.2 Future Program

The contents of this report indicate that the minor constituents of the stratosphere can be detected and measured from a satellite by examining the absorption of solar infrared radiation along a tangent path. The more abundant molecules can be detected using comparitively simple instrumentation while others would require a more sophisticated design. This work must now be extended to put these results on a quantitative basis to estimate accuracy and altitude ranges for the various constituents. Only when this has been accomplished will it be possible to objectively estimate the usefulness of the technique and compare it with other measurement schemes.

Many practical details will have to be considered in this analysis. These include, but are not limited to, horizontal inhomogeneities in concentrations, fine structure in the vertical distribution profile, uncertainties in the temperature profile and in the spectral absorption of the constituents, errors introduced by approximations in the transmittance calculations, the effects of refraction and errors introduced by aerosol layers. It will be necessary to study inversion techniques, that is methods of determining atmospheric distributions from the solar absorption measurements.

The results of the investigations will hopefully lead to specifications for satellite instrumentation and will point out any deficiencies in our knowledge of spectral properties of the constituents, so that laboratory investigations can be made to remedy the situation. Only with a careful analysis and attention to detail can the full potential of this type of satellite experiment be achieved.

References

Drayson, S. R., (1972), Atmospheric Radiative Transfer by Carbon Dioxide. A. M. S. Conference on Atmospheric Radiation, Fort Collins, Colorado.

Hays, P. B., R. G. Roble and A. N. Shah, (1972), Terrestrial Atmospheric Composition from Stellar Occultations. Science, 176, 793.

Appendix

Given the vertical distribution of a minor constituent in the stratosphere, we wish to determine the optical mass along tangent paths at various altitudes in the stratosphere, as well as 'equivalent' pressures and temperatures. It was convenient to write a flexible computer routine to make such calculations. The main application was to determine the optical masses of the constituents considered in this report so that the feasibility of stratospheric measurements of solar absorption could be evaluated. Refraction effects are of some importance but they should not effect a feasibility study and were ignored, but for the reduction of satellite measurements they should be included.

The atmosphere between 1 and 80 km was divided into 1 km thick spherical shells. The temperature, pressure, absorber concentration etc. in each shell was assumed to be the mean of the values at its boundaries. The geometry is illustrated in Fig. A1. Consider a tangent height of h_o km above the surface and consider the shell between K and (K+1) km above h_o. The distance x_K to the tangent point is given by

$$x_K^2 = (a + h_o + K)^2 - (a + h_o)^2$$

$$= K(K + 2(a + h_o))$$

where a is the radius of the earth.

The path length in the layer, $\Delta x_K = 2(X_{K+1} - x_K)$

The optical mass $U(h_o)$ for the entire path is given by the sum over all layers

$$U(h_o) = \sum_K N(K)\Delta x_K$$

where N(K) is the concentration in the K th layer.

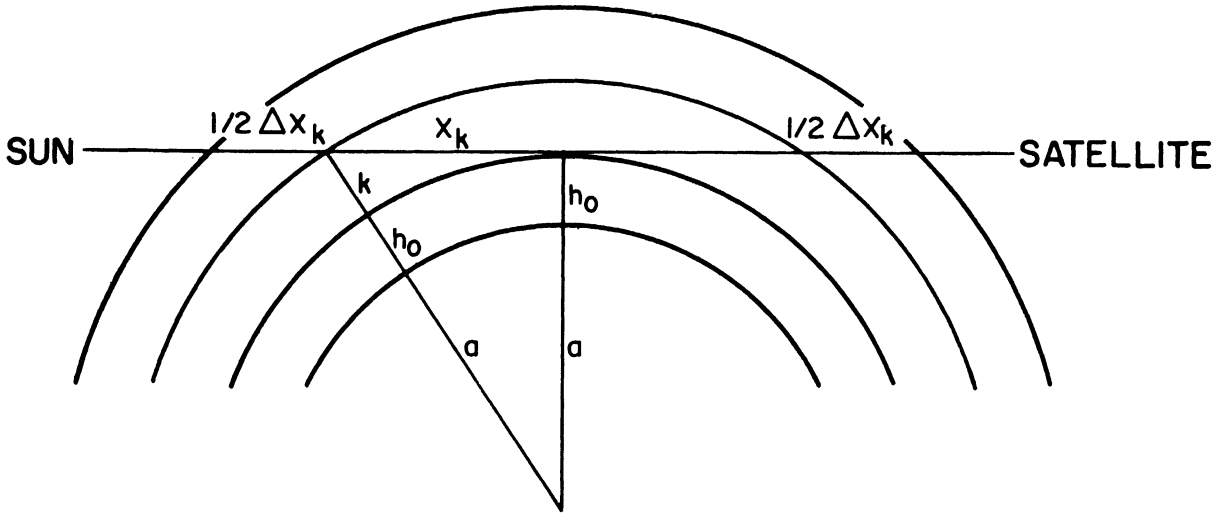

Fig. A.1. Geometry of the solar occultation.

An 'equivalent' or mean pressure is given by

$$\bar{P}(h_o) = \frac{\sum_K P(K)\, N(K)\, \Delta x_K}{\sum_K N(K)\, \Delta x_K}$$

and similarly a mean temperature is defined by

$$\bar{T}(h_o) = \frac{\sum_K T(K)\, N(K)\, \Delta x_K}{\sum_K N(K)\, \Delta x_K}$$

The last two parameters are useful when applying the Curtis-Godson or similar approximation.

A Fortran subroutine OMASS has been written to make the calculations. The arguments are

N	the concentration in molecules cm^{-3} for IS = 1
	or volume mixing ratio for IS = 2
UN	the computed optical mass in molecules cm^{-2}
UATMCM	optical mass in $(atm\ cm)_{300K}$
PBAR	mean pressure in mb
TBAR	mean temperature in ^oK

The calculations are made for the U. S. standard stmosphere (1962). This may be varied by altering the data cards of AP and AT (pressure and temperature respectively). For each vector the subscript I refers to an altitude of I km for I = 1, 2, 3, . . . , 80.

To make the use of OMASS easier an interpolative subroutine INTERP was written. It interpolates linearly the quantities A(1), A(2), . . . , A(L) defined at heights Z(1), Z(2), . . . , Z(L) to give the values X(1), X(2), . . . , X(80) at heights 1, 2, . . . , 80 km. If the interpolated value X becomes negative

at any height, it is set equal to zero. The purpose of INTERP is be able to specify the concentration at a few atmospheric levels rather than all 80 levels required by OMASS.

A Fortran listing of the subroutines and a short calling program is now given. The input data is L, IS, Z, and A. If IS = 1 then the units of A are molecules cm^{-3}. If IS = 2 then A is volume mixing ratio. The program has been tested and run on an IBM 360/67 and has been used in the main body of this report.

```
      REAL N
      DIMENSION N(80),UN(80),UATMCM(80),PBAR(80),TBAR(80),Z(80)
      DIMENSION A(10)
  900 FORMAT (2I20/(8F10.3))
      READ  (5,900) L,IS,(Z(I),I=1,L),(A(I),I=1,L)
      CALL INTERP(Z,A,L,N)
      CALL OMASS(N,UN,UATMCM,PBAR,TBAR,IS)
      WRITE(6,950) (I,N(I),UN(I),UATMCM(I),PBAR(I),TBAR(I),I=1,79)
  950 FORMAT('1'/(I5,4E14.4,F8.1))
      GO TO 100
      END
```

```
      SUBROUTINE OMASS(N,UN,UATMCM,PBAR,TBAR,IS)
      REAL N
      DIMENSION N(80),UN(80),UATMCM(80),PBAR(80),TBAR(80)
      DIMENSION Z(80),AN(80),AP(80),AT(80),X(80)
      DATA Z/1.,2.,3.,4.,5.,6.,7.,8.,9.,10.,11.,12.,13.,14.,15.,16.,
     1 17.,18.,19.,20.,21.,22.,23.,24.,25.,26.,27.,28.,29.,30.,31.,32.,
     2 33.,34.,35.,36.,37.,38.,39.,40.,41.,42.,43.,44.,45.,46.,47.,48.,
     3 49.,50.,51.,52.,53.,54.,55.,56.,57.,58.,59.,60.,61.,62.,63.,
     4 64.,65.,66.,67.,68.,69.,70.,71.,72.,73.,74.,75.,76.,77.,78.,79.,
     5 80./
      DATA AP/  845.6,746.9,657.8,577.5,505.4,440.8,383.0,331.5,285.8,
     1 245.4,209.8,179.3,153.3,131.0,112.0,95.92,81.82,69.95,59.80,
     251.13,43.75,37.46,32.09,27.52,23.62,20.28,17.43,14.99,12.90,
     3 11.11,9.574,8.26,7.13,6.17,5.35,4.65,4.04,3.52,3.07,
     4 2.68,2.35,2.06,1.81,1.58,1.40,1.23,1.09,.961,.849,
     5 .750,.662,.585,.516,.455,.401,.353,.311,.273,.240,
     6 .210,.184,.161,.141,.123,.107,.0926,.0801,.0692,.0595,
     7 .0511,.0438,.0374,.0319,.0271,.0229,.0193,.0162,.0136,.0114/
      DATA AT/ 278.4,271.9,265.4,258.9,252.4,245.9,239.5,233.0,226.5,
     1 220.0,10*216.5,
     2 217.1,218.1,219.1,220.1,221.1,222.0,223.0,224.0,225.0,226.0,
     3 227.0,228.,229.6,232.3,235.1,237.9,240.7,243.4,246.2,248.9,
     4 251.7,254.5,257.3,260.,262.8,265.5,268.3,270.7,270.7,270.7,
     5 270.7,270.7,270.5,268.5,266.6,264.6,262.6,260.7,258.7,256.8,
     6 254.8,252.8,249.1,245.2,241.2,237.3,233.4,229.5,225.6,221.7,
     7 217.7,213.8,209.9,206.0,202.1,198.2,194.3,190.4,186.5,182.6 /
      DATA RZ/6378./,BOLTZ/1.38054E-19/
      AN(80)=0.
      DO 100 I=1,79
100   AN(I)=(N(I)+N(I+1))*.5
      IF (IS.EQ.1) GO TO 110
      DO 102 I=1,79
102   AN(I)=AN(I)*AP(I)/(AT(I)*BOLTZ)
110   CONTINUE
      DO 200 I=1,79
      A=2.*(RZ+Z(I))
      K=0
      X(I)=0.
      DO 201 J=I,79
      K=K+1
201   X(J+1)=SQRT(K*(A+K))
      PBAR(I)=0.
      TBAR(I)=0.
      UN(I)=0.
      DO 202 J=I,79
      U=AN(J)*(X(J+1)-X(J))
      UN(I)=UN(I)+U
      PBAR(I)=PBAR(I)+AP(J)*U
202   TBAR(I)=TBAR(I)+AT(J)*U
      IF (UN(I).EQ.0.) GO TO 210
      PBAR(I)=PBAR(I)/UN(I)
      TBAR(I)=TBAR(I)/UN(I)
      GO TO 211
210   PBAR(I)=PBAR(I-1)
      TBAR(I)=TBAR(I-1)
211   UN(I)=UN(I)*2.E5
200   UATMCM(I)=UN(I)*4.0873E-20
      TBAR(80)=TBAR(79)
```

```
PBAR(80)=PBAR(79)
UN(80)=0.
UATMCM(80)=0.
RETURN
END
```

```
      SUBROUTINE INTERP(Z,A,L,X)
      DIMENSION Z(1),A(1),X(1)
      IJ=2
      DO 100 I=1,80
      Y=I
      DO 110 J=IJ,L
      IF (Z(J).GT.Y) GO TO 111
  110 CONTINUE
      J=L
  111 IJ=J
      X(I)=((Y-Z(IJ-1))*A(IJ)+(Z(IJ)-Y)*A(IJ-1))/(Z(IJ)-Z(IJ-1))
      IF (X(I).LT.0.) X(I)=0.
  100 CONTINUE
      RETURN
      END
```